BIOFILM DEVELOPMENT IN A FLUIDIZED BED BIOREACTOR FOR AEROBIC PHENOL DEGRADATION

A thesis presented in partial fulfilment
of the requirements for the degree of
Master of Technology
in Biotechnology and Bioprocess Engineering at
Massey University, Palmerston North, New Zealand

Kirsten Maushake

1993

Ki te wao nui a Tane,

ki nga awa a Tangaroa ki uta,

ki nga moana a Tangaroa ki tai.

Ki te ika a Maui,

ki te waka a Maui hoki.

To the land of the long white cloud.

ABSTRACT

The main objective of this thesis was to follow the biofilm development during start-up of a fluidized bed bioreactor with the help of digital image processing. A mixed microbial culture immobilized on activated carbon particles was grown on phenol as sole carbon source in an aerobic liquid-solid fluidized bed bioreactor. The effect of different reactor temperatures and of different inlet phenol concentrations on the system behaviour during start-up was investigated.

The phenol inhibition kinetics of the culture was studied in batch culture experiments. Three substrate inhibition models (Teissier-Edwards, Haldane and Aiba-Edwards models) were fitted to the experimental data. There was no statistically significant difference in the goodness of fit between the equations. The phenol concentrations at which the fitted functions go through their maximum value were between 57 and 88 mg/l, corresponding to specific growth rates of between 0.64 and 0.65 h^{-1}.

A fluidized bed system was developed and tested. The test runs showed that the most critical part of the apparatus was the liquid distributor at the bottom of the fluidized bed reactor. Other critical factors that were decided on during the test runs were initial bed expansion, flow rate, support particle size, and amount of support particles used, these parameters all being interdependent.

The fluidized bed experiments proved that the use of image analysis techniques is a very effective means of measuring the mean biofilm thickness on fluidized support particles. Micrographs of the bioparticles were analyzed with the help of a software-controlled system. The software identified the circumference of the particle core and the bioparticle. The mean biofilm thickness was calculated

from the projected areas and the perimeters of the bioparticle and the particle core applying a simple trapezoid formula.

In all fluidized bed experiments, the bed stratified into layers (in most cases two or three) containing bioparticles with different biofilm thickness and different biofilm structure. The main focus was on the development of the biofilm in the top layer. The phenol reduction was only small due to a very short hydraulic retention time. Conversely, the dissolved oxygen concentration in the outlet reached very low values. Thus, the system was oxygen-limited.

Different reactor temperatures led to distinct differences in the morphology of the biofilm in the top layer. Without temperature control, i.e. at ~17°C, and at 30°C, a loose, fluffy, unevenly shaped, thick biofilm developed, whereas at 25°C the biofilm was firm and relatively even in shape, the final thickness remaining far below the values reached by the fluffy biofilm. Since the biofilm that developed at 25°C showed the most favourable characteristics, this temperature was used for the experiments examining the effect of different inlet phenol concentrations.

The biofilm thickness in the top layer increased the fastest at an inlet phenol concentration of 100 mg/l, followed by 35 mg/l, then 330 mg/l and finally 520 mg/l. In the batch culture experiments, the same order had been found for the specific growth rates at phenol concentrations of the above values. In the case of the few observations obtained at non-inhibitory phenol concentrations, the biofilm density increased with increasing phenol concentration. At inhibitory phenol concentrations the flow patterns in the reactor were very different, thus these patterns were the dominating factor influencing the biofilm density.

ACKNOWLEDGEMENTS

I wish to thank Dr Rao S.M. Bhamidimarri for his supervision during the course of this study.

My special thanks are extended to Dr Ian S. Maddox for the attentive reading of the draft and for his encouragement during the write-up stage of this project.

I am particularly grateful to the technical staff of the Department of Process and Environmental Technology; Mr John Alger, Mr Bruce Collins, Mrs Judy Collins, Mrs Ann-Marie Jackson, Mr Don McLean, Mr Wayne Mallett, Mr Mike Sahayam, Mr Mike Stevens and Mr John Sykes. Not only was their help and advice in technical matters exemplary, moreover their friendly nature and sense of humour provided much encouragement and pleasure.

My thanks also go to Dr Graham J. Manderson for the use of his microscope with camera.

I gratefully acknowledge the advice and assistance given by Dr Don G. Bailey of the Image Analysis Unit at Massey University with regard to the processing and analysis of the bioparticle photographs.

I like to express my gratitude to Dr Peter Vogel, my supervisor from a previous project, who never hesitated to reply to faxes from the other side of the world and to give his support when needed.

I am indebted to the Deutscher Akademischer Austauschdienst (DAAD) for the award of a scholarship without which I would not have been able to undertake this study.

Sincere gratefulness is extended to Mr Gary J. Pearson for placing his personal computer at my disposal.

Warm thanks are due to my fellow postgraduate students and to my flatmates for their friendship, support and humour.

With gratitude, I appreciate the tolerance and empathy my parents have demonstrated.

Finally, and most of all, I am profoundly thankful to Mark for his incomparable support, understanding and encouragement.

TABLE OF CONTENTS

LIST OF FIGURES

Page

LIST OF TABLES

NOMENCLATURE

A	projected area of a particle
b	biofilm thickness
CoA	Coenzyme A
d	diameter
d_L	long diameter of an ellipsoid
d_s	short diameter of an ellipsoid
$d_{equiv.}$	equivalent diameter of a sphere
F_{i1}	F-ratio between Model i and Model 1
HRT	hydraulic retention time
i	inhibition constant
K, k_1, k_2	kinetic constants
K_i	inhibition constant
K_s	saturation constant
m, n	constants
NAD	Nicotinamide adenine dinucleotide
NADPH	Nicotinamide adenine dinucleotide phosphate (reduced)
P	perimeter
R^2	coefficient of determination
r_S	volumetric substrate uptake rate
S	substrate concentration
S_0	initial substrate concentration
S'	substrate concentration at the onset of the exponential growth phase
S^*	threshold substrate concentration (below which organisms grow apparently without inhibition)
S_m	total inhibition concentration

Std.	standard deviation
x	biomass concentration
$Y_{x/s}$	growth yield coefficient

Greek letters

μ	specific growth rate
μ_m	maximum specific growth rate
μ^*	maximum observable specific growth rate
σ^2	variance

Subscripts

b	bioparticle
c	carrier particle
i	inlet
o	outlet

CHAPTER 1

INTRODUCTION

Immobilized cell systems are receiving ever-increasing interest for many continuous bioprocess applications. They exhibit many properties that make them preferable to suspended cell systems. These properties include high cell concentrations, enhanced cell retention and increased resistance to toxic substances. The last point causes immobilized cell systems to be particularly advantageous for biological wastewater treatment, where inhibitory substances are a constant threat to the stability of the system.

Phenol has become the most commonly used model compound for the study of inhibitory carbon sources. It is a prevalent organic constituent of effluents from energy and manufacturing industries such as polymeric resin production, oil refineries and coking plants. Because of its frequent occurrence in wastewater streams, and because of the wealth of available data, solutions containing phenol have been used by many researchers to investigate the behaviour of immobilized cell systems for wastewater treatment.

The most commonly used method of cell immobilization in wastewater treatment is adsorption on solid support surfaces, since it represents an inexpensive, simple and natural approach. Of all types of biological fixed film reactors, fluidized bed bioreactors have proved to be the most promising alternative. Reasons for their superiority include extremely high biomass hold-up, excellent contact between liquid and solid phase, and no danger of clogging of biomass in the system. However, fluidized bed bioreactors represent

extremely complex systems with a multitude of interacting factors determining the performance characteristics.

A vast amount of research has been undertaken to investigate the processes prevailing in biological fluidized bed reactors. The most important parameters affecting reactor performance have been found to be the biofilm properties such as biofilm thickness and biofilm density. However, these properties have been investigated only to a small extent, since determination of biofilm thickness and thus in turn biofilm density has provided serious difficulties. Recently, image analysis techniques have proved to be a promising tool for the determination of biofilm thickness and particle size.

The main objective of the present study was to follow the biofilm development during start-up with the help of digital image processing. The biofilm was grown on activated carbon particles in a liquid-solid fluidized bed bioreactor. An aqueous solution containing phenol as sole carbon source was used as model inhibitory wastewater. The study included the determination of the phenol inhibition kinetics of the mixed culture employed, the establishment and testing of the fluidized bed system, and the investigation of the effect of different reactor temperatures and different inlet phenol concentrations on the performance of the fluidized bed system during start-up.

CHAPTER 2

LITERATURE REVIEW

2.1 Basics of Aerobic Phenol Biodegradation

2.1.1 Microorganisms

Although phenol is toxic to most microorganisms, a relatively large number of species has been reported capable of using phenol as a substrate for growth. A bacterium very frequently used in phenol biodegradation studies is *Pseudomonas putida* (Allsop *et al.*, 1993; Bettmann and Rehm, 1984; Ehrhardt and Rehm, 1985, 1987, 1989; Feist and Hegemann, 1969; Hill and Robinson, 1975; Li and Humphrey, 1989; Molin and Nilsson, 1985; Mörsen and Rehm, 1987, 1990; Quail and Hill, 1991; Sokol and Howell, 1981; Sokol, 1987, 1988; Yang and Humphrey, 1975; Zilli *et al.*, 1993). Other phenol degrading microorganisms include *Acinetobacter* sp. (Jones *et al.*, 1973; Livingston and Chase, 1989), *Alcaligenes eutrophus* (Bhamidimarri, 1985), *Bacillus stearothermophilus* (Buswell, 1975; Gurujeyalakshmi and Oriel, 1989; Yanase *et al.*, 1992), *Nocardia* sp. (Mizobuchi *et al.*, 1980), *Streptomyces setonii* (Antai and Crawford, 1983), the yeasts *Candida tropicalis* (Hackel *et al.*, 1975; Shimizu *et al.*, 1973), *Cryptococcus elinovii* (Mörsen and Rehm, 1987, 1990) and *Trichosporon cutaneum* (Neujahr and Varga, 1970; Yang and Humphrey, 1975), and the fungi *Aureobasidium pullulans* (Takahashi *et al.*, 1981) and *Fusarium flocciferum* (Anselmo *et al.*, 1985, 1989, 1992). The capability of algae to degrade phenol has also been reported (Ellis, 1977; Klekner and Kosaric, 1992).

Many researchers employ mixed cultures for biodegradation of phenol. These are often obtained from municipal sewage treatment plants (Beltrame *et al.*, 1980, 1984; D'Adamo *et al.*, 1984; Pawlowsky and Howell, 1973; Rozich *et al.*, 1983a,b, 1985; Szetela and Winnicki, 1981) or from coal conversion effluent (Fan *et al.*, 1990; Holladay *et al.*, 1978; Tang *et al.*, 1987a,b; Wisecarver and Fan, 1989) or isolated from soil (Koch *et al.*, 1991). A commercially available mixed culture for phenol degradation; Phenobac (Worne Biochemical Co., Berlin, N.J., U.S.A.), has also been used (Bhamidimarri, 1985; Bhamidimarri et al., 1987, 1992; Holladay *et al.*, 1978).

2.1.2 Metabolic Pathways

Two different metabolic pathways are responsible for the microbial oxidation of phenol; the *meta*-cleavage pathway or 2,3-oxygenase pathway (Feist and Hegemann, 1969) and the *ortho*-cleavage pathway or β-ketoadipate pathway (Stanier and Ornston, 1973). These pathways are shown in Figure 2.1 and 2.2, respectively. In general, *Pseudomonas* species degrade phenol via the *meta*-cleavage pathway (Bayly and Dagley, 1969; Feist and Hegemann, 1969), whereas yeasts metabolize the aromatic ring by using the *ortho*-cleavage pathway (Mörsen and Rehm, 1990; Neujahr and Varga, 1970).

2.1.3 Kinetic Models

Considerable work has been undertaken to delineate kinetic models depicting the microbial growth on phenol. The toxic nature of phenol results in inhibition of growth at higher phenol concentrations. Thus the relationship between the specific growth rate, μ, and the phenol concentration, S, is best described by a

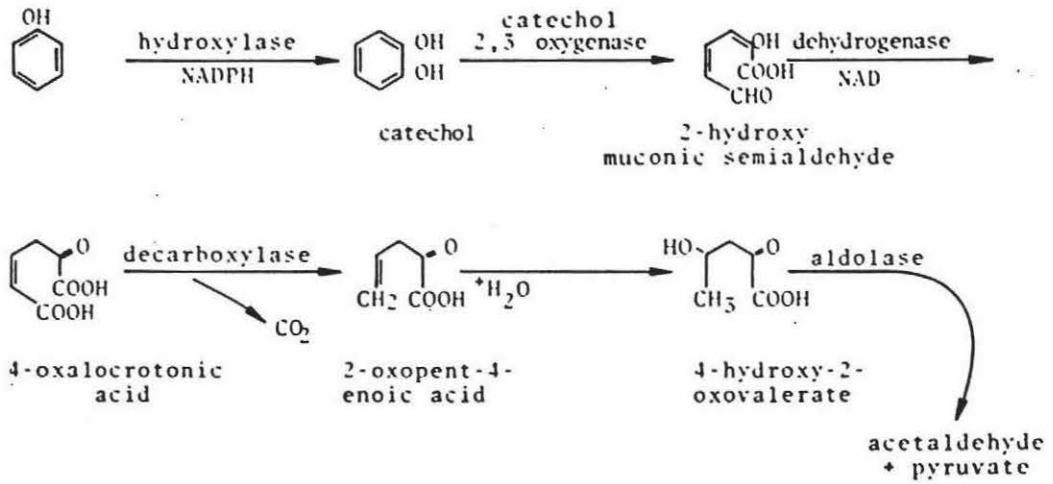

Figure 2.1 *Meta*-cleavage pathway of phenol degradation (Yang and Humphrey, 1975)

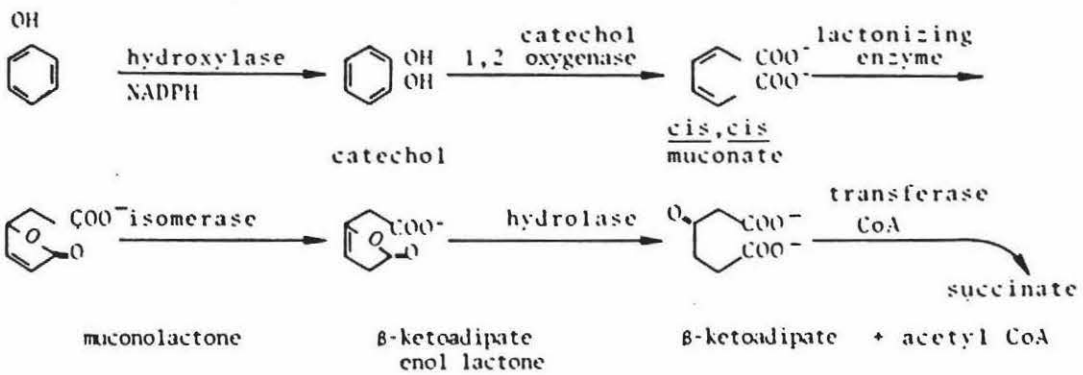

Figure 2.2 *Ortho*-cleavage pathway of phenol degradation (Yang and Humphrey, 1975)

substrate inhibition model. However, some researchers have found a hyperbolic, non-inhibitory relationship, e.g. the Monod function, satisfactory for modelling the degradation of phenol by acclimated populations (Beltrame *et al.*, 1980; Kim *et al.*, 1981). The typical shapes of non-inhibitory and inhibitory kinetic models are shown in Figure 2.3. The plot for non-inhibitory models is represented by the Monod function,

$$\mu = \mu_m S / (K_s + S),$$

the plot for inhibitory models by the Haldane function,

$$\mu = \mu_m S / [(K_s + S) (1 + S/K_i)],$$

where μ_m is the maximum specific growth rate in the absence of inhibition; S is the substrate concentration; K_s is the saturation constant, the lowest substrate concentration at which, in the absence of inhibition, the specific growth rate is half the maximum specific growth rate, μ_m; and K_i is the inhibition constant, which numerically equals the highest substrate concentration at which the specific growth rate is equal to one half the maximum specific growth rate, μ_m.

Substrate inhibition can be caused by different mechanisms. Some actions that can cause a reduction in the metabolic activities of cells are summarized in Table 2.1. For phenol, the injury of membrane functions has been regarded as the mechanism of action (Davidson and Branen, 1981; Heipieper *et al.*, 1991; Keweloh *et al.*, 1990). However, Allsop *et al.* (1993) concluded from their investigations that the most probable site of inhibitory action is at the level of phenol permease or phenol hydroxylase.

Several different substrate inhibition models have been proposed in the literature. Edwards (1970) tested the goodness of fit of five kinetic models (Models 1-5 in Table 2.2). Subsequently, these models have been used by other

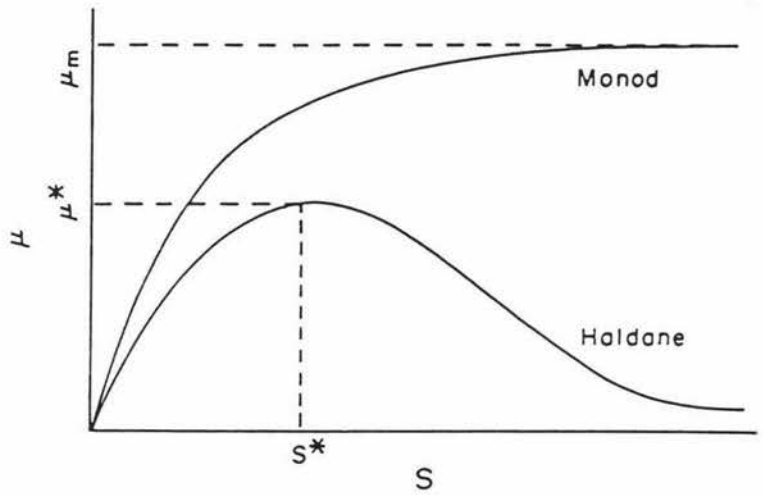

Figure 2.3 Non-inhibitory (Monod) and inhibitory (Haldane) kinetic models (Rozich *et al.*, 1985)

Table 2.1 Possible types of inhibitor action (adapted from Edwards, 1970)

1. Modify chemical potential of substrates, intermediates, or products.
2. Alter cell permeability.
3. Change activity of one or more enzymes.
4. Dissociation of one or more enzyme or metabolic aggregates.
5. Affect enzyme synthesis by interaction with genome or transcription process.
6. Influence functional activity of the cell.
7. Modification of physicochemical variables of the external solution.

Table 2.2 Kinetic models for substrate inhibition

Model No.	Commonly Used Name	Equation	Reference
1a	Haldane	$\mu = \dfrac{\mu_m S}{(K_s + S)(1 + S/K_i)}$	Edwards (1970)
1b	Haldane	$\mu = \dfrac{\mu_m S}{K_s + S + S^2/K_i}$	Pawlowsky and Howell (1973)
2	Webb	$\mu = \dfrac{\mu_m S (1 + S/K)}{K_s + S + S^2/K_i}$	Edwards (1970)
3	Yano	$\mu = \dfrac{\mu_m S}{K_s + S + (S^2/K_i)(1 + S/K)}$	Edwards (1970)
4	Aiba-Edwards	$\mu = \dfrac{\mu_m S \exp(-S/K_i)}{K_s + S}$	Edwards (1970)
5	Teissier-Edwards	$\mu = \mu_m [\exp(-S/K_i) - \exp(-S/K_s)]$	Edwards (1970)
6	Two-parameter Haldane-type	$\mu = \dfrac{k_1 S}{k_2 + S^2}$ where $k_1 = \mu_m K_i$, $k_2 = K_s K_i$	Sokol and Howell (1981)
7	Wayman-Tseng	$\mu = \dfrac{\mu_m S}{K_s + S}$ when $S < S^*$ $\mu = \dfrac{\mu_m S}{K_s + S} - i (S - S^*)$ when $S > S^*$ where i = an inhibition constant	Wayman and Tseng (1976)
8	Luong	$\mu = \dfrac{\mu_m S}{K_s + S} (1 - S/S_m)^n$ where S_m = total inhibition concentration	Luong (1987)
9	Han-Levenspiel	$\mu = \dfrac{\mu_m S}{S + K_s (1 - S/S_m)^m} (1 - S/S_m)^n$ where S_m = total inhibition concentration	Han and Levenspiel (1988)
10		$\mu = \dfrac{\mu_m S}{K_s + S} (1 - i S)$ where i = an inhibition constant	Van Ede *et al.* (1993)

researchers to fit their phenol inhibition data (D'Adamo *et al.*, 1984; Pawlowsky and Howell, 1973; Rozich *et al.*, 1985; Yang and Humphrey, 1975). Equation 1a and 1b are both referred to as the Haldane model in the literature. Equation 1a becomes Equation 1b for $K_s \ll K_i$, which is generally the case. However, Model 1a describes the case of noncompetitive substrate inhibition, whereas Model 1b describes competitive inhibition by the substrate itself (Hill and Robinson, 1975). Models 2 and 3 are also borrowed from enzyme kinetics, whereas Model 4 is an empirical model and Model 5 is derived from the assumption of diffusion-controlled substrate supply.

All investigations came to the conclusion that all five models are suitable for describing substrate inhibition data and that it is not possible to eliminate any of the models as less suitable than the others. However, in some cases (Edwards 1970) the four-parameter models (No. 2 and 3 in Table 2.2) gave a slightly inferior fit than the three-parameter models (No. 1, 4 and 5 in Table 2.2). More important, a higher number of fittable parameters increases the difficulty of the task of fitting a function to a given data set. Thus, the three-parameter models are advantageous. However, Equation 4 and 5 contain the substrate concentration as an exponent. This results in a rather unwieldy equation for the substrate concentration when these models are inserted into biological reactor mass balance equations. Hence, it has been concluded that the Haldane equation, Model 1, is the best choice out of the five models for fitting substrate inhibition data. Consequently, many researchers have used the Haldane function to fit phenol inhibition data (Colvin and Rozich, 1986; Hill and Robinson, 1975; Jones *et al.*, 1973; Livingston and Chase, 1989; Mizobuchi *et al.*, 1980; Molin and Nilsson, 1985; Ong and Bowers, 1990; Rozich *et al.*, 1983a,b; Szetela and Winnicki, 1981; Tang *et al.*, 1987a,b).

Sokol and Howell (1981) proposed a two-parameter simplification of the

Haldane equation (Model 6 in Table 2.2) which fitted their phenol inhibition data significantly better than the three-parameter Haldane equation.

All these models fail to predict the substrate concentration above which growth will cease, but imply that the cells are capable of growing indefinitely. Yet, most observations prove that the latter is not the case. Wayman and Tseng (1976) proposed and tested a model that predicts the total inhibition substrate concentration (Model 6 in Table 2.2). The major drawback of this model is its discontinuity. Further, literature data indicate that the relationship between μ and S above the threshold substrate concentration S^* (the concentration below which the organisms grow apparently without inhibition and the Monod equation is obeyed) is not always linear, as assumed by the model.

Luong (1987) proposed a continuous substrate inhibition model which is capable of predicting the maximum substrate concentration above which growth is completely inhibited (Model 8 in Table 2.2). For inhibitory substrate concentrations, when $n = 1$ the function is linear, when $n > 1$ a rapid initial drop in growth rate is followed by a slow decrease to zero (concavity upward), and when $n < 1$ a slow initial decrease in growth rate is followed by a rapid decrease to zero (concavity downward).

Han and Levenspiel (1988) proposed a generalized form of the Monod expression which accounts for all kinds of substrate, product and cell inhibition and, like the previous two models, assumes that there exists a critical inhibitor concentration above which cells cannot grow. For substrate inhibition it takes the form given in Model 9, Table 2.2, which is similar to that suggested by Luong (1987).

Van Ede *et al.* (1993) assumed linear substrate inhibition kinetics (in spite of

the above mentioned contradicting observations) and thus developed the model given as Model 10 in Table 2.2. It is identical to the linear case of the Luong model (n = 1).

All these models that are capable of predicting the critical substrate concentration above which growth will cease, fitted the inhibition data presented in the publications well, but, apart from Model 10, they were not tested on phenol inhibition data. Since the Haldane equation has the advantage of simplicity and since it has been found satisfactory to describe substrate inhibition by phenol, its use is preferable as long as the kinetic behaviour at very high substrate concentrations and the value of the total inhibition concentration is not of importance.

However, notwithstanding the advantages and the popularity of the Haldane model, when applied to continuous reactors, discrepancies between the model predictions and the experimental data have been observed (Allsop *et al.*, 1993; Rozich *et al.*, 1983a,b, 1985).

2.1.4 Kinetic Parameters and Behaviour

In order to determine kinetic parameters, data on the growth rate at various substrate concentrations are needed. These data are commonly obtained in batch experiments, since this is the most simple approach. Further, some workers regard batch experiments as the most reliable means of obtaining kinetic growth data, although there are others who disagree (Pawlowsky and Howell, 1973).

The most frequently used means of fitting kinetic models to experimental data is the nonlinear least squares fit (D'Adamo *et al.*, 1984; Edwards, 1970; Hill

and Robinson, 1975; Livingston and Chase, 1989; Pawlowsky and Howell, 1973; Rozich *et al.*, 1983a,b, 1985; Sokol and Howell, 1981; Sokol, 1987; Tang *et al.*, 1987a,b). Other methods that have been used are linearization of the growth rate model (Anselmo *et al.*, 1989; Hill and Robinson, 1975; Jones *et al.*, 1973; Mizobuchi *et al.*, 1980) and transformation of the kinetic equation into a quadratic polynomial (Szetela and Winnicki, 1981). For comparison of the goodness of fit of different functions to a set of data, the F-test for equality of variances (Edwards, 1970) is commonly used.

Another parameter of interest is the yield coefficient, $Y_{x/s}$, which corresponds to the slope of the straight line obtained by plotting biomass produced versus substrate removed. Because of the high carbon to oxygen ratio in phenol, relatively high growth rates are the rule (Yang and Humphrey, 1975).

A summary of kinetic parameters for phenol degradation obtained by various researchers is given in Table 2.3. In all cases, phenol was the sole carbon source. The values of D'Adamo *et al.* (1984) give the range of values obtained in six separate growth studies conducted under unchanged conditions. D'Adamo *et al.* suggested that normal changes in predominating microbial species of the mixed culture were the reason for the high variation. Overall, the presented data exhibit large discrepancies, with the kinetic constants varying greatly.

The concentration of phenol at which inhibition occurs also differs widely. For continuous culture, for example, Beltrame *et al.* (1980) reported that at concentrations below 300 mg/l in the bulk liquid no inhibition was evidenced, while Jones *et al.* (1973) observed inhibition even at concentrations below 10 mg/l. Apart from the fact that different cultures were used, these differences can also be attributed to the fact that the inhibition effect does not only depend on the prevailing phenol concentration but also on the history of the culture,

Table 2.3 Kinetic parameters for substrate inhibition of phenol

Culture	Kinetic Model	μ_m (h^{-1})	K_s (mg/l)	K_i (mg/l)	K (mg/l)	$Y_{x/s}$ (g/g)	Culture System	Temp. (°C)	pH	Reference
Acineobacter sp.	Haldane	0.29	< 1	110		0.59	continuous	20	6.8	Jones *et al.* (1973)
Nocardia sp.	Haldane	0.29	< 1	730		0.88	batch	30		Mizobuchi *et al.* (1980)
Pseudomonas sp.	Haldane	0.369	5.94	227			continuous	28	6.8	Chi and Howell (1976)
Pseudomonas putida	Haldane Aiba-Edwards	0.534 0.481	< 1 < 1	470 840		0.52	batch	30	6.7	Hill and Robinson (1975)
Pseudomonas putida *Trichosporon cutaneum*	Haldane Aiba-Edwards Haldane Aiba-Edwards	0.567 0.504 0.464 0.443	2.386 1.876 1.66 1.47	106 218 380 624		0.85	batch	30 30	6.0 4.5	Yang and Humphrey (1975)
Mixed culture	Monod	0.17	245			0.45	continuous	20	7.2	Beltrame *et al.* (1980)
Mixed culture	Aiba-Edwards	0.401	21.76	312.1		0.92	batch	30	6.7	Bhamidimarri (1985)
Mixed culture	Haldane Webb Yano Aiba-Edwards Teissier-Edwards	0.131 - 0.363 0.124 - 0.461 0.124 - 0.340 0.134 - 0.353 0.134 - 0.237	5 - 266 10 - 197 16 - 281 16 - 247 24 - 272	142 - 1199 45 - 638 165 - 1434 281 - 1315 315 - 1443	 225 - 2.6×10^5 726 - 4.8×10^{11}		batch	26	6.8 - 7.0	D'Adamo *et al.* (1984)

continued...

Table 2.3 *...continued*

Culture	Kinetic Model	μ_m (h^{-1})	K_s (mg/l)	K_i (mg/l)	K (mg/l)	$Y_{x/s}$ (g/g)	Culture System	Temp. (°C)	pH	Reference
Mixed culture	Haldane	0.418	2.9	370.0			batch	30	6.7 - 6.9	Livingston and Chase (1989)
Mixed culture,							batch	28	6.6	Pawlowsky and Howell (1973)
nonfilamentous	Haldane	0.260	25.4	173.0		0.545				
	Webb	1.01	160.0	14.7	371.0					
	Yano	0.251	23.7	190.5	10756.0					
	Aiba-Edwards	0.185	10.7	546.3						
	Teissier-Edwards	0.164	16.85	611.6						
filamentous	Haldane	0.223	5.86	934.5		0.616				
	Webb	0.660	86.70	34.2	225.0					
	Yano	0.220	5.20	1020.0	15220.0					
	Aiba-Edwards	0.205	2.00	1564.0						
	Teissier-Edwards	0.205	16.07	1550.0						
Mixed culture	Haldane	0.19	35	135			batch and continuous	25		Rozich *et al.* (1983b)
Mixed culture	Haldane	0.326	19.2	229.3			batch	20	6.8	Szetela and Winnicki (1981)
Mixed culture	Haldane	0.365	10.95	113.00		0.496	batch	23	8.5	Tang *et al.* (1987a,b)

especially on the phenol concentrations the microorganisms have been exposed to in the past (Chi and Howell, 1976; Sokol and Howell, 1981; Sokol, 1988).

The observations reported in the literature regarding the lag phase in batch culture studies are markedly different, too. Pawlowsky and Howell (1973), for example, state that the lag phase in their batch experiments was usually short. In some cases, however, high initial phenol concentrations resulted in a somewhat longer lag phase. In the experiments conducted by Szetela and Winnicki (1981), the duration of the lag phase was relatively short in all cases, even at high substrate concentrations. Conversely, Hill and Robinson (1975) commonly observed lag times in the order of 10 h, increasing to 7 d for phenol concentrations of about 700 mg/l, even though phenol acclimatized inoculum was used. However, the length of the lag phase does not affect the specific growth rate (Pawlowsky and Howell, 1973).

2.2 Immobilized Microorganisms in Aerobic Phenol Degradation

2.2.1 Immobilized Cell Systems

2.2.1.1 Overview

The study of immobilized cells and their application is one of the most rapidly growing topics in biotechnology with a very large volume of literature having been published in this area. Immobilization of cells, compared with freely suspended cell systems, involves a number of features which are summarized in Table 2.4. An overview of different methods for cell immobilization, their properties and applications can for example be found in Bucke (1986), in Karel *et al.* (1985), in Klein and Vorlop (1985), in Klein (1988), in Phillips and Poon

Table 2.4 Features of immobilized cell systems (Atkinson and Mavituna, 1991b)

- ♦ Facilitates cell separation
- ♦ Leads to high cell concentrations within the reactor
- ♦ Leads to internal gradients of physicochemical conditions within microbial aggregates, for example substrate and product concentrations, oxygen and pH
- ♦ Leads to the possibilities for gaseous product evolution in the centre of microbial aggregates
- ♦ Leads to heterogeneous and possible syntrophic, though ordered, populations of organisms within microbial aggregates
- ♦ Affects overall rates of growth
- ♦ Affects overall stoichiometry
- ♦ Allows continuous fermenters to be operated beyond the nominal washout flow rate
- ♦ Allows batch fermenters to be operated on a drain and fill basis
- ♦ May protect against contamination
- ♦ Permits manipulation of growth rate in continuous systems, independent of dilution rate
- ♦ Permits the manipulation of the cells as a discrete phase
- ♦ Allows possibilities for the use of optimum aggregate sizes leading to maximum microbial activities
- ♦ Provides possibilities for the co-immobilization of different cell populations within the same bioreactor
- ♦ May affect morphology, physiology and metabolism of cells

(1988) and in Scott (1987). For the degradation of phenol by immobilized microorganisms, besides entrapment in polymeric networks, adsorption onto carrier matrices has mainly been used as the form of immobilization.

2.2.1.2 Biofilms

Cells and their associated extracellular by-products attached to a solid surface are collectively known as biofilm. Biofilms form as a consequence of the natural tendency of microorganisms to adsorb to surfaces and accumulate in films. They represent an inexpensive, but effective form of immobilization. An abundant amount of research has been undertaken on the formation and properties of biofilms.

A number of physical, chemical and biological processes govern biofilm formation at a surface/liquid interface, including cell-particulate transport to the substratum, adhesion, cellular growth and replication, extracellular polymer production, shear removal, and sloughing (Applegate and Bryers, 1991). The rate of initial biofilm formation depends to a large degree on the microorganisms, and on the roughness and physicochemical properties of the carrier surface. Factors affecting the biofilm development are summarized in Table 2.5. An overview over the processes governing initial adhesion is given in Bhamidimarri (1990) and in Rouxhet and Mozes (1990).

Physical, chemical and biological properties of the biofilm are dependent on the microorganisms forming the biofilm and on the surrounding environment. The most important properties of biofilms are their thickness and density, which determine the extent of diffusional limitations within the biofilm and the substrate conversion rate. Further, they influence to a large degree their

Table 2.5 Factors affecting biofilm development (modified from Senthilnathan and Ganczarczyk, 1990a)

- **Character of the solid surface**
  - Type of solid
  - Surface chemistry
  - Concentration
  - Size and shape
  - Surface area
  - Roughness and porosity
- **Character of microorganisms**
  - Species
  - Surface chemistry
  - Concentration
  - Culture age and conditions
  - Size and shape
- **Character of the environment**
  - Hydrogen ion concentration, pH
  - Ionic strength
  - Substrate loading
  - Hydrodynamics
  - Presence of competing species
  - Presence of mediating species
  - Time of contact
  - Temperature

mechanical strength. The biochemical composition of the biofilm is also of importance, i.e. the amount and character of extracellular substances in the biofilm. A problem encountered when modelling biofilms is the fact that biofilm properties change as the biofilm develops causing spatial variations in the microbial population and in the physical and chemical characteristics within the biofilm. Properties of biofilms are summarized in Shieh and Keenan (1986).

Biofilms have been modelled extensively. An overview over some models is given by Wanner and Gujer (1986). Some of the more recent models are those by Annachhatre and Khanna (1987), Kim and Suidan (1989), Muslu (1992), Rittmann and Manem (1992), Sáez and Rittmann (1988), and Skowlund (1990). A model for biofilm on activated carbon, incorporating adsorption of a substrate, has been proposed by Chang and Rittmann (1987). Biofilms for utilization of inhibitory substrate have been modelled by Gantzer (1989) and van Ede *et al.* (1993).

2.2.2 Effect of Immobilization on Phenol Tolerance

Many researchers have reported that phenol tolerance is improved and phenol uptake is increased if a culture system contains immobilized microorganisms compared to a system solely containing freely suspended microorganisms (Anselmo and Novais, 1992; Molin and Nilsson, 1985; Pawlowski and Howell, 1973).

Rehm and co-workers investigated in detail the difference in the response of free and immobilized cells to the inhibitory action of phenol. Bettmann and Rehm (1984) entrapped *Pseudomonas* sp. in alginate and polyacrylamide-hydrazide. The immobilized culture showed better degradation rates than the

free cells. Moreover, the immobilized bacteria could be exposed to higher phenol concentrations without loss of cell viability (e.g. cells immobilized in polyacrylamide-hydrazide tolerated concentrations up to 3 g/l phenol, whereas free cells degraded phenol only up to a concentration of 1.5 g/l). The authors concluded that diffusional limitations protect the culture against the toxicity of phenol.

Based on the investigations of Bettmann and Rehm (1984), Keweloh *et al.* (1989) examined the phenol tolerance of free and immobilized cells of *Pseudomonas putida*, *Escherichia coli* and *Staphylococcus aureus*, the latter two cultures lacking the potential for phenol degradation. The microorganisms were immobilized in calcium alginate beads. A medium with glucose as carbon source was used for all three species, thus preventing a change in phenol concentration by degradation in the case of *Pseudomonas putida*. It was found that, independent of culture conditions, growth rates and the ability to degrade phenol, immobilized cells tolerated higher phenol concentrations than free cells in all cases. The size of the microcolonies in the gel matrix determined the extent of phenol tolerance. Dissolution of the gel particles resulted in the liberated bacteria responding with similar sensitivity to phenol as cells grown in the free state. It was assumed that physiological alterations of cells that are part of a colony protect the microorganisms against the toxic action of phenol.

Subsequently, Keweloh *et al.* (1990) reported on membrane changes in free and immobilized *Escherichia coli* induced by phenol. They found that phenol at sublethal concentrations induces an increase in protein-to-lipid ratios of membranes. The increase in the protein proportion is an adaptive reaction which slows down the increase in membrane permeability caused by phenol. The experiments also showed that immobilization causes an increase of the protein-to-lipid ratio of the outer membrane by changing the microenvironment of the

cells. Thus, an explanation for the increased resistance of immobilized bacteria to phenol was offered.

In addition to this, Heipieper *et al.* (1991) proposed that an increase in membrane permeability is less critical for immobilized cells than for free cells because the lost cellular material is not instantaneously diluted. Therefore, the efflux is smaller and slower, and a re-uptake can be carried out easily and quickly. Thus, from the investigations of Rehm and co-workers it can be concluded that the protection of immobilized cells from the toxicity of phenol is not only due to phenol concentration gradients in the bioaggregates caused by diffusional limitations.

2.2.3 Effect of Immobilization Material on Phenol Tolerance

Anselmo *et al.* (1985) studied the degradation of phenol by *Fusarium flocciferum* immobilized by entrapment in agar, K-carrageenan, alginate and polyurethane, and by adsorption on preformed polyurethane foams. They found that the initial rate of phenol uptake was much faster in the agar, carrageenan and alginate entrapped systems than in the systems using polyurethane. This was explained by the higher capacity of the former matrices to adsorb phenol. Thus, the phenol adsorption which takes place in the first minutes of contact, masks the actual initial rate of phenol oxidation. The reaction to increasing phenol concentrations was studied only with polyurethane beads and foams. Cells entrapped in polyurethane could be exposed to higher phenol concentrations without losing their catalytic activity (i.e. up to 4 g/l) than cells adsorbed on the foams (i.e. up to 2.5 g/l). Free cells showed complete inhibition at 1.3 g/l of phenol.

Anselmo *et al.* (1989) found that with cells of *Fusarium flocciferum* inserted in porous celite beads total inhibition occurred at 2.5 g/l. Celite does not have the ability to adsorb phenol as polyurethane does. However, the rates of consumption the authors obtained with cells immobilized in celite were much higher than those obtained with polyurethane beads. This was attributed to physical differences between the two types of support, e.g. pore and particle sizes.

Worden and Donaldson (1987) reported that biofilms for aerobic phenol degradation form more rapidly and are more stable on anthracite coal particles than on glass or polystyrene beads.

2.2.4 Activated Carbon as Carrier Matrix

Activated carbon is inexpensive and easily available. It has a large adsorptive surface which is advantageous for the immobilization of microorganisms. The specific surface area of activated carbon varies from 500 m^2/g to over 2000 m^2/g, depending on the starting material and the activation conditions (Diamadopoulos *et al.*, 1992). However, the diameter of the outer pores of activated carbon particles is relatively small. Therefore, cells mainly attach to the external surface of the particles and to the inside of a few big macropores, thus forming a biofilm around the particle (Ehrhardt and Rehm, 1985).

Further, activated carbon has a high adsorption capacity for phenol which results in a buffer effect against the toxicity of phenol. Ehrhardt and Rehm (1985) and Mol *et al.* (1992) found that the activated carbon they used as carrier matrix adsorbed phenol to about half of its own weight. However, Diamadopoulos *et al.* (1992) reported that the phenol adsorption capacity of activated carbon is

variable. It is mainly affected by the carbon surface area and by the ash content of the activated carbon. The quantity of phenol adsorbed increases with increasing surface area and decreasing ash content.

Ehrhardt and Rehm (1985) investigated the phenol degradation of microorganisms attached to activated carbon particles in batch experiments. Pure cultures of *Pseudomonas putida* and *Cryptococcus elinovii* were used. The high adsorptive capacity of activated carbon for phenol makes it difficult to distinguish between phenol adsorption to the activated carbon and phenol degradation by immobilized microorganisms. They found that after its addition, the phenol was rapidly adsorbed onto the activated carbon. At a phenol concentration of 1 g/l immobilized cells delayed the phenol adsorption slightly. The adsorption at higher phenol concentrations was not affected by the immobilization of microorganisms. The immobilized cells remained active in spite of the addition of high phenol concentrations of up to 15 g/l, whereas free cells were completely inhibited at 1.5 g/l phenol concentration. This was attributed to the buffer and depot characteristics of the activated carbon. After the phenol in the medium had been used up, the cells continued to grow, using the phenol previously adsorbed to the activated carbon. However, Mol *et al.* (1992) reported that some of the phenol stays irreversibly adsorbed to the activated carbon.

Mörsen and Rehm (1987) used a mixed culture of *Pseudomonas putida* and *Cryptococcus elinovii*. The immobilized mixed culture was able to degrade phenol up to a concentration of 17 g/l. The degradation was faster than it was using the pure cultures. At all phenol concentrations tested, the microorganisms started growing out into the medium as soon as the phenol concentration had gone down to about 1 g/l. A phenol concentration of 20 g/l was toxic to the microorganisms. Subsequent exposure of the immobilized culture to a low

phenol concentration did not result in regeneration of the biocatalyst. Scanning electron micrographs showed that *Pseudomonas putida* is capable of growing through the pore system of the activated carbon into the inside of the carbon particles. The biocatalyst could be stored for 12 months without decrease in degradation capacity.

Following these batch experiments, Ehrhardt and Rehm (1989) conducted experiments with *Pseudomonas putida* in semicontinuous and continuous culture in a packed bed reactor. The amount of bacteria immobilized on the activated carbon surface depended on the cell concentration used during the immobilization process; the higher the concentration, the more cells were adsorbed. Further, the immobilization capacity of the particles decreased with increasing particle diameter, because the surface to volume ratio of the particles decreased. The microorganisms grew especially in the caverns and in the entrances of the macropores. The cells were partially connected by network-like structures. After six days, the amount of adsorbed cells had increased ten fold. The biofilm hindered phenol adsorption by the activated carbon. This was also observed by Kindzierski *et al.* (1992). Consequently, it was assumed that after some time the phenol is metabolized immediately by the biofilm before it can adsorb to the activated carbon. Phenol degradation rates up to 625 mg/l·h were reached. These high rates could only be maintained for a short period of time, because with time, the fixed-bed became increasingly blocked by biomass. Free cells of *Pseudomonas putida* in a continuous airlift reactor achieved degradation rates up to only 300 mg/l·h.

Mörsen and Rehm (1990) compared the degradation of phenol by microorganisms adsorbed to activated carbon to that by microorganisms adsorbed to sintered glass. They used a mixed culture of *Pseudomonas putida* and *Cryptococcus elinovii*. More bacteria adsorbed to the activated carbon than

to the sintered glass. For the yeast it was vice versa. Higher phenol degradation rates and better phenol tolerance were achieved with the activated carbon system. This was attributed to the fact that sintered glass does not adsorb phenol, whereas activated carbon has a high phenol adsorption capacity. Further, the biomass build-up on the activated carbon particles was considerably higher than on the sintered glass beads.

This is somewhat contrary to the findings of Nishijima *et al.* (1992). They reported that the porous structure of the activated carbon did not lead to an increased population of the particles in comparison to anthracite which was used as reference support material without pores and without adsorbability. Yet, the rate of biodegradation in the completely mixed activated carbon reactors was approximately three times as high as in the reactors with anthracite. It was found that the rate of biodegradation per attached bacteria was higher in the activated carbon system than in the anthracite system. Thus, the conclusion was drawn that activated carbon as bacterial support medium stimulates the biodegradation activity of microorganisms.

2.2.5 Effect of Temperature on Phenol Degradation

Bettmann and Rehm (1984) investigated the influence of temperature on the phenol degradation of *Pseudomonas* sp. immobilized in polyacrylamide-hydrazide. Temperatures between 17°C and 35°C were tested. The optimum temperature was 25°C. The outgrowth of microorganisms increased with rising temperature, being the highest at 35°C.

2.2.6 Effect of Phenol Concentration on Substrate Consumption

Anselmo *et al.* (1985) investigated the effect of different phenol concentrations on the phenol uptake of *Fusarium flocciferum* entrapped in polyurethane and adsorbed on polyurethane foam. Anselmo *et al.* (1989) studied the same relationship for *Fusarium flocciferum* adsorbed in porous celite particles. The investigations were conducted in batch culture. For the systems with cells entrapped in polyurethane and with cells adsorbed to celite particles, they found that the rate of phenol degradation was constant over a wide range of phenol concentrations (i.e. 700 - 1500 mg/l for celite particles and 1500 - 4000 mg/l for polyurethane beads) after it had gone through a maximum. For the celite beads the plateau was followed by a drop in degradation rate, reaching total inhibition at 2500 mg/l phenol concentration. Employing the polyurethane foams only a very short plateau was observed. The occurrence of these plateaux was explained by the protective effect of immobilization. It makes it impossible to fit the data to the Haldane equation, which is commonly used for free cell systems. The oxygen uptake rates of the cells immobilized in celite were very similar for all phenol concentrations used. They were much lower than the ones obtained with free cells.

Phenol degradation in a completely mixed continuous flow reactor using *Fusarium flocciferum* immobilized in polyurethane foam was studied by Anselmo and Novais (1992). The behaviour at different feed substrate concentrations was studied at a hydraulic retention time of 5.1 h. Above 1 g/l inlet phenol concentration the phenol was not removed completely. The outlet phenol concentration increased progressively with increasing inlet concentration. A linear relationship between inlet phenol concentration and volumetric phenol uptake rate (i.e. no inhibitory effect) was observed in the tested range (500 - 1500 mg/l). The investigations proved that a system employing immobilized

cells is more stable and provides a higher degree of treatment than a conventional system using suspended cells.

2.3 Fluidized Bed Bioreactors in Aerobic Phenol Degradation

2.3.1 General Characteristics of Fluidized Bed Bioreactors

In fluidized bed bioreactors a bed of bioparticles is held in suspension by the upward flow of one or more fluids. In the case of biological treatment of liquid media liquid-solid (two-phase) and gas-liquid-solid (three-phase) fluidized beds are employed. The bioparticles are most commonly support particles coated with a biofilm.

Fluidization can only be achieved if the upward velocity of the fluid exceeds the minimum fluidization velocity, i.e. if the pressure drop across the bed is equal to the weight of the bed. Above this velocity, the bed is set in motion and expanded, ultimately leading to elutriation if the force exerted on an individual particle exceeds its weight. The force exerted by the fluid on a particle is related to its size and density by Stokes' law. In liquid fluidized beds the fluidization is normally particulate, i.e. the bed can be considered pseudo-homogeneous. An important requirement for uniformity of the bed is an even distribution of the liquid by the liquid distributor at the bottom of the fluidized bed. The expansion of a liquid fluidized bed is commonly described by the Richardson-Zaki equation. If the particles are of mixed size and/or density, the particles stratify, i.e. larger and/or denser particles collect towards the bottom of the bed, whereas smaller, lighter particles are found towards the top. Engineering fundamentals of fluidized beds are well presented in Kunii and Levenspiel (1991) and Trambouze *et al.* (1988).

Microbial growth on the support particles results in expansion of the bed because it reduces the overall bioparticle density. If natural attrition is not strong enough, elutriation can be prevented by controlled removal of biomass from the particles to balance growth. Further, the development of very thick biofilms is disadvantageous because the effectiveness of the biomass is reduced by diffusional limitations, leading to the biomass close to the support particle becoming inactive. However, diffusional limitations can be of advantage in systems with substrate inhibition, as discussed in Section 2.2. Overall, biofilm thickness is the single most important parameter affecting biomass effectiveness and thus the overall performance of fluidized bed bioreactors, there being an optimum biofilm thickness for every system (Shieh and Keenan, 1986). The density of the biofilm and the size of the support medium are similarly important (Shieh *et al.*, 1982). A summary of fundamentals of biological fluidized beds can be found in Atkinson and Mavituna (1991a), in Cooper and Atkinson (1981), in Cooper (1985), and in Shieh and Keenan (1986).

The most common application of fluidized bed bioreactors is in wastewater treatment. A summary of the history of the employment of fluidized bed bioreactors for wastewater treatment can be found in Cooper (1985). Some process examples are given in Atkinson and Mavituna (1991a), Cooper and Atkinson (1981), Cooper (1985, 1986), Shieh and Keenan (1986), Tanaka *et al.* (1993), and Vembu and Tyagi (1990). Advantages and disadvantages of fluidized bed bioreactors for wastewater treatment are well summarized in Vembu and Tyagi (1990).

The main advantage of biological fluidized bed reactors over other biofilm reactor configurations is the very large surface area per unit volume which is available for growth. This results in a much higher possible biomass hold-up, which in turn leads to a high rate of reaction per unit volume. Therefore, a

higher dilution rate (which is independent of the growth rate of the microorganisms, as it is in all other continuous cultures using immobilized microorganisms) or a smaller reactor volume can be chosen than for other reactor types. Important advantages over packed bed reactors are that clogging is avoided and intimate contact between liquid phase and solid phase is achieved because of the free movement of the bioparticles. Holladay *et al.* (1978) demonstrated that a fluidized bed bioreactor is much more efficient for the biodegradation of phenolic waste liquors than a stirred tank bioreactor or a packed bed bioreactor.

The major drawback of fluidized bed bioreactors is the complexity of the system resulting in highly complex models, consisting of a kinetic model for the biological process, a biofilm model, a fluidization model and a reactor flow model (Characklis *et al.*, 1985), the latter three especially being highly complex in themselves. A lot of work has been published on the modelling of biological fluidized bed reactors (e.g. Bignami *et al.*, 1991; Lin, 1991; Mulcahy *et al.*, 1981; Shieh, 1980; Shieh *et al.*, 1981, 1982;). The models are commonly based on many simplifying assumptions, such as; immobilization does not change the kinetic parameters describing growth rate and substrate consumption, the biofilm is uniform in thickness, composition and reactivity, the various species of a mixed culture can be treated as one single imaginary species, the support particles are spherical in shape and of uniform size. Models for aerobic degradation of phenol in fluidized bed bioreactors have been proposed for example by Bhamidimarri (1985), Bhamidimarri and Greenfield (1990), Livingston and Chase (1989), Tang *et al.* (1987a,b), Wisecarver and Fan (1989), and Worden and Donaldson (1987).

2.3.2 Operating Conditions

Several researchers have investigated fluidized bed bioreactors for aerobic phenol biodegradation. An overview of the work undertaken by various investigators is given in Table 2.6. Some of the workers used fluidized beds fitted with an internal draft-tube to promote internal circulation of the liquid and solid phases (Fan *et al.*, 1987, 1990; Livingston and Chase, 1989; Tang *et al.*, 1987a,b). This configuration proved superior to conventional fluidized bed bioreactors (Fan *et al.*, 1987). The main observations stated in the literature are described below.

2.3.3 Effect of Oxygen Concentration

Lee *et al.* (1979), operating their tapered fluidized bed reactor in two-phase and in three-phase mode, observed that significantly higher phenol conversion rates were found with the use of higher oxygen concentrations and concluded that the phenol degradation rate was oxygen-limited.

Worden and Donaldson (1987) investigated the effect of oxygen concentration on the biofilm reaction rate in a liquid-solid fluidized bed reactor with pre-aeration. The phenol concentration was held at about 75 mg/l. Since the new steady state was achieved typically within an hour, the effect of biofilm growth could be neglected. It was found that oxygen was strongly rate limiting below 20% oxygen saturation, and weakly rate limiting up to 80% saturation. Mass transfer of oxygen from the bulk liquid to the biofilm was regarded the rate limiting step. The results show that if air (21% oxygen) was used as a source of oxygen, the reaction rate would be limited to about half the maximum rate.

Table 2.6 Research conducted on fluidized bed bioreactors for aerobic phenol degradation

Reference	Type of Experiment	Culture and Temp.	Carrier (Size in μm)	Reactor, Type and Volume	Fluid Flow (ml/min)	Gas Flow (ml/min)	Phenol-In (mg/l)	Phenol-Bulk (mg/l)	Oxygen-Bulk (mg/l)	Biofilm Thickness (μm)	Biofilm Density (kg/m^3)
Holladay *et al.* (1978)	steady state	mixed culture, 21°C	anthracite coal (150-180)	tapered 3-phase, 3 l 10 l	13 - 24 190 - 800	3000	580 - 2200 45 - 260	<1 - 700 <1 - 30	1 - 24		
Lee *et al.* (1979)	steady state	*Pseudomonas* sp., mixed culture	anthracite coal (150-180, 420-700)	tapered 3-phase, 10 l	300 - 800		9 - 260	<0.025 - 100			
Bhamidimarri (1985), Bhamidimarri *et al.* (1987, 1990)	conc. profiles with reactor height, diffusivities	mixed culture, 30°C	activated carbon	2-phase, 3-phase, ~0.5 l							
Fan *et al.* (1987)	dynamic (biofilm)	mixed culture, 25°C	activated carbon (300, 710)	3-phase draft-tube, 5.1 l			100	<1	<1		
Tang and Fan (1987a)	steady state	mixed culture, 22-23°C	activated carbon	3-phase draft-tube, 1 l	33.5 38.3 38.3 33.5	1420	38.09 49.17 96.20 72.71	2.69 3.50 6.49 3.54	8.4 8.1 7.1 5.1	12.83 17.76 40.35 48.06	151.06 152.47 78.24 72.16
Tang *et al.* (1987b)	dynamic (phenol steps)	mixed culture, 22-23°C	activated carbon	3-phase draft-tube, 1 l	38.3 33.5 33.5 33.5	1420	100% step 100% step 40% step 200% step	3.50→6.49 2.69→3.54 0.34→0.41 2.09→0.67	8.1→5.1 8.4→7.1 8.5→8.3 8.3→4.8	17.8→ 40.4 12.8→ 48.1 40.2→ 36.8 30.2→159.3	152.5→78.2 151.1→72.2 85.5→86.0 119.1→27.1

continued...

Table 2.6 *...continued*

Reference	Type of Experiment	Culture and Temp.	Carrier (Size in μm)	Reactor, Type and Volume	Fluid Flow (ml/min)	Gas Flow (ml/min)	Phenol-In (mg/l)	Phenol-Bulk (mg/l)	Oxygen-Bulk (mg/l)	Biofilm Thickness (μm)	Biofilm Density (kg/m^3)
Worden and Donaldson (1987)	steady state (oxygen), dynamic (phenol pulses)	mixed culture, 30°C	anthracite coal (250-500)	tapered 2-phase with recycle, 0.14 l	fresh medium: 20 recycle: 140						
Livingston and Chase (1989)	steady state	mixed culture, 30°C	celite (750-1180)	3-phase draft-tube, 1.2 l	54.42 61.38 51.90 55.32 56.28	900	82.7 92.3 131.7 108.5 83.0	2.55 4.05 12.02 5.84 3.79	4.69 4.24 4.54 5.58 6.25	23.1 22.1 24.4 26.2 26.2	141.3 194.5 217.0 222.6 218.5
Wisecarver and Fan (1989)	steady state	mixed culture, 25°C	activated carbon (310)	3-phase, 5.1 l	40	2070 1525	242 256 262 220 245 192 240 256	<1	~2	41.2 59.8 22.8 123.3 31.6 28.5 29.1 88.8	78 81 70 47 74 73 73 73
Fan *et al.* (1990)	phenol adsorption and diffusion	mixed culture	activated carbon (310)	3-phase draft-tube, 5.1 l							
Ro and Neethling (1990, 1991)	terminal settling characteristics	mixed culture	sand (420-590)	reactor with recycle							

Livingston and Chase (1989) investigated the interdependence of dissolved oxygen concentration and phenol concentration. The results show that as the oxygen concentration in the bulk liquid is decreased, the phenol concentration initially stays unaffected. In this region, phenol is the limiting substrate in the biofilm. As the dissolved oxygen concentration is progressively decreased, the rate of reaction becomes oxygen-limited. The critical value of bulk phenol concentration to bulk oxygen concentration, at which the transition from phenol-limited to oxygen-limited biofilm kinetics occurs, was found to be in the range of 0.9-1.1. Thus, a criterion was established for determining whether the degradation rate is oxygen- or phenol-limited.

2.3.4 Effect of Phenol Concentration

Fan *et al.* (1987) observed phenol conversion fractions greater than 99% for volumetric phenol loading rates up to 750 mg/(l·h), using activated carbon particles (d = 300 μm) in a three-phase draft-tube reactor. For phenol loading rates greater than that, the conversion fraction decreased with increasing loadings. Using larger particles (d = 710 μm) and about half initial solids loading, the decrease in conversion fraction started at 170 mg/(l·h) due to a decreased capacity for biomass hold-up.

The model developed by Wisecarver and Fan (1989) for a three-phase bioreactor using activated carbon particles predicts that the rate of biodegradation rises nearly linearly with inlet phenol concentration until a break point is reached at an inlet phenol concentration of around 800 mg/l. Beyond this point the rate decreases with a further increase in inlet phenol concentration, due to substrate inhibition. Experiments to verify these predictions were not conducted.

Tang *et al.* (1987b) studied the transient response of a three-phase draft-tube fluidized bed reactor to different magnitudes of step increase in inlet phenol concentration. The observed response was very fast in all cases. At a 100% step increase in inlet phenol concentration, the height of the transient change and the time required to regain a new steady state increased with increased initial phenol concentration under otherwise almost identical conditions. Stable operation was restored even when the system was subjected to a 200% step increase in inlet phenol concentration. Yet, a drastic transient change was observed. The authors concluded that the high reactor biomass hold-up and the adsorptive capacity of the activated carbon particles employed as carrier, contributed significantly to the fast response and the operating stability.

Worden and Donaldson (1987) investigated the response of a two-phase fluidized bed bioreactor with recycle to pulses of phenol. Anthracite coal particles were used as carrier matrix for a mixed culture. Relatively high oxygen concentrations were employed to avoid oxygen limitation. A small pulse increase (increase of phenol concentration in the reactor from 10 mg/l to 65 mg/l) was followed by an immediate increase in reaction rate. With pH control, as the phenol concentration dropped back to its original value, the reaction rate did so, too. Without pH control, the return to the steady state was oscillatory. Following larger pulses (increase of phenol concentration in the reactor from 15 mg/l to 170 mg/l), the reaction rate initially decreased, suggesting substrate inhibition by phenol, and then recovered as the phenol concentration declined.

2.3.5 Biofilm Properties

Holladay *et al.* (1978) observed in their tapered three-phase reactor that once the mixed culture had achieved an operable concentration, the biomass could double

in a matter of hours. Spheres of up to 6500 µm diameter were formed (diameter of anthracite coal particles: 150-180 µm).

The growth behaviour of the biofilm (mixed culture on activated carbon particles) in a three-phase draft-tube reactor was analyzed by Fan *et al.* (1987). During the first 50 days they obtained thin, uniform and dense biofilm, slowly and steadily increasing to about 50 µm. Then, a drastic expansion of the biofilm was observed. Microscopic examination showed that a bulky, loose, filamentous matrix had grown over the original thin and dense biofilm. As a consequence, the biodegradation rate decreased. The reason for the switch in the predominant microbial species from nonfilamentous to filamentous is unknown. However, at low substrate concentrations as present in this study, the filamentous organisms, once attached to the existing biofilm surface, obviously have the advantage in uptake of phenol. In the same reactor with the draft-tube removed but otherwise identical conditions, the biofilm was thicker and less dense than in the draft-tube reactor before the occurrence of the switch in biofilm consistency. This was due to the reduced shear stress in the conventional reactor configuration.

Tang *et al.* (1987b), investigating the response to step-changes in inlet phenol concentration in a three-phase draft-tube fluidized bed bioreactor using a mixed culture, observed close to the end of one experiment a drastic increase in biofilm thickness, accompanied by a sharp decrease in overall biofilm dry density. Microscopic examination showed that filamentous microorganisms had developed on top of the original dense biofilm. The very low bulk phenol concentration at this stage of the experiment is assumed to favour filamentous microorganisms.

Worden and Donaldson (1987) grew a mixed culture on anthracite particles in a solid-liquid fluidized bed. They observed gradual, spontaneously occurring

variations in several biofilm properties, including appearance, density, and growth rate, without investigating these changes further.

Livingston and Chase (1989) observed that during the initial start-up period of their three-phase draft-tube reactor a bulky, fibrous biofilm with trailing tendrils developed until a biomass loading of 0.154 g/g was reached. At this point the gas flow rate was increased from 660 ml/min to 1200 ml/min for a period of four days. After this period the biomass loading had decreased to 0.04 g/g and the biofilm was smooth. The gas flow was then set to 900 ml/min for the steady state runs. Thus, the nature of the biofilm and its density depend heavily on the conditions of shear in the fluidized bed bioreactor; formation of smooth, dense biofilm is favoured by turbulent conditions.

For biofilm thicknesses below 250 μm, the biofilm dry density is reported to increase with increasing biofilm thickness (Bhamidimarri, 1985; Bhamidimarri *et al.*, 1987). However, Fan *et al.* (1987) observed that the biofilm dry density initially increased and then after reaching a maximum decreased with increasing biofilm thickness. The maximum biofilm dry density occurred at a thickness of about 20 μm.

Tang and Fan (1987a) noticed that the biofilm dry density decreased as the biofilm thickness increased (see Table 2.6). Comparing their results with other work, the authors concluded that variation of biofilm dry density with biofilm thickness strongly depends upon the species of microorganisms forming the biofilms, the substrate loading rates, the reactor configuration, and the operating conditions in which the biofilms are cultivated. For example, the biofilm dry densities obtained in three-phase fluidized bed systems are higher than those obtained in two-phase systems, because in the former systems, the cells have to pack more tightly to resist the higher shear. Tang *et al.* (1987b) also reported

that the biofilm dry density decreases with increasing biofilm thickness. They concluded that this variation implies a non-uniform cell distribution along the radial locus of the bioparticle.

Ro and Neethling (1991) specifically investigated the relationship of biofilm thickness and density of a mixed culture. They found that the biofilm density decreased as the biofilm thickness increased as a function of the relative biofilm thickness (ratio between bioparticle size and support particle size). Their results show that the biofilm dry density decreased rapidly as the biofilm thickness increased to a relatively constant value of approximately 10-20 kg/m^3 for thick biofilms (relative thickness > ~2). However, it must again be emphasized that the characteristics of biofilms depend on all environmental conditions and on the microbial culture used.

Tang and Fan (1987a) and Livingston and Chase (1989) found that as the biofilm density increases, the biofilm substrate diffusivities decrease. This is to be expected as a smaller biofilm dry density implies looser packing and thus larger void fraction within the biofilm (Tang *et al.*, 1987b). Fan *et al.* (1990) investigated the diffusion of phenol through a biofilm on activated carbon particles in more detail. Their results confirm that the phenol diffusivity decreases with increasing biofilm density. Phenol was found not to adsorb to the biofilm. Apart from diffusional limitations within the biofilm, liquid-bioparticle mass transfer resistance contributes markedly to the transport resistance of substrates (Livingston and Chase, 1989; Tang *et al.*, 1987b).

2.4 Quantitative Image Analysis of Bioparticles

2.4.1 Basics of Digital Image Processing

Digital image processing serves the analysis of visual information. The latter is transformed into numerical data with the help of computer systems. Contrary to the manual evaluation procedures used in the past, digital image processing is fast, accurate and objective. Further, it enables complex phenomena to be evaluated, which could not be adequately accessed with conventional measuring techniques.

Image processing consists of several steps. It begins with the capturing of an image with a suitable acquisition system. The image sensed is then transformed into digital information (digitization) which can be treated by the computer. Thus, an array of picture elements, or pixels, is produced. The first actual processing step is image restoration, i.e. correction of known disturbances in the image. This can include, for example, correction of errors in the sensor or in the transmission of image signals, optimization of brightness and contrast of the image, and noise reduction. To analyze the image, adequate filtering procedures must be applied in order to distinguish the objects of interest from other objects and from the background. Then the regions of interest are separated from the background (segmentation), i.e. each individual pixel is checked whether it belongs to an object of interest or not. The result is a binary (black and white) image. Thus, knowing the exact geometrical shape of the object of interest, information such as the mean grey value, the area, perimeter, and other parameters for the form can easily be gained. Further information on digital image processing can be obtained from a multitude of books on the topic. An example is Jähne (1991).

In addition to personal computers and workstations having become powerful enough to process image data, they have also become cheap enough to be widely used. Thus, image processing has been applied amongst other disciplines to virtually all natural sciences. In biotechnology, image analysis has for example been used for measurements on filamentous microorganisms (Adams and Thomas, 1988; Reichl *et al.*, 1990) and for measurements on bioparticles (see below).

2.4.2 Measurement of Bioparticles

Conventionally, bioparticles have been measured with the help of light microscopes equipped with an eye-piece with ocular scale. However, since bioparticles are in general not spherical and biofilms often vary in thickness, it is difficult or even impossible to determine particle size and biofilm thickness, and thus biofilm density, accurately by direct observation.

For determination of particle diameter and biofilm thickness from microscopic measurements, Lu and Ganczarczyk (1983) suggested that each particle should be regarded as an ellipse. The bioparticle long diameter ($d_{b,L}$) and short diameter ($d_{b,s}$), and the carrier long diameter ($d_{c,L}$) and short diameter ($d_{c,s}$) should be measured for each particle. The equivalent volume diameter of a sphere ($d_{equiv.}$) can then be calculated as

$$d_{equiv.} = \sqrt[3]{(d_L \cdot d_s^2)},$$

and the thickness of the biofilm (b) as

$$b = \frac{(d_{b,L} - d_{c,L}) + (d_{b,s} - d_{c,s})}{4}.$$

Ro and Neethling (1990, 1991) used a similar approach for measurement of bioparticle size and shape. They took pictures of the bioparticles with a camera attached to a microscope and then characterized the bioparticle shape as an ellipsoid by selecting the best fit from various ellipsoidal forms differing in size and projection angles. The lengths of the major and minor ellipsoidal axes were recorded to determine the equivalent volume diameters according to the formula given above. Ro and Neethling (1990) also provided formulae for calculation of equivalent projected-area diameter and equivalent surface-area diameter. The authors claimed that their technique allows efficient and accurate size measurement of many irregular bioparticles. However, it is clear that the method is time consuming and can be improved in accuracy.

McFeters (1984) suggested the possibility of employment of computer-enhanced image processing in combination with light microscopy for quantitative measures of biofilm growth. This method was used by Livingston and Chase (1989) for measurement of biofilm thickness on bioparticles. The video input into the image analyzer was directly from a microscope. From the projected area of the bioparticle the diameter of a sphere which would project an equal area was calculated. The same was done for the particle core after the biomass had been burned off in a furnace. The biofilm thickness was calculated as half the difference in diameters between the biomass-laden sample and the biomass-free sample. As discussed later (Section 3.4.4), this approach overestimates the value of the mean biofilm thickness for non-spherical particles.

Senthilnathan *et al.* (1990b, 1991) suggested a more accurate way of calculating the mean biofilm thickness from the data obtained from digital image processing. A simple trapezoid formula was used to determine the mean biofilm thickness (b) from the projected area of the bioparticle, A_b, the projected area of the particle core, A_c, and the perimeters of the biofilm, P_b, and the particle

core, P_c;

$$b = \frac{(A_b - A_c)}{(P_b + P_c) / 2} .$$

This formula provides a much more reliable estimate of the biofilm thickness and can be used for any shape of particle core and bioparticle.

In order to measure the bioparticles, Senthilnathan *et al.* (1990b) embedded them in agar in a petri dish. The particles could be observed through the transparent agar medium. The image of the bioparticle was captured using a camera adapted to a microscope. The circumference of the particle core and of the bioparticle was traced using a light pen. This step clearly reduces the objectivity of the procedure and introduces operator errors. After the object of interest was defined, the longest dimension, breadth, area, and perimeter were determined by the software.

For the purpose of calculating the biomass volume, which is important for the determination of the biofilm density, the projected image of the carrier was approximated by either a circle, an ellipse, or a sector of a circle. Since the biofilm was thin, the shape of the bioparticle did not differ significantly from that of the carrier. The measured perimeter was used to check the goodness of fit of the various shapes. Much better agreement was found for the elliptical and sector shape assumption than for the assumption of a circular cross-sectional area. After a shape had been decided on, the volume of the three-dimensional particles could easily be derived by simple geometric relationships. Thus, the volume of the retained biomass could be calculated as the difference between the volume of the carrier with and without biofilm. Formulae for characteristic dimensions of the assumed geometric forms were provided.

Dudley *et al.* (1993) employed two-dimensional image analysis for counting and sizing (area and equivalent circle diameter) of granules in upflow anaerobic sludge blanket digesters. As with Senthilnathan *et al.* (1990b), the authors embedded bioparticle suspensions in agar in a petri dish. This method was found advantageous because the aqueous nature of the medium prevents shrinkage of the bioparticles, the medium is transparent, and the bioparticles can be largely separated from one another. The samples were analyzed within 12 h of preparation. The image was directly captured by a camera without the use of a microscope. The volume of the granules, needed for the density determination, was calculated assuming spherical shape.

CHAPTER 3

MATERIALS AND METHODS

3.1 Culture and Growth Medium

3.1.1 Culture

The culture used for all the experiments was a mixed culture held in the Department of Process and Environmental Technology, Massey University. It was first developed by Bhamidimarri (1985) for degradation of phenol. After application to various waste treatment problems, it had been freeze dried and mixed with a filler material. It is known to contain strains of *Pseudomonas putida* and *Alcaligenes eutrophus* (Bhamidimarri, 1985).

The culture was activated by inoculating 50 ml of the growth medium (see Section 3.1.2), at a phenol concentration of 100 mg/l, with about a quarter teaspoon of the dried mixture. It was incubated at 30°C in 250 ml shake flasks on a shaker (Gyrotory Shaker, Model G10, New Brunswick Scientific Company, New Brunswick, New Jersey, U.S.A.) at 250 rpm for 24 h. To ensure sufficient oxygen supply the flasks were fitted with lids with holes. After this period the mixture was left for the filler material to settle. Then, 10 ml of the supernatant liquid was transferred into 40 ml of fresh medium and incubated as before. The last step was repeated twice before the culture was regarded as well established.

During the course of the kinetic studies the culture was kept active by transferring it daily into fresh medium, whereas for the fluidized bed studies activation of fresh culture was conducted for each experiment.

3.1.2 Growth Medium

A buffered inorganic salt solution with phenol as the sole carbon source was used as growth medium throughout the study. Its composition is listed in Table 3.1. The pH of the solution was 6.9 and adjustment was not necessary.

Table 3.1 Composition of synthetic growth medium (Bhamidimarri, 1985)

Component	Concentration (mg/l)
Potassium dihydrogen orthophosphate, KH_2PO_4	420
Dipotassium hydrogen orthophosphate, K_2HPO_4	375
Ammonium sulphate, $(NH_4)_2SO_4$	244
Sodium chloride, NaCl	30
Calcium chloride, $CaCl_2 \cdot 2H_2O$	30
Magnesium sulphate, $MgSO_4 \cdot 7H_2O$	30
Iron(II) chloride, $FeCl_2 \cdot 4H_2O$	4.6
Phenol, C_6H_5OH	varying
Distilled or tap water to volume	

When dissolving the components of the medium in water, magnesium sulphate must be added to the solution before calcium chloride to avoid precipitation.

The chemicals used to make up the medium were of analytical grade (obtained from BDH Laboratory Supplies, Poole, Dorset, England, and Rhône-Poulenc Prolabo, Paris, France).

Sterilization of the medium was not necessary because phenol is inhibitory to most microorganisms.

3.2 Batch Culture Kinetic Studies

3.2.1 Experimental Design

Experiments were carried out in 2 l shake flasks with a liquid volume of 500 ml. Cultures were incubated in a 'Lab-Line' Incubator-Shaker (Lab-Line Instruments Inc., Melrose Park, Illinois, U.S.A.) at 30°C and 250 rpm. To minimize any decrease in liquid volume by evaporation the flasks were sealed with tightly packed cotton plugs. For aeration, compressed air was provided through rubber tubings and bubbled directly into the liquid. Control of the pH was not necessary.

3.2.2 Inoculation

An inoculation volume of 10% (v/v) was used. The inoculum was developed by transferring 50 ml of the established culture (see Section 3.1.1) into 450 ml of growth medium with a phenol concentration of 100 mg/l. The mixture was incubated under the conditions described above (Section 3.2.1). After seven hours (approximately the end of the exponential growth phase), this culture was used as inoculum.

To ensure a constant inoculum size for all experiments, the concentration of suspended biomass in the inoculum was determined. It was about 90 mg/l dry weight in all cases.

The growth medium was prepared up by combining the correct quantities of concentrated salt solution, concentrated phenol solution and distilled water so that after addition of the inoculum the mixture had the concentrations given in Table 3.1, assuming that all the nutrients in the inoculum had been consumed. For phenol this was proven by measurement of the phenol concentration at the end of the inoculum development.

3.2.3 Sampling

Sample size was restricted to 6 ml in order to minimize the reduction of the culture volume. The intervals between sampling depended on the rate of growth. During the exponential growth phase of the cultures, i.e. the period of interest for determination of the specific growth rate, samples were taken at intervals of 0.5 h to 1.0 h. Immediately after sampling, phenol concentration and suspended biomass concentration were determined (see Section 3.4).

3.3 Fluidized Bed Studies

3.3.1 Process Description

A flow diagram of the liquid-solid fluidized bed reactor system is given in Figure 3.1 and a photograph of the system can be seen in Figure 3.2.

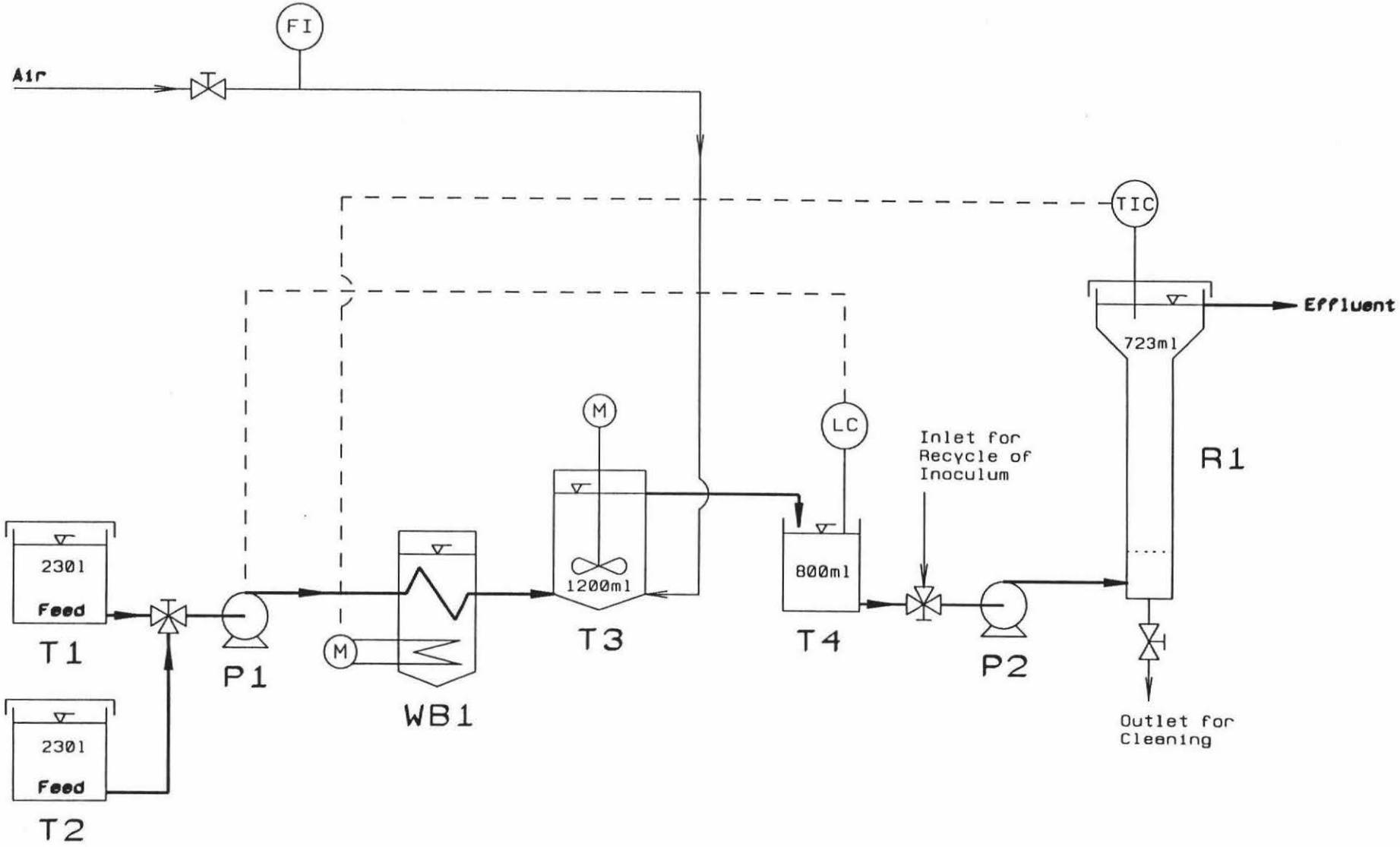

Figure 3.1 Flow diagram of the fluidized bed reactor system (Symbols according to N.Z. Standard 582)
Volumes given are liquid volumes of the vessels

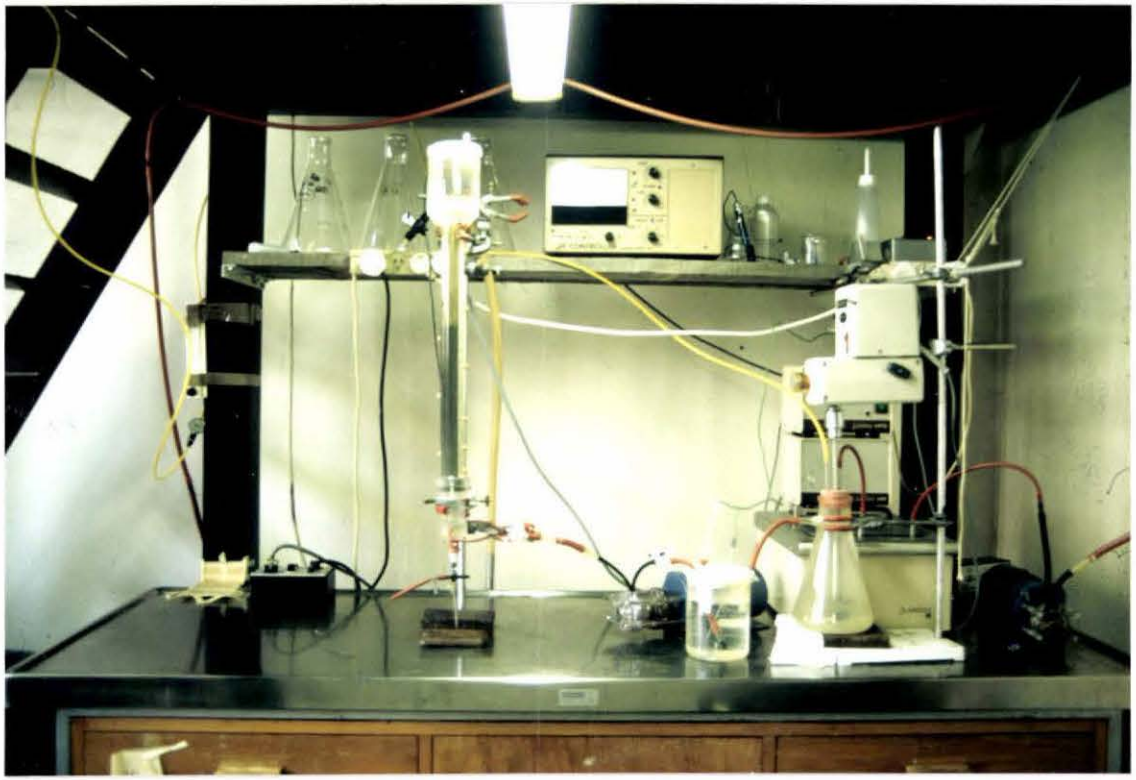

Figure 3.2 Photograph of the experimental apparatus used for fluidized bed experiments

The synthetic growth medium was pumped from the feed tanks T1 and T2 through a coil in the water bath WB1 (Julabo 8, type HTC-HP, Julabo Labortechnik GmbH, Seelbach, Germany) into the well mixed aeration tank T3, where the medium was aerated using compressed air through a porous sintered glass sparger. From here the medium overflowed into the gas-liquid disengagement tank, T4, before being pumped through a liquid distributor into the column reactor, R1. To ensure a constant liquid temperature in the reactor the thermostat of the water bath was connected to a PT 100 temperature transducer in the solid-liquid disengagement Section at the top of the column. Control of the pH was not necessary, but for reassurance the value was checked occasionally. The overflowing effluent from the reactor was disposed of, i.e. recycle was not employed.

The pumps P1 and P2 were Masterflex peristaltic pumps (Cole-Parmer Instrument Co., Chicago, Illinois, U.S.A.). Norprene tubings were used in the pump heads. Pump P1 was operated with a standard pump head series 7015 at a flow rate of 480 ml/min. The pump was periodically switched off by a level controller in the gas-liquid disengagement tank T4. Pump P2 was equipped with a standard pump head series 7016. After the preliminary studies (see Section 5.2) it was set to pump at a flow rate of 245 ml/min for all following experiments. The flow rate was checked daily by measuring the effluent flow. The pulsed flow had a negligible effect on the expansion of the fluidized bed.

3.3.2 Fluidized Bed Reactor

A diagram of the fluidized bed reactor is shown in Figure 3.3. It was made of circular Perspex tubings.

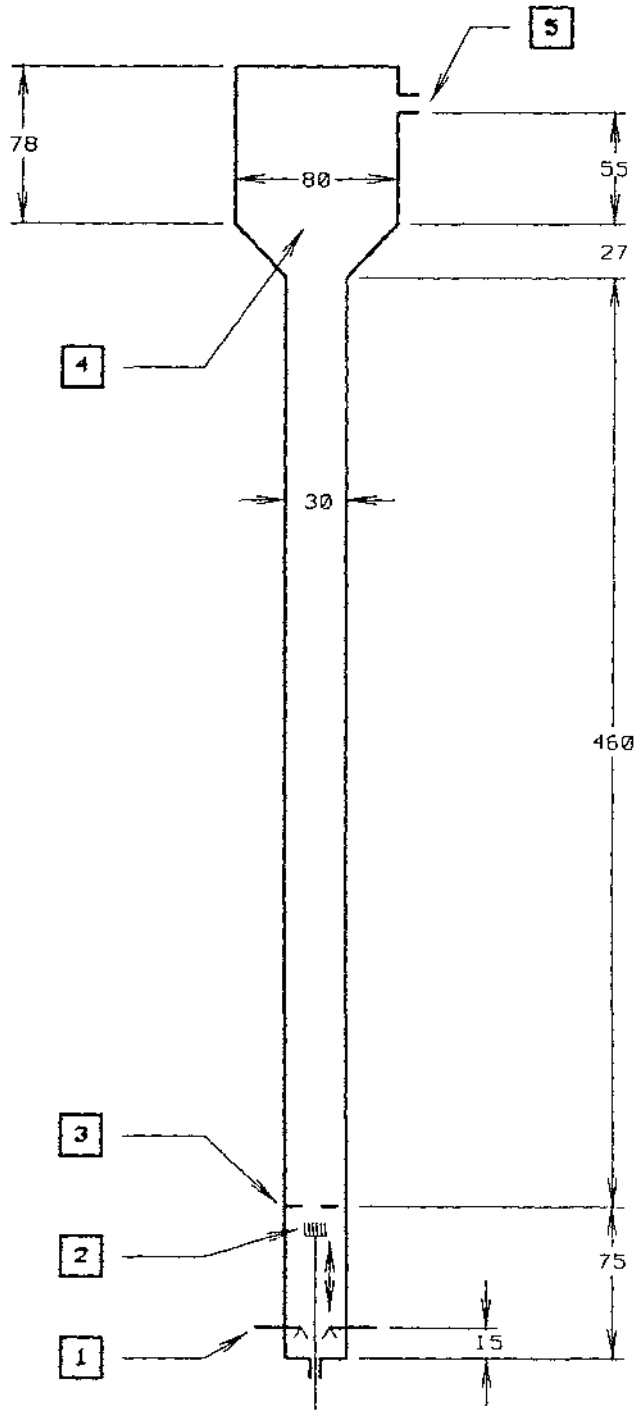

1: Primary liquid distributor
2: Movable stainless steel brush
3: Stainless steel mesh
4: Solid-liquid disengagement zone
5: Effluent overflow

Figure 3.3 Diagram of the fluidized bed reactor (Dimensions in mm)

A stainless steel mesh, mesh size 80/80 (no. of strands per inch both ways) separated the liquid inlet zone from the actual fluidized bed zone of the reactor. It also served as a secondary liquid distributor. To make the mesh easily removable and to facilitate the cleaning of the reactor between experiments, the column was subdivided at the height of the mesh. The mesh was sandwiched tightly between these two sections. An o-ring assured perfect sealing of the intersection.

A stainless steel brush was installed in the liquid inlet zone for periodical cleaning of the mesh. It could be moved to the very bottom of the column when not in use. Air bubbles, which coalesced underneath the sieve at the beginning of all experiments, were removed using a syringe inserted through a septum positioned immediately beneath the mesh.

A diagram of the primary liquid distributor can be seen in Figure 3.4. The holes were in the underside of the tubings.

The reactor had a total liquid volume of 723 ml. The working volume of the fluidized bed itself, when expanded to the bottom of the solid-liquid disengagement section was 325 ml. Thus, operating at a flow rate of 245 ml/min, the hydraulic retention times in the whole of the reactor and in the fully expanded bed were 2.95 min and 1.33 min, respectively. The superficial liquid upflow velocity in the fluidized bed zone was 34.65 cm/min.

3.3.3 Immobilization Medium

Activated carbon was used as immobilization medium. The activated carbon available (Calgon Granular Activated Carbon, Calgon Carbon Co., Pittsburgh,

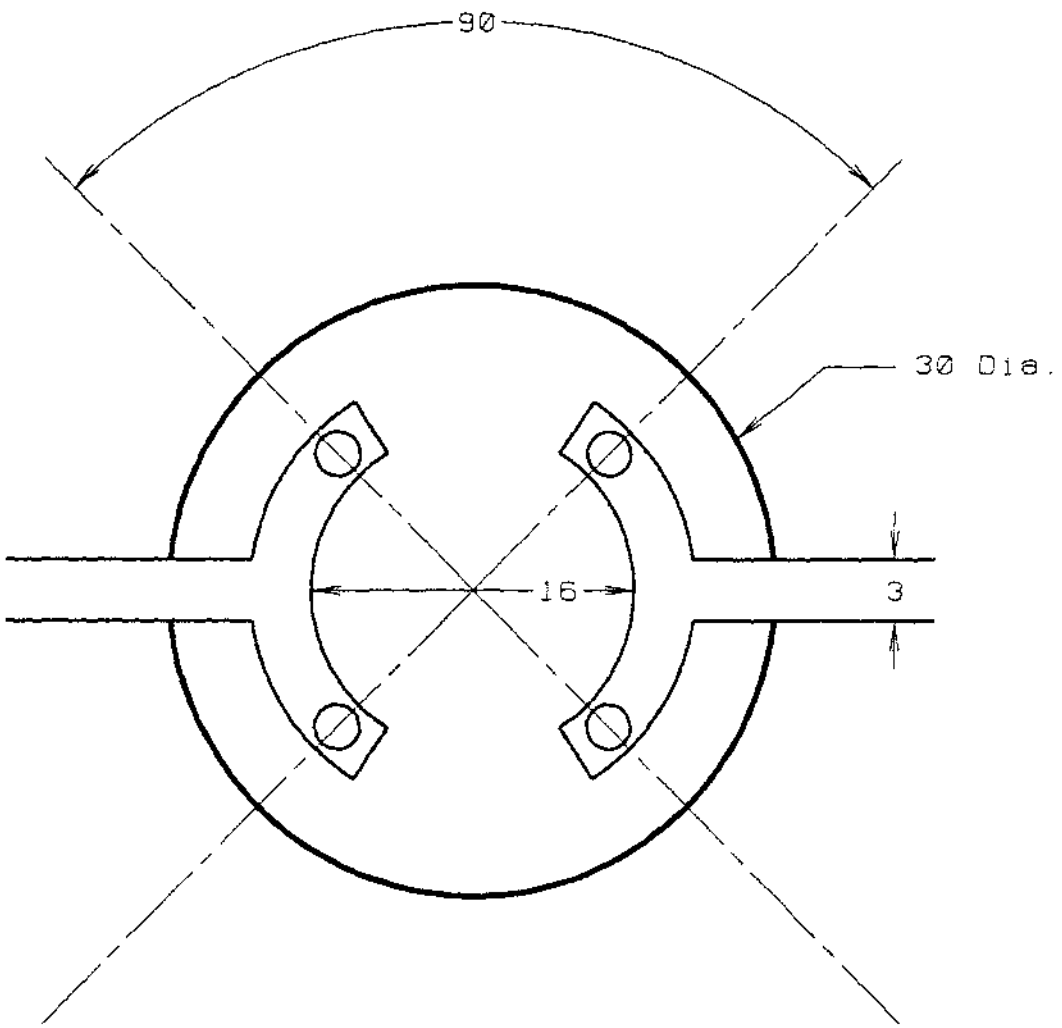

Figure 3.4 Diagram of the primary liquid distributor (Dimensions in mm)

Pennsylvania, U.S.A.) consisted of comparatively large particles of a very wide size range. In order to obtain smaller sized particles, the activated carbon was crushed using a pestle and mortar. This method was very straightforward and did not require any special equipment. However, it was rather ineffective because the particles did not break, i.e. only dust was rubbed off their outside.

After crushing, the activated carbon was sieved into the desired fractions using a mechanical sieve shaker (Endecotts Test Sieve Shaker, Endecotts Ltd., London, England). To ensure complete separation of the fractions, only about 50 g of activated carbon was sieved at a time, for a duration of half an hour. Since the shape of the particles was usually far from spherical, the actual particle size range was larger than suggested by the aperture size of the sieves used.

In order to remove the carbon dust, the desired particle fraction was washed overnight in a column reactor by continuous pumping of clean tap water through the system. Subsequently, the carbon was dried in an oven (Contherm Series Five, Contherm Scientific Company, Lower Hutt, New Zealand) at 105°C for 24 h.

After the preliminary studies (see Section 5.2), the sieving aimed to obtain particles in the diameter size range of 250-300 μm. With the employed flow rate of 245 ml/min, this resulted in an initial bed expansion of about four times. For most experiments, 8 g of activated carbon was used. This equalled a volume of settled activated carbon particles of 5.7% (v/v) of the fluidized bed zone of the reactor.

3.3.4 Start-up Procedure

Before starting a new experiment, all the equipment of the experimental apparatus that comes in contact with the growth medium was sanitised using Savlon solution (Imperial Chemical Industries Australia Operations Pty. Ltd., Melbourne, Victoria, Australia) and subsequently rinsed with tap water.

After placing the activated carbon in the column reactor, 2 l of growth medium containing twice the concentration of salts given in Table 3.1, and 200 mg/l phenol, was circulated continuously through the column for 16 h. The three-way-valve in front of pump P2 (Figure 3.1) was used for this purpose. Measurements at the end of the circulation period showed that the phenol was completely adsorbed by the activated carbon. Thus, it was ensured that substrate was provided during the initial stage of the subsequent seeding phase.

After the circulation of medium, 2 l of inoculum was circulated through the reactor. The inoculum was developed as described under Section 3.2.2 with the exception that the culture was grown for 16 h before being used to seed the activated carbon. After 26 h of circulating the culture through the column the fluidized bed experiment was started. This was done by switching the three-way-valve in front of pump P2 so that the medium from the previously filled tank T4 was pumped through the reactor instead of the circulated seed culture. The reactor effluent was subsequently send to waste.

3.3.5 Preparation of Growth Medium

Growth medium was prepared once a day in each of the feed tanks T1 and T2. Before mixing new medium, the tanks were completely emptied and thoroughly

washed with tap water, thus reducing the possibility of growth of microorganisms in the feed. The tanks were filled with tap water to a level of about 5 l below the desired volume of medium to prepare. The liquid was mixed with a stirrer (Pioneer Mixer, Model 2600, Premier Colloid Mills Ltd., England) at 1500 rpm while the components of the medium were weighed in. After the disturbance in the liquid, caused by the stirrer, had ceased, water was added to the desired volume using a calibrated measuring stick for volume measurement.

3.3.6 Sampling

Samples of the phenol solution were taken once or twice a day. The inlet sample was taken using a syringe through the septum below the mesh. The outlet was sampled using a glass pipette from immediately above the fluidized bed. The samples were used to determine the inlet and outlet phenol concentrations.

Dissolved oxygen concentration and pH were measured in the gas-liquid disengagement tank, T4, and in the solid-liquid disengagement zone at the top of the reactor. Dissolved oxygen concentration was determined once a day, pH only occasionally as it was never observed to change.

The height of the expanding fluidized bed was measured three times a day using a scale attached to the outside of the fluidized bed zone of the reactor.

Bioparticles were sampled daily. When stratification of the fluidized bed occurred, samples from the top layer were taken every day, and samples from the bottom layer taken occasionally. The particles were removed from the

reactor using a long glass pipette, the tip of which had been cut off. Pipetting had to be done very slowly and carefully to minimize damage to the biofilm. The bioparticles were returned into the reactor after measurement of the biofilm thickness.

3.4 Analytical Methods

3.4.1 Determination of Dissolved Oxygen and pH

Dissolved oxygen concentration in the phenol solution was measured using a portable dissolved oxygen meter with a polarographic type probe incorporating a thermistor for automatic temperature compensation (HANNA Model HI 8043, HANNA Instruments, Limena/PD, Italy). Calibration was conducted using the zero calibration solution HI 7040 (HANNA Instruments, Limena/PD, Italy).

Determination of the pH was performed using a Horizon pH Controller, Model 5997-20 (Horizon Ecology Co., Chicago, Illinois, U.S.A.) equipped with a combination pH probe (Broadley James Co., Santa Ana, California, U.S.A.). The meter was calibrated prior to measurements using pH 4.0 and pH 7.0 colour key buffer solutions (Laboratory reagent grade, BDH, Poole, England).

3.4.2 Determination of Phenol Concentration

Phenol concentration was determined photometrically using a Philips spectrophotometer (Model PU 8625 UV/VIS, Philips Analytical, Cambridge, England) equipped with quartz sample cells (Starna Ltd., Romford, England). This direct method, without protracted sample preparation, could be employed

because the aromatic ring of the phenol molecule absorbs UV light. Maximum UV absorbance was found at 274 nm. Thus, this wavelength was used for all measurements.

In order to have a pure sample without turbidity caused by suspended biomass, the sample was centrifuged (Biofuge 13, Heraeus Sepatech GmbH, Germany) in 1.5 ml Eppendorf tubes at 13000 rpm for 10 min prior to determination of phenol concentration.

UV absorbance and phenol concentration showed a linear relationship up to a phenol concentration of 120 mg/l. Beyond this value the sample needed to be diluted. When this was necessary, the measurements were conducted in replicate to decrease the possible error caused by dilution. However, replicated measurements could not be conducted in the kinetic experiments because the sample size had to be kept small (see Section 3.2.3).

The salts in the growth medium, and the water quality (tap water or distilled water), were found to influence the absorbance. However, the salt concentrations in the growth medium were abundant. Thus, for the kinetic experiments it could be assumed that the salt concentrations decreased only to a small extent in the beginning of the exponential growth phase of the culture, i.e. the important period for determination of the specific growth rate, μ. In the fluidized bed experiments, the decrease in salt concentration during the passage of the medium through the reactor could be regarded as negligible. In consequence, the salt solution given in Table 3.1, without phenol, was used for reference and for dilution of the sample where necessary. The solution was made up with water of the same quality as the growth medium being analyzed.

3.4.3 Determination of Suspended Biomass Concentration

Suspended biomass concentration was measured by determination of the optical density of the culture broth. This was done using a spectrophotometer (Varian Series 634 UV-Visible Spectrophotometer, Varian Associates Inc., Sunnyvale, California, U.S.A.) at a wavelength of 620 nm using quartz sample cells (Starna Ltd., Romford, England).

In order to establish the correlation between optical density and suspended biomass dry weight concentration, the dry weight of samples with known optical density was determined. To do this, 0.45 μm pore size membrane filters (MF-Millipore Membrane Filters, type HA, diameter 47 mm, Millipore Co., Bedford, Massachusetts, U.S.A.) were pre-dried in a microwave oven (Microwave Oven - 630 D, Samsung, Korea) at level four for 4 min. After they had been left to cool in a desiccator in the presence of silica gel for 30 min, they were weighed, thus obtaining their dry weight. Under vacuum, 20 ml of sample was then passed through the filters before being rinsed twice with distilled water. Subsequently, the filters with the biomass were dried in the microwave oven at level four for 7 min. After equilibration in the desiccator, they were again weighed. The difference in the obtained values represents the biomass dry weight per 20 ml of culture broth.

Since the correlation between measured optical density and suspended biomass concentration was linear in the range of biomass concentrations occurring, dilution of the samples was not necessary at any time. The solution given in Table 3.1, without phenol, was used as reference.

3.4.4 Determination of Biofilm Thickness

The biofilm thickness was determined with the help of light microscopy and image analysis techniques. The samples were placed on a glass slide and the excess liquid was removed using a tissue. Since the biofilm had a light yellowish colour and the carbon particles were black, staining was not necessary.

In order to have an immediate idea of the course of biofilm development, the biofilm thickness was measured under a light microscope (Olympus CHA, Olympus Corp., Scientific Instruments Div., Lake Success, New York, U.S.A.) with the help of a previously calibrated eye-piece with ocular scale. A magnification of 100 times was used. To get a representative value, the biofilm thickness of each bioparticle was measured at three to four locations around the particle and at least ten bioparticles were measured per sample.

For more accurate results, photographs of the bioparticles were taken under a light microscope equipped with a camera (Leitz Ortholux II, Leitz, Wetzlar, Germany) using a magnification of 50 times. After initial usage of black and white films, colour pictures were taken. For the latter, a blue filter was inserted in the ray to prevent the pictures having a red tinge. The best results were generally obtained using an exposure time of 1/15 s. Usually pictures of 10 to 25 bioparticles were taken per sample.

The photographs were analyzed with image analysis techniques in the Image Analysis Unit, Massey University. The captured image of a photographed bioparticle was processed by a computer program written by the staff of the Image Analysis Unit, Massey University. The software automatically identified the circumference of the bioparticle, and the particle core to biofilm interface

by segmentation, thus determining the exact geometrical shape of the projected objects of interest. The software output contained the projected areas of the bioparticle and of the particle core, the length and breadth of the particle core, and the mean biofilm thickness. The latter was determined from the projected area of the bioparticle, A_b, the projected area of the particle core, A_c, and the perimeters of the biofilm, P_b, and the particle core, P_c;

$$\text{Mean biofilm thickness} = \frac{(A_b - A_c)}{(P_b + P_c) / 2} .$$

This trapezoid formula provides a reliable estimate of the mean biofilm thickness for any shape of particle core and for nonuniform bioparticles.

From the values of the projected areas, A, given by the computer program, the equivalent diameters of a sphere,

$$d_{equiv.} = 2 \sqrt{(A/\pi)},$$

was calculated for the particle core and for the bioparticle.

An example of a captured image of a bioparticle and the boundary lines detected by the computer program can be seen in Figure 3.5. Since the outline of the particle core (white line in Figure 3.5) was often very uneven, the length of this line would overestimate the value of the perimeter of the particle core, which in turn would result in an underestimation of the mean biofilm thickness. Thus, a slightly straightened boundary line was used to determine the perimeter of the particle core. Because of statistical variations, the boundaries detected by the computer program varied slightly from time to time. Therefore, each bioparticle was analyzed twice and the average of the determined values was taken.

In some cases the software was not capable of detecting the boundary between

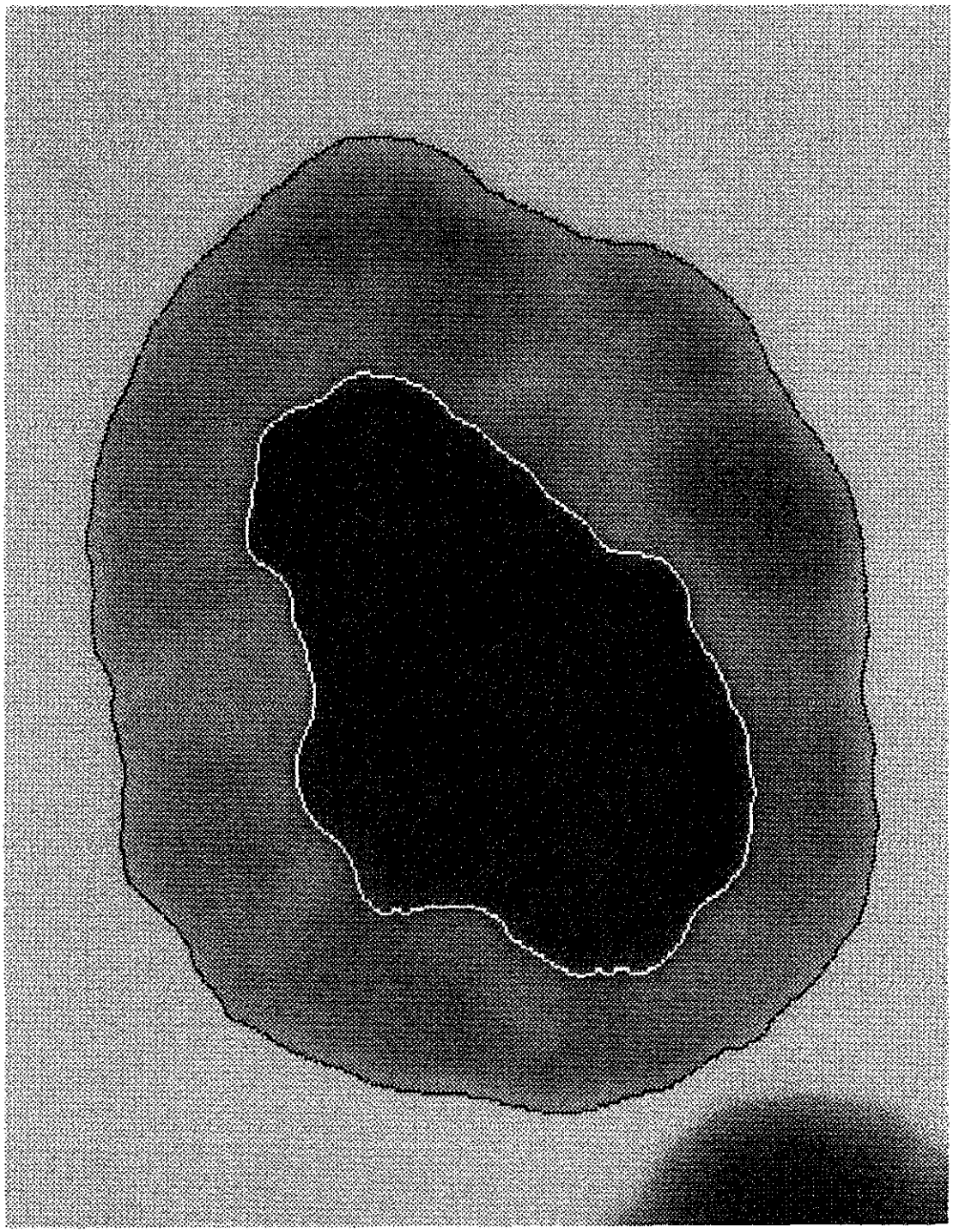

Figure 3.5 Captured image of a bioparticle with boundary lines detected by the software

particle core and biofilm even though it was visible to the human eye. To overcome this problem these bioparticles were redrawn with colour pens on transparent foil which was put on top of the photographs. The drawings were then analyzed by the image analysis system.

In one experiment, however, the interface between particle core and biofilm was not detectable at all. In this case only the area of each bioparticle was determined by the computer program. An estimate of the mean biofilm thickness was calculated as follows;

$$\text{Mean biofilm thickness} = (d_{b,equiv.} - \bar{d}_{c,equiv.}) \; / \; 2 \;,$$

where the equivalent diameter of each bioparticle and an average over the equivalent diameters of all measured particle cores was used. However, this formula overestimates the value of the mean biofilm thickness, because it assumes the projected areas to be circular in shape, which in turn means that the shortest possible perimeters are assumed.

During biofilm thickness measurements, the density and morphology of the biofilm were observed visually.

CHAPTER 4

BATCH CULTURE KINETIC STUDIES

4.1 Introduction

Initially it was of interest to determine the kinetic behaviour of the system to gain a basic impression of the influence of the initial concentration of the substrate phenol on the growth characteristics of the culture used. It is known that for phenol degradation, as in general for aerobic wastewater treatment systems treating toxic but biodegradable organics, the microbial growth kinetics can be best described by a substrate inhibition mechanism. In order to be able to fit a substrate inhibition model, and to determine the kinetic parameters, data on the actual growth rate at various substrate concentrations were needed. The easiest means to obtain these is the batch process. According to some authors, the latter is also regarded as the most reliable means of determining maximum specific growth rates (Pawlowsky and Howell, 1973). Thus, the growth characteristics at different phenol concentrations were investigated in batch culture.

Bhamidimarri (1985) conducted kinetic studies with the culture used in this work before it was applied to various waste treatment problems. It was assumed that the culture became more adapted to inhibitory systems in the course of its application. Hence, the present study was not only conducted to gain a general impression of the kinetic behaviour of the culture but also to determine to what extent the culture performance had changed following its adaptation to different waste treatment processes.

4.2 Results

A total of 40 experiments were conducted in eight sets. The initial phenol concentrations ranged from 12 to 1720 mg/l. Since it is more difficult to accurately determine values of the specific growth rate where growth is fast and concentrations are low, a large number of experiments were conducted with phenol concentrations up to 100 mg/l.

4.2.1 Growth Characteristics

An example of a typical growth history is shown in Figure 4.1.

The duration of the lag phase often varied considerably in different sets of experiments for similar initial phenol concentrations. Up to an initial phenol concentration of about 160 mg/l the lag phase lasted in general between one and three hours. At higher concentrations it was significantly longer. Here, the differences in the duration of the lag phase in different sets of experiments were especially obvious, with 21 h and 31 h at about 450 mg/l and 590 mg/l, respectively, in one set, and 6 h, 8 h and 13 h at about 400 mg/l, 560 mg/l and 690 mg/l, respectively, in another.

The specific growth rate, μ, was not affected by the duration of the lag phase. For each experiment, its value was obtained by plotting the natural logarithm of the biomass concentration versus the time elapsed. A straight line was fitted to the data points in the exponential growth phase using a linear least squares fit. The slope of the line represents the value of the specific growth rate of the culture at the initial phenol concentration employed. However, since the uptake of phenol during the lag phase has to be taken into account, the specific growth

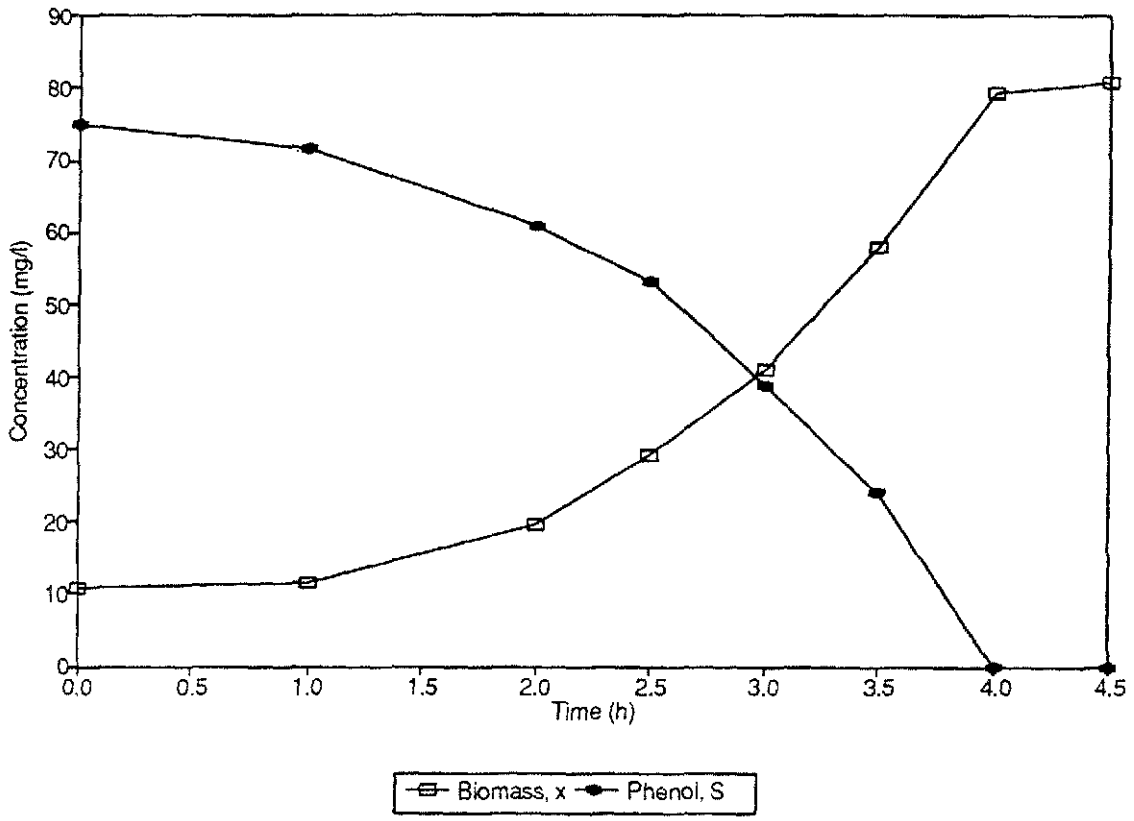

Figure 4.1 Typical growth history of a batch experiment (S_0 = 75 mg/l)

rate was not related to the actual initial phenol concentration, S_0, but to the phenol concentration at the onset of the exponential growth phase, S'. An example of a plot for determination of the specific growth rate is given in Figure 4.2, the data being from the same experiment as the data in Figure 4.1.

The values of the specific growth rate and the duration of the lag phase for all the conducted experiments are given in Table 4.1. The specific growth rates showed a considerable degree of variation in different experiments with similar initial phenol concentrations. The extent of the variation was independent of whether the results came from the same set of experiments or not.

For phenol concentrations, S', between 25 and 150 mg/l, the specific growth rates were all in the same range. At lower and higher concentrations the specific growth rates were distinctly lower, for higher concentrations decreasing as S' was increasing. At the two highest concentrations tested, i.e. about 830 mg/l and 1720 mg/l no obvious growth occurred during an observation period of 74 h.

In the experiments with an initial phenol concentration, S_0, of about 400 mg/l and more, growth decelerated without the phenol being used up completely, whereas at lower concentrations the exponential growth phase came to an abrupt end, when the phenol was entirely consumed. The higher the initial phenol concentration, the more phenol was remaining when deceleration of growth occurred. The biomass concentration at this point was between 320 mg/l and 350 mg/l in all cases. An example of a growth history without complete phenol consumption can be seen in Figure 4.3.

For each experiment, the biomass yield was obtained from the data of the exponential growth phase. The mean value of the yield from all experiments

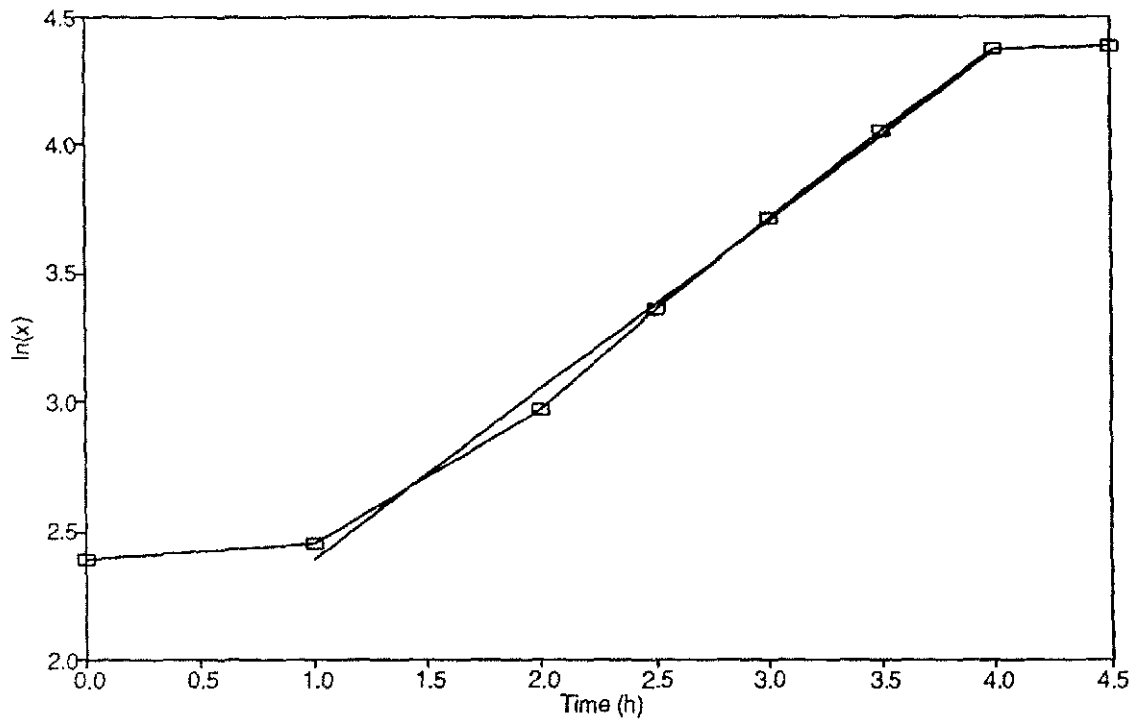

Figure 4.2 Semilogarithmic plot of data from a batch experiment, slope of fitted straight line equals specific growth rate
(Data set is the same as in Figure 4.1)

Table 4.1 Results of batch culture kinetic experiments

Set no.	S_0 (mg/l)	S' (mg/l)	μ (h^{-1})	Lag phase (h)
5	12.6	12.6	0.415	0
4	14.2	12.7	0.390	3
4	14.2	13.0	0.398	3
4	14.2	14.2	0.371	3
6	15.1	13.8	0.389	2.5
7	32.7	25.1	0.642	1
7	32.7	26.7	0.640	1
7	32.7	27.2	0.605	1
5	34.1	30.4	0.641	1
6	38.4	32.4	0.481	2.5
3	39.5	32.5	0.651	2
7	54.9	43.3	0.599	1.5
7	54.9	47.1	0.660	1
7	54.9	47.2	0.643	1
5	55.8	51.2	0.675	1
3	58.8	50.0	0.664	2.5
6	62.4	56.1	0.595	2
5	75.2	71.6	0.656	1
4	76.2	69.3	0.617	3
4	76.2	69.9	0.617	3
4	76.2	71.2	0.614	3
3	77.0	70.8	0.633	3
6	84.7	75.9	0.590	2.5
5	92.9	90.3	0.675	1.5
1	104.4	101.6	0.598	1
6	105.3	94.0	0.604	2
5	126.5	115.5	0.618	2
6	157.7	149.2	0.634	2
1	162.1	157.2	0.529	2
1	276.2	245.3	0.518	7
8	395.7	376.2	0.412	6
8	395.7	376.5	0.426	6
2	454.4	435.9	0.372	21
8	558.8	542.0	0.327	8
8	558.8	544.2	0.324	8
2	585.0	559.2	0.293	31
8	693.1	664.6	0.253	13
8	693.1	667.2	0.245	13
1	826.6	no growth occurred		
1	1716.5	no growth occurred		

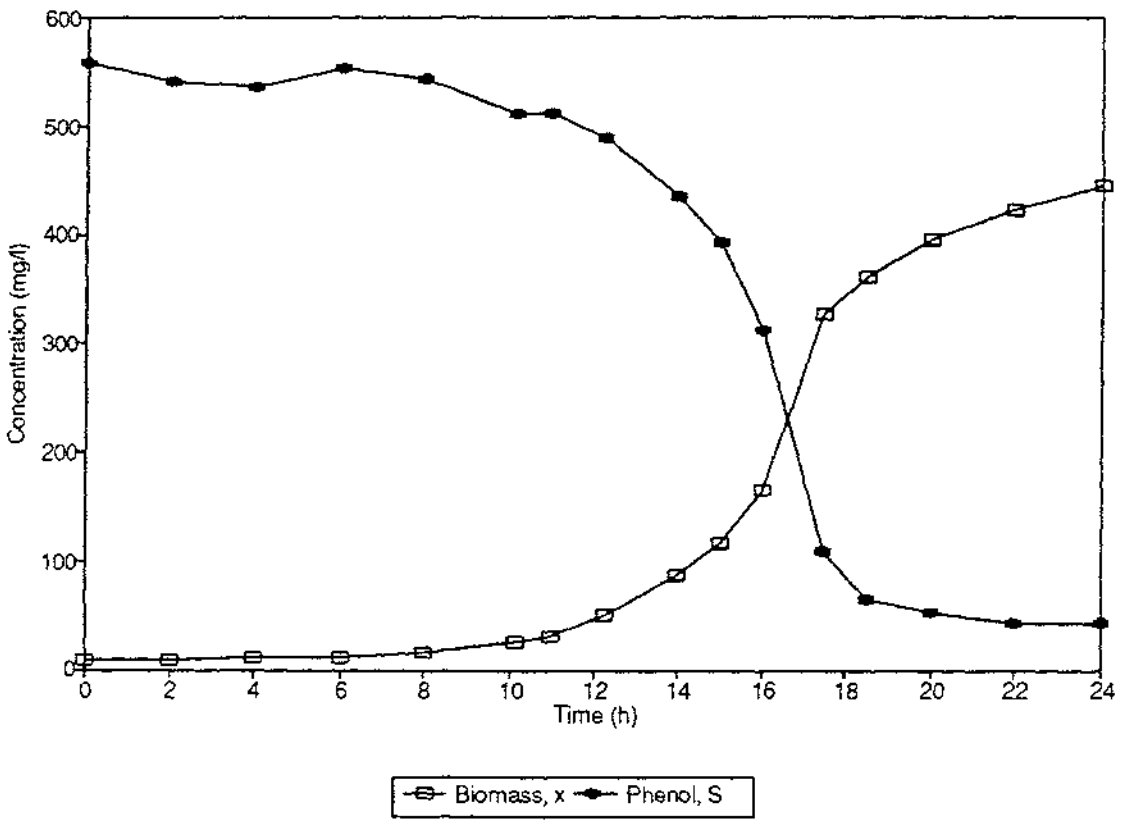

Figure 4.3 Growth history of a batch experiment without complete phenol consumption ($S_0 \approx 559$ mg/l)

was 0.815 ± 0.029 mg biomass/mg phenol at a confidence level of 95%.

4.2.2 Substrate Inhibition Model

The three-parameter substrate inhibition models used by Edwards (1970) were tested. They are not only easier to handle but have also been found to give generally slightly better results (Edwards, 1970) than the four-parameter models. The functions of the tested inhibition models are given in Table 4.2.

Table 4.2 Substrate inhibition models tested (Edwards, 1970)

Teissier-Edwards	$\mu = \mu_m [\exp(-S/K_i) - \exp(-S/K_s)]$
Haldane	$\mu = \mu_m S / [(K_s + S)(1 + S/K_i)]$
Aiba-Edwards	$\mu = \mu_m S \exp(-S/K_i) / (K_s + S)$

These functions were fitted to the experimental data using a nonlinear least squares method. With the kinetic parameters thus obtained for each equation, the substrate concentration, S^*, at which each function goes through its maximum value, and the corresponding specific growth rate, μ^*, were calculated. The goodness of fit of the tested models to the data set was compared using the F-test for equality of variances in accordance with Edwards (1970).

A plot of the experimentally obtained specific growth rates versus the phenol concentrations at the onset of the exponential growth phase, together with the fitted equations, is shown in Figure 4.4. From the summary of the results of the model fitting (Table 4.3) it can be seen that the Teissier-Edwards model fits the

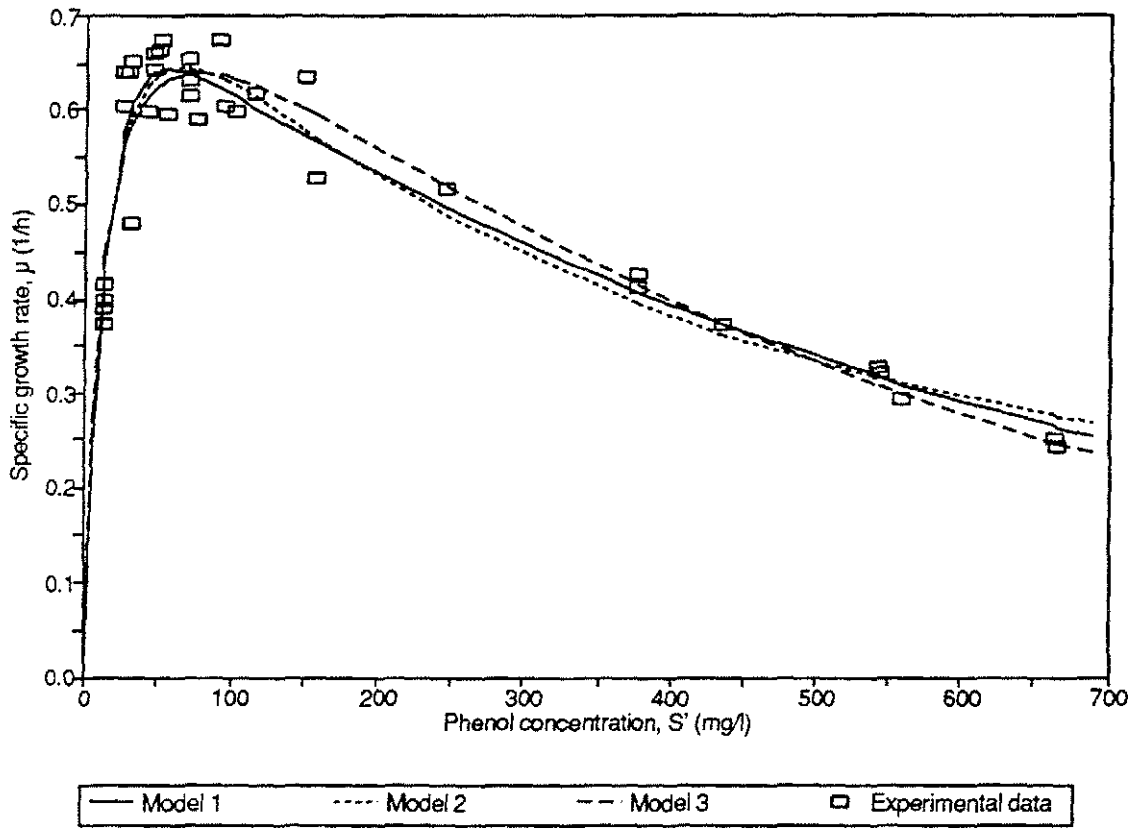

Figure 4.4 Results of batch culture kinetic experiments with curves of fitted models
(Models: 1 = Teissier-Edwards, 2 = Haldane, 3 = Aiba-Edwards)

Table 4.3 Results from least squares fit of substrate inhibition models to the experimental data

Model	μ_m (h^{-1})	K_s (mg/l)	K_i (mg/l)	S^* (mg/l)	μ^* (h^{-1})	R^2 (%)	σ^2 $*10^{-3}$	F_{il}
Teissier-Edwards	0.717	14.56	666.25	56.91	0.644	91.28	1.61	
Haldane	1.032	17.54	251.12	66.37	0.646	89.86	1.87	1.163
Aiba-Edwards	0.857	12.39	542.87	88.44	0.639	89.28	1.97	1.230

data the best. However, the differences between the tested models are statistically not significant at the 95% confidence level.

4.3 Discussion

All three substrate inhibition models tested fitted the experimental data well, giving an R^2 value of about 90%. Statistically, there was no significant difference in the goodness of fit between the models. However, the lowest variance was obtained with the Teissier-Edwards model, followed by the Haldane model and then the Aiba-Edwards model.

The experimental results gave a scatter cloud of data points where the curves of the models go through their maximum. The same phenomenon has been found by other workers (e.g. Pawlowsky and Howell, 1973; Szetela and Winnicki, 1981). It is probably caused by the fact that in this region accurate measurements are most difficult because growth is fastest while the increase of biomass concentration during the course of the experiment is only small due to the low initial phenol concentrations. In the present study, the effect of inaccurate measurements on the results of the kinetic modelling was reduced by conducting a high number of experiments in the region where growth is fastest.

Since it has been found that the inhibition characteristics are influenced by the phenol concentration prevailing in the culture from which the microorganisms were taken (Chi and Howell, 1976; Sokol and Howell, 1981; Sokol, 1988), it is not surprising that the highest growth rates were found near a phenol concentration of 100 mg/l, the concentration used for growing the inoculum.

At very high initial phenol concentrations (about 830 and 1720 mg/l), growth

was completely inhibited. This exposes the weakness of the tested models which imply that cells are capable of growing at indefinitely high initial phenol concentrations, and fail to predict the maximum substrate concentration above which growth will cease.

The fitted parameters obtained for the three functions are relatively similar, with the exception of the K_i value for the Haldane equation which is less than half of the ones for the other two equations. The substrate concentrations at which the functions go through their maximum value are considerably different for the three models tested, while the maximum values are almost the same. The reason for this discrepancy lies in the fact that for a relatively wide range of substrate concentrations the specific growth rates are scattered in the same area.

The maximum specific growth rates, μ_m, determined by fitting the models are distinctly higher than those found by other researchers (see Table 2.3). Compared to the results of Bhamidimarri (1985), who investigated the kinetic behaviour of the culture used in this study before it was applied to various waste treatment problems, the present μ_m values were on average about twice as high, while the K_s values were slightly lower (Bhamidimarri: $\mu_m = 0.401\ h^{-1}$, $K_s = 21.76$ mg/l).

Bhamidimarri found that the Aiba-Edwards inhibition model provided the best fit to his data, giving a value for K_i of 312.1 mg/l. This value is clearly lower than the one found in the present study (542.9 mg/l). The same applies to the K_i value determined by the Haldane model (144.4 mg/l as compared to 251.12 mg/l). The Teissier-Edwards model was not tested by Bhamidimarri. These results verify the assumption that the use of the culture in various waste treatment applications has led to an adaptation of the microorganisms to inhibitory systems.

The biomass yield determined by Bhamidimarri was slightly higher than the one found in the present study (0.922 as compared to 0.815 mg biomass/mg phenol). This means that more phenol was consumed for the same increase in biomass. Other workers have reported yields in the same range, e.g. 0.85 mg cells/mg phenol (Yang and Humphrey, 1975). The generally high value can be explained by the high carbon to oxygen ratio in phenol.

The increase in the length of the lag phase with increasing initial phenol concentrations shows that the microorganisms need to acclimatize to the given phenol concentrations. As the concentration increases, more time is needed for this process.

The observed distinct variations in the duration of the lag phases for similar initial phenol concentrations remain unexplained, since all experiments were performed under the same conditions, and the same inoculum size and development procedure were used throughout the study. However, as also stated by other researchers (e.g. Pawlowsky and Howell, 1973), the length of the lag phase did not affect the specific growth rate and, thus, the results of the kinetic studies were not influenced by it.

For initial phenol concentrations, S_0, of about 400 mg/l and above, the salts in the growth medium probably became the growth limiting factor after some time, causing the growth to decelerate without the phenol having been consumed. Thus, for experiments with high initial phenol concentrations, the concentrations of the salts in the medium should be increased. Nevertheless, the obtained values of the specific growth rates remained unaffected by the deceleration of growth, since they were determined from the initial period of the exponential growth phase.

4.4 Conclusion

Good agreement was found between the experimental data and the three tested inhibition models; the Teissier-Edwards, Haldane and Aiba-Edwards models. There was no statistically significant difference in the goodness of fit between the equations. However, the lowest variance was obtained for the Teissier-Edwards model.

The culture proved to be better adapted to the phenol-inhibited system than it had been when last investigated by Bhamidimarri (1985) before its application to various waste treatment problems. In addition, it was much faster growing than other cultures described in the literature.

For initial phenol concentrations of about 400 mg/l and above, the concentration of salts in the growth medium should be increased to prevent the possibility of the salts becoming the growth limiting factor.

Since the highest specific growth rates were obtained for initial phenol concentrations of between 30 and 130 mg/l, a phenol concentration of about 100 mg/l was chosen for the subsequent preliminary fluidized bed studies.

CHAPTER 5

PRELIMINARY FLUIDIZED BED STUDIES

5.1 Introduction

After design and establishment of an experimental apparatus, several trials were conducted to test and improve the system, the details of the system as described in Section 3.3 being the result of these studies. Apart from improving the performance of the apparatus, especially that of the fluidized bed reactor, the preliminary investigations were needed to be able to decide on the particle size and the amount of activated carbon particles used, and on the liquid velocity in the column reactor.

The size of the particles and the liquid velocity had to be chosen so that sufficient particle movement was provided to avoid the formation of big lumps of particles, which could result in blockage of the reactor. At the same time, the liquid velocity had to be low enough not to cause excessive shear stress and to enable the microorganisms to utilize the phenol. The amount of particles was restricted on the one hand by the necessity for sufficient surface area so that the biomass concentration in the fluidized bed would be high enough to allow noticeable phenol consumption, and on the other hand by the need for the bed to be able to expand as the biofilm thickness increased.

5.2 Results

Conditions and results of the six runs conducted to establish the final experimental design are given in Table 5.1.

A noticeable phenol consumption was observed in Runs 1 to 3. Phenol concentrations were not measured in Runs 4 and 5, since the duration of these runs was only very short. In Run 6 no phenol degradation took place.

Oxygen concentrations were measured in Runs 1 to 3. In all three runs, the oxygen in the growth medium was almost completely used up at the top of the fluidized bed after a biofilm layer had established itself on the particles. The inlet oxygen concentration did not change notably when air instead of oxygen was used for aeration.

In Run 6, only a very thin layer of biomass developed, merely filling the crevices on particle surfaces, whereas in Runs 1 to 3, marked biofilm formation took place. The other two experiments were of too short duration to allow comparison of biofilm development.

5.3 Discussion

In Run 1, considerable bacterial growth was observed in tanks T3 and T4 (see Figure 3.1). In consequence, the residence time of the growth medium in these tanks was decreased by decreasing their size by about half. This measure was successful as hardly any growth was noticed in these two tanks in the subsequent runs.

Table 5.1 Conditions and results of preliminary studies (Refer to Figure 3.1 for illustration of experimental apparatus) (Phenol concentration: 100 mg/l, Temperature: 30°C)

Run No.	Act. Carb. Amount (g)	Act. Carb. Diameter (μm)	Flow Rate (ml/min)	Initial Bed Expansion (times)	Aeration	Duration of Run (d)	Important Observations	Alterations after Run
1	20	420-500	210	1.5	O_2	6	- Big air bubbles under mesh - High amount of growth in tanks T3 and T4 - Biomass accumulates under mesh - Mesh installation unsatisfactory - Turbulence in bottom of bed - Channelling and blockage	- Size of tanks T3 and T4 decreased - Installation of brush under mesh - Fixation of mesh
2	20	420-500	220	1.5	O_2	5	- Big air bubbles under mesh - Particles are washed out after 4 d - Turbulence in bottom of bed - Channelling and blockage	- Attachment of solid-liquid disengagement zone to top of column - Installation of septum under mesh - Alteration of mesh installation
3	10	420-500	215	1.5	Air	3	- Strong turbulence in bottom of bed - Blockage	- Alterations to liquid inlet zone
4	10	420-500	285	2	Air	0.5	- Strong turbulence in bed - Column has crack	- Repair of column
5	10	250-300	240	4	Air	1	- Strong turbulence in bed	- Installation of primary liquid distributor
6	10	420-500	440	3	Air	7	- Hardly any growth on particles	- Use of smaller particles at lower flow rate

In order to deal with the problem of air bubbles and biomass accumulating under the mesh as observed in the first run, a brush was installed in the liquid inlet zone. It was hoped that by brushing, the biomass could be removed from beneath the mesh and the air bubbles could be dispersed. Whereas this worked for the biomass it did not work for the air bubbles. Thus, after Run 2, a septum was placed in the reactor wall immediately beneath the mesh. Consequently, air bubbles could be removed using a syringe inserted through the septum. This system worked very well and air bubbles which coalesced under the mesh at the start of all experiments provided no further concern.

To prevent elutriation of particles due to a thick biofilm layer developing on their surface (as occurred in Run 2), a solid-liquid disengagement zone was installed at the top of the fluidized bed zone. The principle of this zone is to decrease the upward force on the particles by decreasing the superficial liquid velocity which in turn is achieved by increasing the diameter of the column. This simple, commonly used measure is very successful provided that the overall density of the bioparticles does not drop below the point where the force exerted by the fluid on an individual bioparticle in the solid-liquid disengagement zone exceeds the gravitational force on the particle.

Since the fluidized bed expanded up to the top of the column rather quickly, and at the same time the phenol consumption was considerable, the amount of activated carbon used was halved after the first two runs. This led to satisfactory conditions and thus, an amount of 10 g activated carbon was used for all subsequent runs in the preliminary investigations.

In Run 3, air was tested for aeration instead of oxygen. This did not cause a noticeable change in the inlet dissolved oxygen concentration. This behaviour was not unexpected because after aeration the medium passed through an open

system (gas-liquid disengagement tank, T4), causing the dissolved oxygen concentration to drop to the saturation concentration in the presence of air even after aeration with pure oxygen. Therefore, as air is more readily available and less costly, all aeration was subsequently conducted using air.

Blockage of the reactor caused by bioparticles sticking together presented a serious problem. Before altering the flow rate and/or particle size, which can help solve the problem by allowing a larger bed porosity, alterations were made to the equipment which focused on improving the flow patterns in the reactor. These alterations at the same time aimed at reducing the turbulence at the bottom of the fluidized bed. The flow patterns were especially critical as the diameter of the column reactor was small. The small diameter in turn had been chosen to keep the volumetric flow rate (for a given superficial liquid velocity) to a practicable level, which was important as recycle was not employed.

The installation of a brush and a septum were two of the alterations made which helped alleviate the aforementioned problems as they served to remove biomass and air bubbles from beneath the mesh which originally disturbed the liquid flow and thus had a negative effect on the movement of the particles in the fluidized bed. Other steps taken included the alteration of the mesh installation and the liquid inlet zone. The former resulted in the removal of a rim sticking into the column on which the mesh was mounted. This rim was suspected to be the cause for the observed lack in movement of particles near the wall just above the mesh. The changes to the liquid inlet zone aimed at a general improvement of the liquid distribution.

All these alterations produced definite improvements to the reactor design. However, this was not sufficient to solve the problem of blockage and turbulence. Therefore, the initial bed expansion was increased by raising the

flow rate and using smaller sized particles. In order to minimize the recurring turbulence at the bottom of the fluidized bed, the primary liquid distributor (see Figure 3.4) was installed. With these steps the phenomena of blockage and strong turbulence in the fluidized bed were finally eliminated.

However, the combination of particle size and flow rate employed in the last run in order to achieve a larger bed expansion than in the initial runs, proved to be unsuitable for the system as very little biofilm developed on the particles. It is assumed that the high shear stress and the low hydraulic retention time of the growth medium in the reactor, caused by the high flow rate used, made it impossible for the biofilm to develop beyond a very thin layer. Thus, it was necessary to use smaller sized particles in order to be able to achieve a high initial bed expansion with lower flow rates.

5.4 Conclusion

Blockage of the reactor by bioparticles sticking together, and turbulence in the bottom of the fluidized bed were the most serious problems encountered in the preliminary studies. They were solved by improving the flow patterns in the reactor and by employing an initial bed expansion of three to four times.

The flow patterns were improved by alterations to the fluidized bed reactor such as the installation of devices for removal of accumulating biomass and air bubbles from beneath the mesh at the bottom of the fluidized bed zone, and by improvement to the liquid inlet configuration culminating in the installation of the primary liquid distributor (see Figure 3.4) in the reactor.

Since the original particle size of 420-500 μm allowed sufficient bed expansion

only when using very high flow rates which hindered the biofilm development, particles in the diameter range of 250-300 µm, coupled with a flow rate of 245 ml/min (resulting in an initial bed expansion of about four times), were used in the subsequent studies. An amount of about 10 g activated carbon proved to be a suitable quantity of support medium to be used. However, for all but one of the following experiments it was reduced to 8 g.

CHAPTER 6

FLUIDIZED BED STUDIES USING DIFFERENT REACTOR TEMPERATURES

6.1 Introduction

Temperature is one of the most important environmental factors influencing the growth of microorganisms. It is well known that as temperature rises, enzymatic reactions proceed at more rapid rates and growth becomes faster. However, above a certain temperature inactivation reactions set in. Moreover, temperature also influences physical processes such as diffusion of substrate into and within the biomass and adsorption of substrate onto the carrier matrix, both important factors influencing the growth of immobilized cultures.

The temperature used in the preceding studies was chosen according to Bhamidimarri (1985). However, investigations into the effect of different temperatures on the growth of the culture are not reported in his work. In fact, even though temperature is known to influence biofilm development (see Table 2.5), no report on the influence of different temperatures on the rate or structure of biofilm development in biological fluidized bed fermenters was found in the literature. Hence, the present work was conducted in order to gain an insight into the effects of different reactor temperatures on the performance of the fluidized bed system, especially on the biofilm development.

6.2 Results

Experiments were conducted at 30°C, 25°C and without temperature control (i.e. average: 17.2°C, maximum: 18.7°C, minimum: 15.3°C). In consequence of the results of the batch culture kinetic studies (Chapter 4), a phenol concentration of about 100 mg/l was employed. In the experiment conducted at 30°C, 10 g of activated carbon was used, in contrast to 8 g in the other two experiments. All other conditions were as described in Section 3.3.

6.2.1 Biofilm Development

In all three experiments, the biofilm did not develop evenly throughout the fluidized bed, but stratification occurred into layers of particles with different biofilm thicknesses. Between the different layers, the size range of the particle cores did not differ significantly. A top layer separated from the initially homogenous bed shortly after start of the experiments. It originally contained only a few particles which soon circulated to the top of the fluidized bed zone. The number of particles in the top layer increased with time. Therefore, no gradual increase in total bed height with growth of the biofilm took place. In the experiment conducted without temperature control, the bed stratified into three layers; a top, middle and bottom layer. In the other two experiments, for most of the time two layers were observed. The development of the fluidized bed is illustrated in Figure 6.1, using the experiment conducted at 30°C as an example. For all three experiments, the heights of the different layers as a function of time is given in Figure 6.2.

Bioparticles were sampled daily from the top layer of the stratified bed. For the experiment at 30°C, only very few photographs of bioparticles were taken,

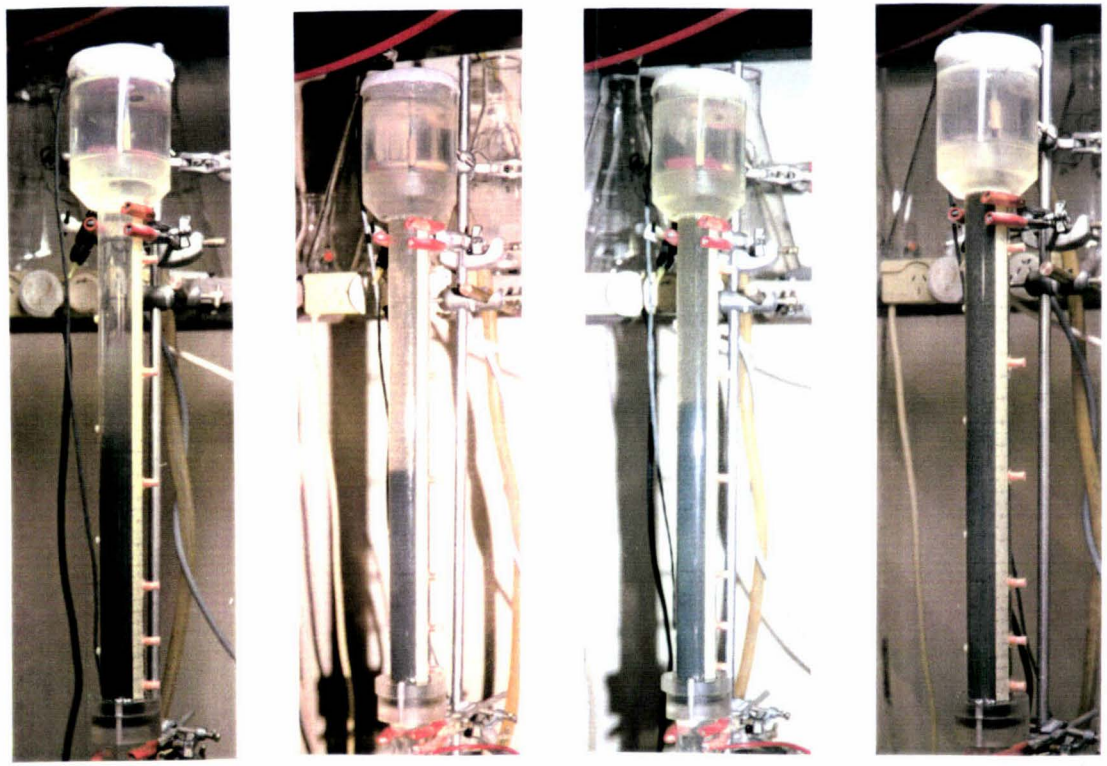

c. 60 h c. 80 h c. 100 h c. 150 h

Figure 6.1 Photographic illustration of the fluidized bed development (Reactor temperature: 30°C)

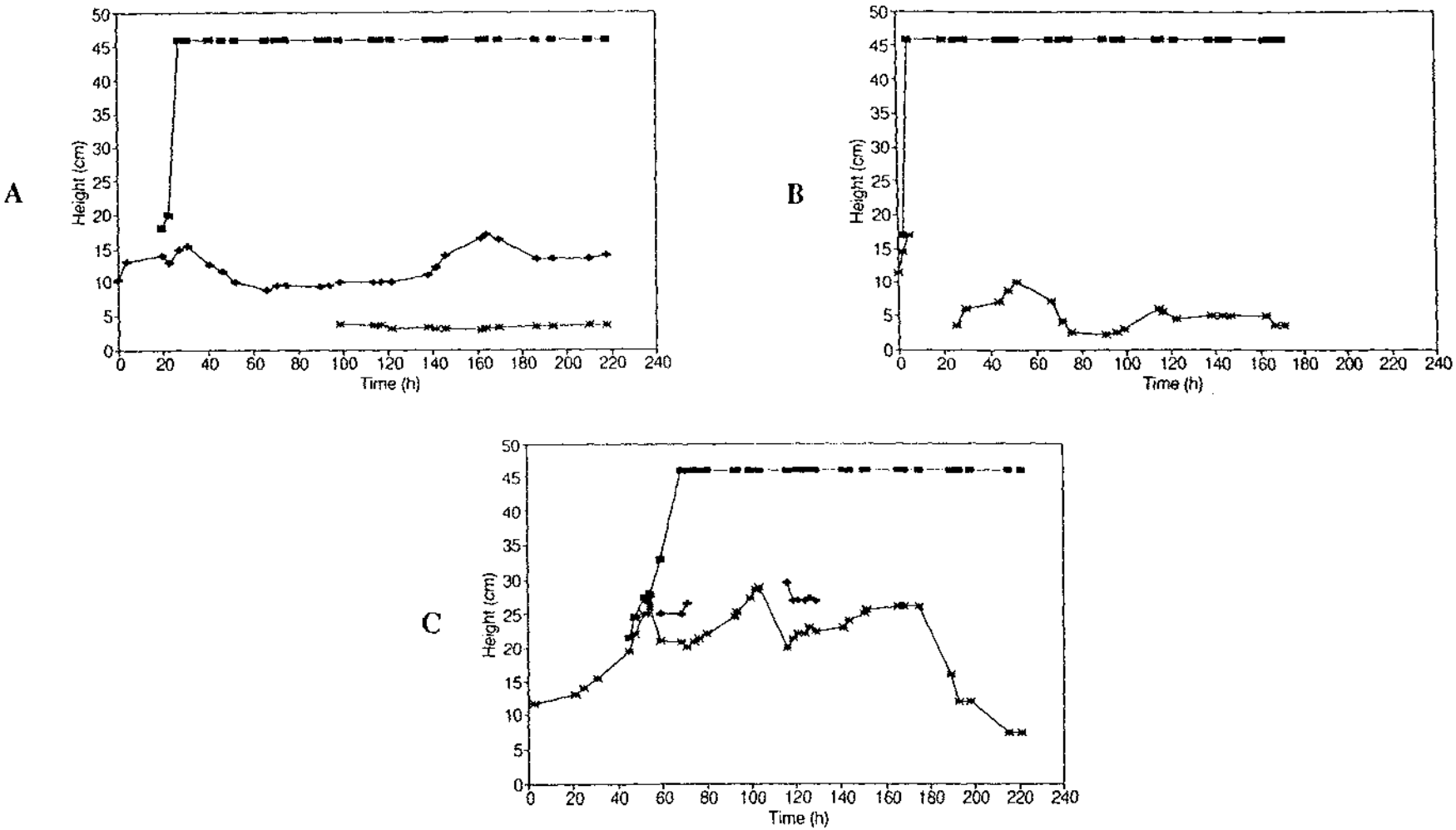

Figure 6.2 Time course of the heights of the different layers of the fluidized bed at different reactor temperatures (**A**: ~17.2°C, **B**: 25°C, **C**: 30°C)

commencing after five days (c. 120 h) only. The observed increase in biofilm thickness over time for all temperatures tested is shown in Figure 6.3. In the experiment conducted with no temperature control, the biofilm was irregular in shape, and loose and fluffy in structure throughout the whole experiment (Figure 6.4). Mycelium-like filaments (Figure 6.5) were observed on the outside of the biofilm after about five days (c. 120 h). After about six days (c. 140 h) the biofilm thickness had decreased and the remaining biofilm appeared, on average, slightly denser. At 30°C, the biofilm was also loose in structure, but initially of relatively uniform thickness. Only after eight days (c. 190 h) did the biofilm become very fluffy and irregular in shape, accompanied by a sudden, extreme increase in thickness. In both experiments, sampling of the bioparticles was difficult because the biofilm broke very easily and parts detached themselves. Conversely, the biofilm grown at 25°C was relatively dense and even in shape and structure throughout the experiment (Figure 6.6). In this case, the variation in the thickness of the biofilm of the same sample was much smaller than in the other two experiments.

From the middle layer of the experiment without temperature control and from the bottom layer of the experiment at 30°C, bioparticles were sampled occasionally. Here, the biofilm was thinner, denser, smoother in structure and more even in shape than in the top layers. In the experiment with no temperature control, the mean biofilm thickness in the middle layer reached about 50 µm at the end of the experiment (c. 220 h). In the bottom layer at 30°C it was about 35 µm after seven days (c. 170 h).

Particles from the bottom layers of the experiment with no temperature control and the experiment conducted at 25°C were not sampled. Nevertheless, in these cases it was clearly visible that the particles had only very little biomass on their surfaces. The same applied for the bottom layer at 30°C towards the very

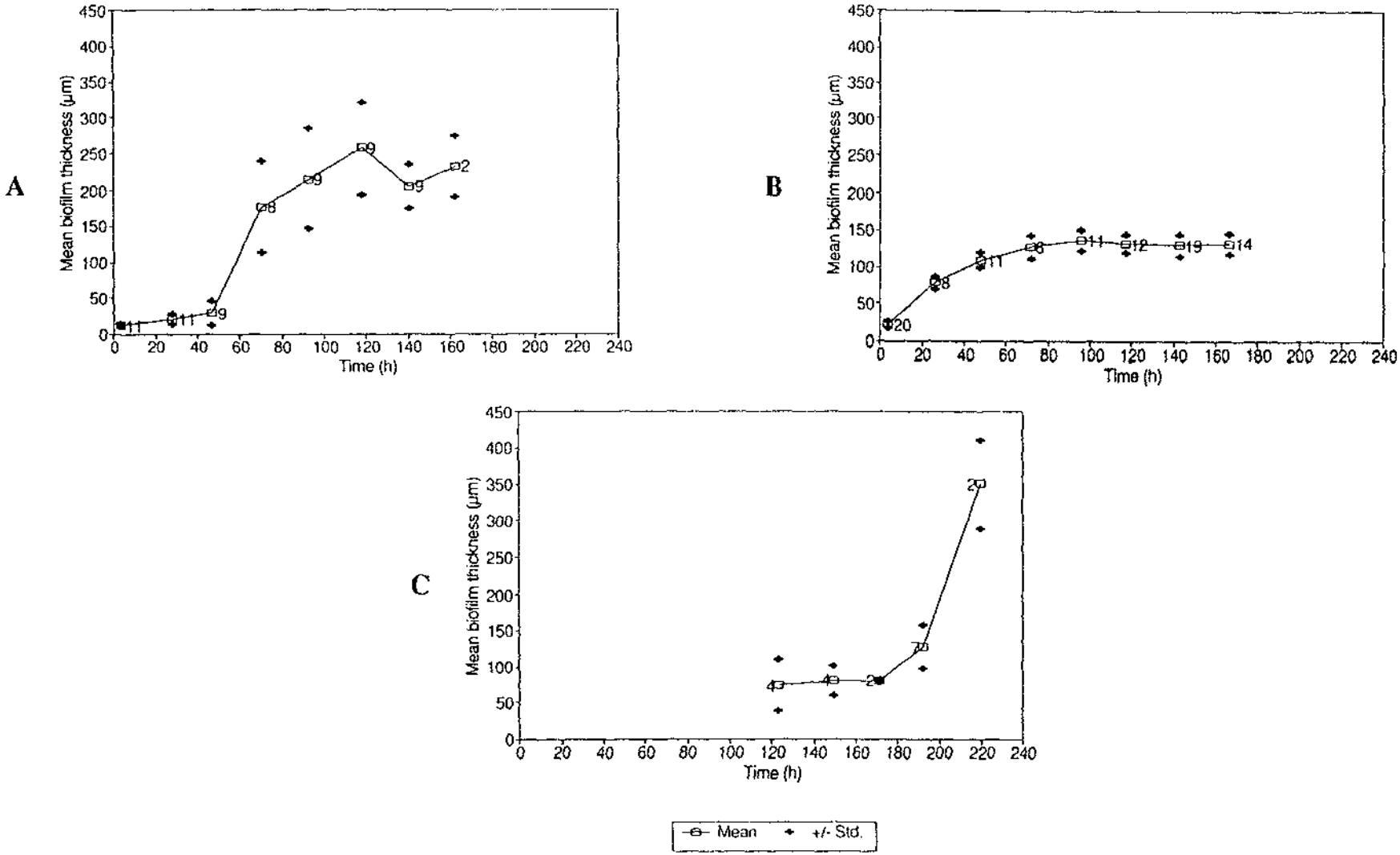

Figure 6.3 Time course of the mean biofilm thickness in the top layer at different reactor temperatures, Interior labels: sample size (**A**: -17.2°C, **B**: 25°C, **C**: 30°C)

Figure 6.4 Photograph of biofilm grown in the top layer at ~17.2°C, time: c. 70 h (72.5x)

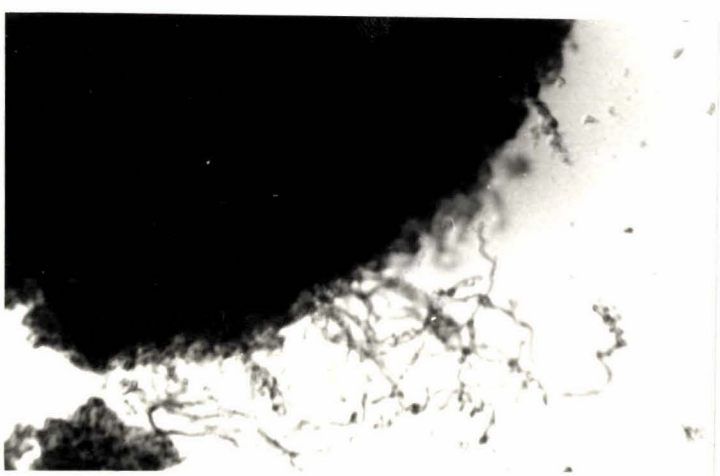

Figure 6.5 Photograph of mycelium-like filaments at the outside of the biofilm, grown in the top layer at ~17.2°C, time: c. 120 h (79x)

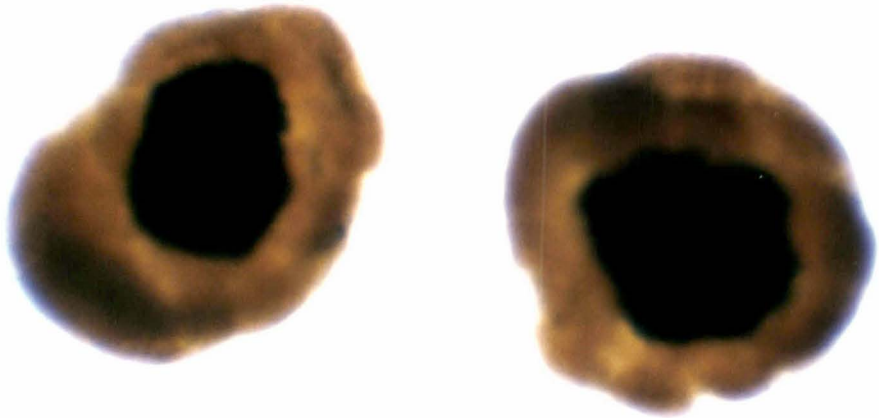

Figure 6.6 Photograph of biofilm grown in the top layer at 25°C, time: c. 120 h (70.5x)

end of the experiment.

In all experiments, the colour of the biofilm was darker in the lower layers than in the top layer. It also darkened with time. Further, within the biofilm, areas of different shades were observed.

6.2.2 Substrate Consumption

The reduction of phenol concentration in the growth medium during its passage through the fluidized bed was only small as can be seen in Figure 6.7. However, high phenol removal was observed at the very start of each experiment, increasingly high with increasing temperature. In the subsequent course of the experiments, the volumetric uptake rates reached about 190 mg/(l·h), 220 mg/(l·h) and 270 mg/(l·h), at ~17.2°C, 25°C and 30°C, respectively. However, in the experiments conducted at 17.2°C average temperature and at 30°C, the phenol uptake decreased towards the end of the experiments to values of about 120 mg/(l·h) and 200 mg/(l·h), respectively. The time course of the volumetric phenol uptake rate for the three temperatures tested is given in Figure 6.8. The volumetric uptake rates relate to the volume of the fluidized bed zone of the reactor, i.e. the area between the mesh and the bottom of the solid-liquid disengagement zone (Figure 3.3).

The measured dissolved oxygen concentrations in the inlet and outlet for all three experiments conducted can be seen in Figure 6.9. The inlet concentration decreased as the temperature rose (9.0-9.6 mg/l at ~17.2°C, 7.9-9.2 mg/l at 25°C, and 7.3-8.5 mg/l at 30°C). It also decreased slightly with time in the experiments conducted at 25°C and 30°C. In these experiments the dissolved oxygen was almost completely consumed after a short operation time of the

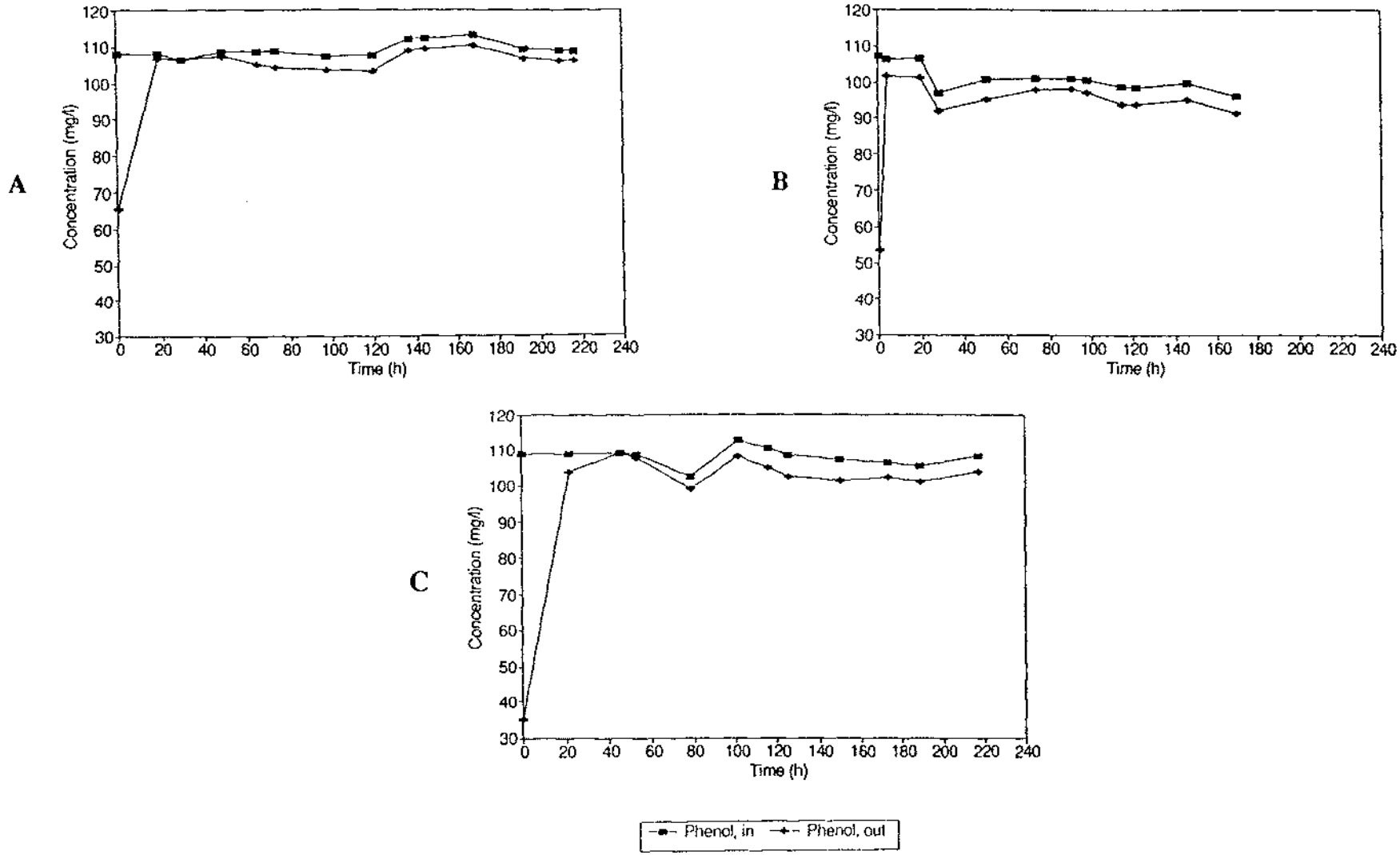

Figure 6.7 Time course of the phenol concentration at different reactor temperatures (**A**: ~17.2°C, **B**: 25°C, **C**: 30°C)

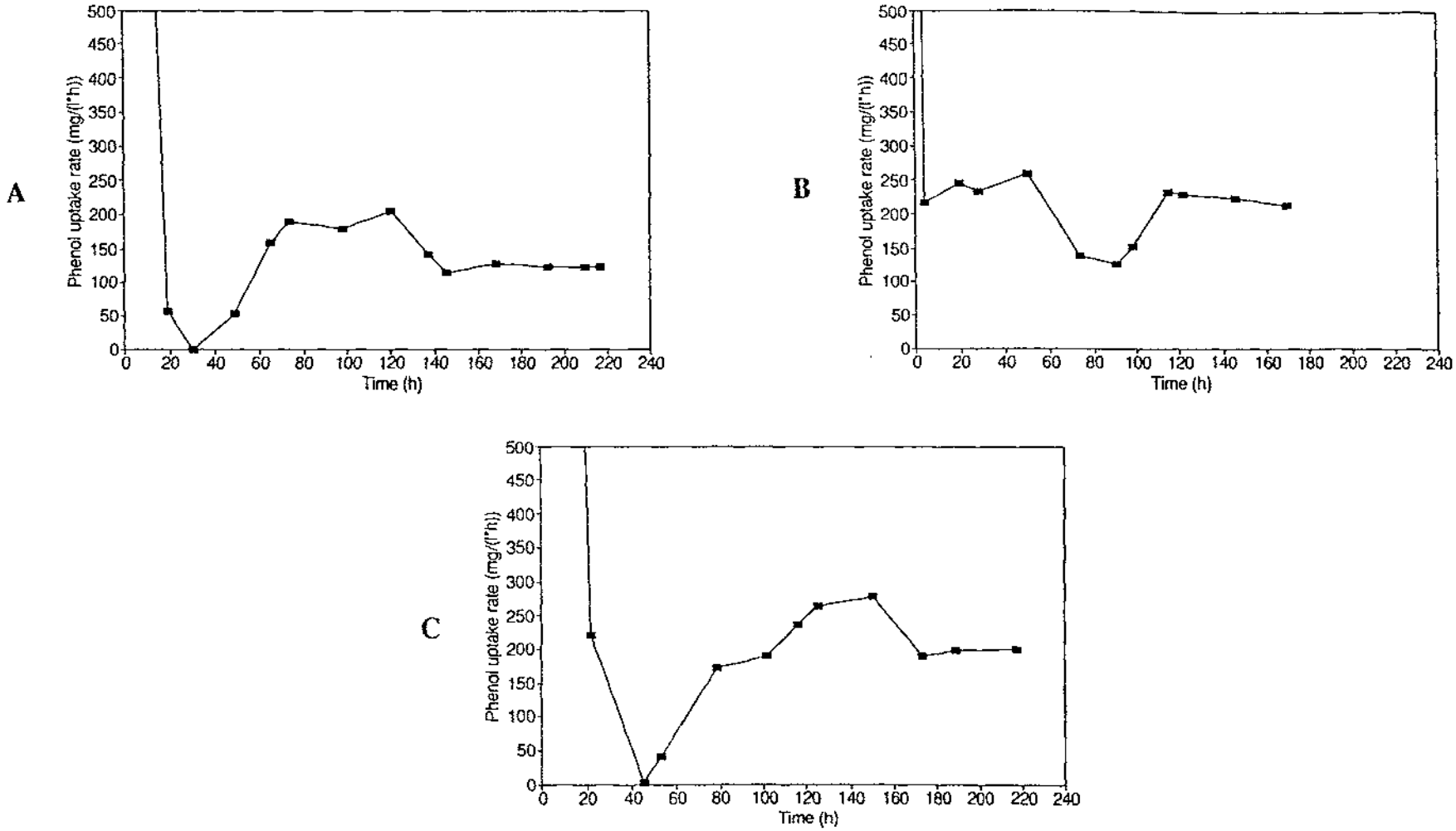

Figure 6.8 Time course of the volumetric phenol uptake rate at different reactor temperatures (**A**: ~17.2°C, **B**: 25°C, **C**: 30°C)

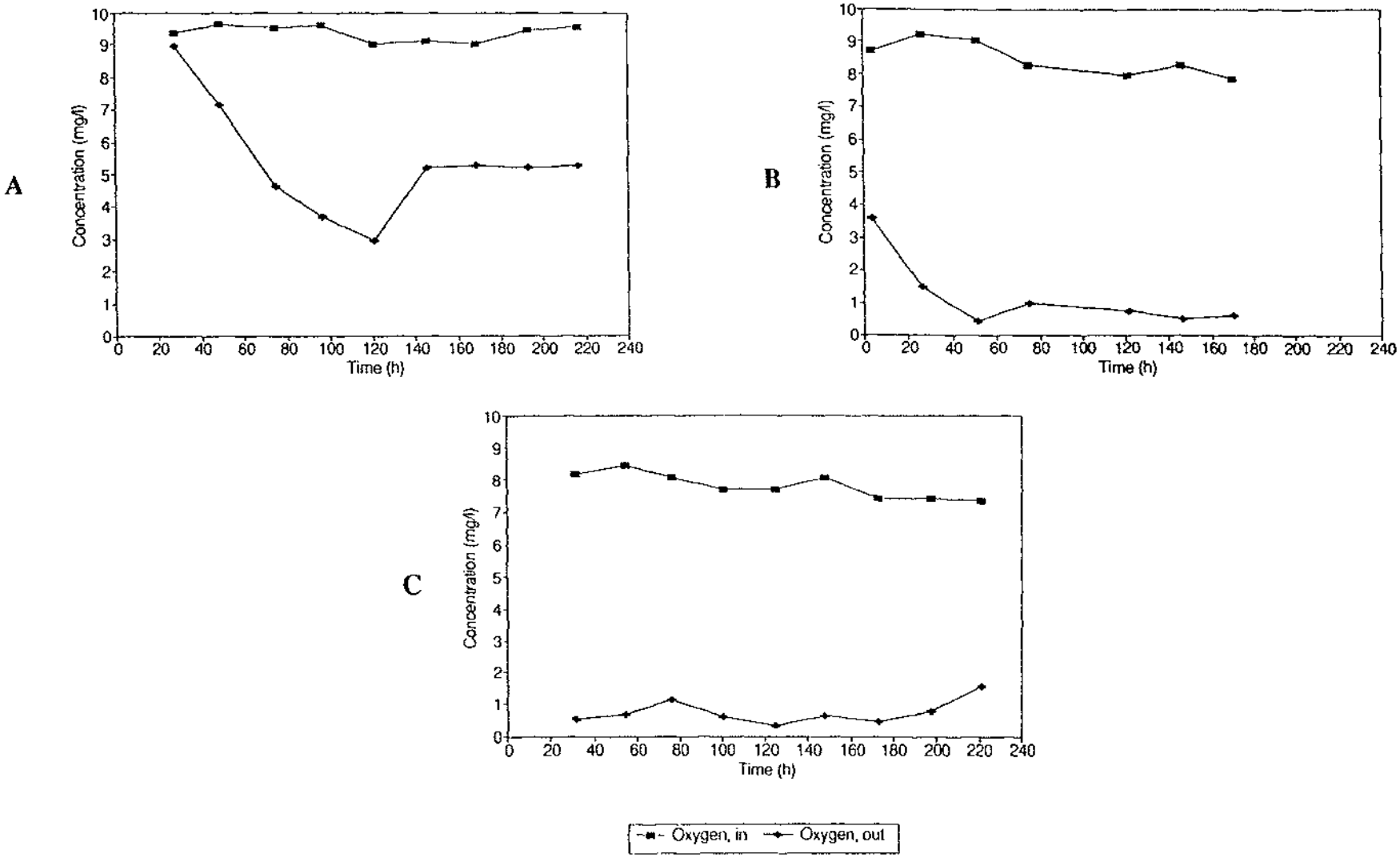

Figure 6.9 Time course of the oxygen concentration at different reactor temperatures (**A**: ~17.2°C, **B**: 25°C, **C**: 30°C)

system, i.e. the oxygen uptake was in general over 90%. However, towards the end of the experiment at 30°C, the oxygen uptake decreased to about 80%. Without temperature control, the oxygen uptake first increased to a value of about 65% before decreasing to about 45%.

The amount of dissolved oxygen required for the degradation of phenol was about 1.5 mg O_2/mg phenol in all three experiments.

6.3 Discussion

In all the experiments conducted, the fluidized bed stratified into different layers. The results show that the stratification did not take place due to differently sized particle cores, but due to differences in the biofilm thickness and structure. The latter causes the bed to stratify, because the overall density of the bioparticles and thus the gravitational force on them, decreases with increasing biofilm thickness and with decreasing biofilm density. Hence, as the biofilm grew, or became thinner due to shearing, bioparticles moved along the height of the fluidized bed zone forming new layers or changing the height and consistency of existing layers. The formation of differently structured layers in a laboratory fluidized bed bioreactor has also been reported by Gorris *et al.* (1988, 1989).

Since a multitude of factors affect biofilm development (see Table 2.5), there are many possible reasons for the observed differences in rate and structure of biofilm development on different support particles, which resulted in stratification of the bed. One of the reasons is that differences in the shape of the support particles and in their surface area and structure may have caused differences in the initial attachment of microorganisms, resulting in different

microbial compositions and proliferation rates. Further, different environmental conditions at different heights of the bed might have influenced the biofilm development.

Where a separate, thin layer of particles at the bottom of the fluidized bed developed, it contained very little growth. The particles in this layer probably consisted on the one hand of particles that had never had much growth on their surface and on the other hand of particles that had lost their biofilm due to shearing. It is assumed that the more turbulent flow patterns observed at the bottom of the fluidized bed zone made it difficult for a marked biofilm to (re)develop in this area.

The observed differences in the darkness of the biofilm were assumed to be caused by different biofilm densities, the biofilm appearing darker as the density increased. Thus, the colour difference between the biofilm in the top layer and the biofilm in the lower layers manifests the observation made by looking at the structure of the biofilm, i.e. that in the top layer a less dense biofilm developed than in the lower layers. Further, the colour revealed that generally the biofilm density increased with time. However, it has to be assumed that the increase in biofilm thickness also contributed to the observed darkening of the biofilm. Finally, biofilm properties did not just vary with different layers and with time, but also within the biofilm of one particle, as can be concluded from the existence of differently shaded areas within the biofilm.

The determined values for the mean biofilm thickness are all slight overestimates since the three-dimensional bioparticles became somewhat flatter when put on a glass slide for microscopy (see Section 3.4.4). Image analysis in combination with the trapezoid formula employed, proved to be very useful for determination of the mean biofilm thickness, giving representative values even

for bioparticles with very nonuniform biofilm thicknesses.

At the three temperatures tested, the biofilm that developed in the top layer of the stratified bed was significantly different. The reason for the different appearance could be, on the one hand, that at different temperatures different microorganism species were favoured, and on the other hand that the same species showed different attachment and growth characteristics at different temperatures. In any event, the results clearly show that temperature had an important effect on biofilm development.

Low temperatures (~17.2°C) seemed to induce the development of a fluffy, loose, irregularly shaped biofilm. Even though the biofilm developed unevenly around the particles with appendage-like structures from the very start, it is assumed that the irregular shape was enforced by the detachment of parts of the loose biofilm in the course of the experiment. The decrease in biofilm thickness after several days and the observation that the remaining film was slightly denser, accompanied by the increase in height of the middle layer and the appearance of the bottom layer containing particles with hardly any growth on their surface, suggests that sloughing of the very loose biofilm took place. The last data point in the biofilm thickness graph of this experiment, which implies that the thickness might have increased again, has to be regarded with strong reservation since the sample size was very small. The high variation in the biofilm thickness per sample was due on the one hand to the fluffy, irregular structure itself and on the other hand to the difficulties that were encountered when sampling the bioparticles, as breaking and detachment of the loose biofilm could not be completely avoided even though extreme care was taken. The latter also suggests that the results might be somewhat inaccurate.

At the highest temperature tested the biofilm was also loose in structure, causing

the same problems as mentioned above. Here, the accuracy of the values for the biofilm thickness is even more in question as the sample size was small throughout the experiment. However, the results clearly show that, conversely to the experiment without temperature control, at the start the biofilm grew comparatively slowly, forming a layer of relatively uniform thickness. The subsequent, sudden expansion of the biofilm after about a week, accompanied by a change in structure to a very fluffy consistency and an irregular shape, was probably due to a switch of the predominant microbial species from nonfilamentous to filamentous organisms. The cause of the sudden switch is unknown, but similar behaviour has been observed by other workers (Fan *et al.*, 1987). Possibly, the nonfilamentous microorganisms outperformed the filamentous ones in the attachment and initial growth phases but once the latter had established themselves they produced a rapidly expanding biofilm. The reason why this phenomenon was observed only in the experiment conducted at 30°C, is likely to be due to the fact that the adhesion capacities and growth characteristics of different species are differently influenced by temperature. At the same time as the sudden biofilm expansion occurred, the bottom layer decreased in height leading to a small layer of particles with hardly any biofilm attached to their surface. This suggests that some particles from the bottom layer moved into the top layer, whereas particles that had been very poorly seeded, and particles that had lost their biofilm due to the increased shear stress caused by the decrease in void space in the top layer, accumulated at the bottom. It is to be assumed that if the experiment had been continued, sloughing of the fluffy biofilm in the top layer would have taken place as was the case in the experiment with no temperature control.

At 25°C, a firm biofilm of relatively uniform thickness was observed in the top layer throughout the experiment. The biofilm grew relatively quickly during the initial stage of the experiment reaching its maximum thickness after a

comparatively short time interval. The final thickness was much lower than in the other two experiments, but because of the differences in densities, the thicknesses cannot be directly compared. The fluidized bed was more uniform than at the other temperatures tested, only developing two layers with the bottom layer being very thin. Therefore, in order to achieve a uniform biofilm development, 25°C proved to be the best temperature out of the three tested.

In all three experiments, only a small reduction in phenol concentration in the growth medium during its passage through the fluidized bed was achieved (Figure 6.7). Yet, the volumetric uptake rates obtained were averagely high (Figure 6.8). This had been expected as the hydraulic retention time in the fluidized bed zone was only 1.33 min. Other workers who achieved much higher reductions at similar inlet phenol concentrations, employed substantially higher hydraulic retention times, resulting in similar volumetric uptake rates (e.g. Livingston and Chase, 1989; S_i = 108.5 mg/l, S_o = 5.84 mg/l, r_S = 284 mg/(l·h), HRT = 21.69 min). The hydraulic retention time used in the present work was based on the preliminary studies (see Chapter 5).

The high phenol removal at the start of each experiment was due to adsorption of phenol to the activated carbon particles. Since adsorption is temperature dependent (Tchobanoglous, 1991), more phenol was removed from the medium as higher temperatures were used. However, it has to be taken into consideration that the first measurement of phenol concentrations was taken half an hour after start of the experiments and that the adsorption of phenol onto activated carbon is a rather fast process (Ehrhardt and Rehm, 1985). Thus, the measurements represent an instantaneous value only.

The fluctuations in the inlet phenol concentration can be explained by inaccuracies in the liquid volume measurement when mixing the growth

medium due to the procedure employed (see Section 3.3.5). Further, the hygroscopic nature of phenol causes errors when measuring the amount of phenol required.

The highest phenol uptake rate was reached in the experiment conducted at 30°C, followed by the one at 25°C and then the one at 17.2°C average temperature. This was according to expectations since biochemical reactions and diffusional processes proceed at more rapid rates as temperature rises. Further, in the experiment at 30°C a slightly higher amount of support material was used, providing more surface for microbial growth and thus in turn contributing to an increased phenol uptake. However, in this case the uptake rate was not retained at its high level until the end of the experiment. The decrease was obviously caused by the sudden development of fluffy, thick biofilm, i.e. by the change in the composition of the microbial population. Fan *et al.* (1987) also observed a decrease in biodegradation rate after the sharp increase in biofilm thickness. Consequently, at the end of the experiments the highest phenol uptake rate was observed at 25°C.

A decrease in phenol uptake also took place in the experiment with no temperature control, caused by sloughing of the biofilm. An explanation for the phenol uptake rate passing through a trough in the experiment at 25°C cannot be given. However, since the differences between inlet and outlet phenol concentrations were only small, the accuracy of the results has to be questioned and not too much significance can be placed on the results of the phenol uptake rate.

Since the biofilm at 25°C grew rapidly immediately after the start of the experiment, the phenol uptake did not decrease as much as in the other two experiments after the adsorptive capacity of the carbon had been reached. In the

latter experiments, the observed phenol uptake decreased to zero even though growth took place at the time. This is attributed to the fact that the microorganisms were utilizing phenol previously adsorbed to the activated carbon and that at the same time the adsorption equilibrium changed because the increasing growth on the carbon particles hindered the phenol adsorption (Ehrhardt and Rehm, 1989; Kindzierski *et al.*, 1992).

The observed decrease in inlet dissolved oxygen concentration with increasing temperature was expected as the solubility of oxygen decreases as temperature rises. The slight decrease in oxygen concentration with time in the experiments at 25°C and 30°C was caused by microorganisms that started growing in the aeration tank and in the gas-liquid disengagement tank after some time.

The fact that the dissolved oxygen concentration in the outlet was low whereas the phenol concentration was high leads to the conclusion that the phenol degradation was oxygen-limited. This conclusion is supported by the findings of other workers (see Section 2.3.3). Livingston and Chase (1989), for example, found that above a critical value of bulk phenol concentration to bulk oxygen concentration of 0.9-1.1, the biofilm kinetics changes from phenol-limited to oxygen-limited. In the present work this ratio was much higher. In order to increase the bulk oxygen concentration, the inlet oxygen concentration would need to be increased. This in turn requires a different aeration device, as with the system employed in this study the dissolved oxygen concentration cannot be increased above the normal saturation concentration in the presence of air due to the medium passing through an open system after aeration.

The observed decrease in oxygen uptake in the experiments at ~17.2°C and at 30°C occurred at about the same time as the phenol uptake decreased in these experiments. Hence, it was obviously caused by the same reason, i.e. sloughing

at ~17°C, and change in composition of the microbial population at 30°C.

The amount of oxygen required for the degradation of phenol found in this study (1.5 mg O_2/mg phenol) was in agreement with the values found by other workers. Klein *et al.* (1979), for example, reported a value of 1.36 mg O_2/mg phenol for a pure culture of *Candida tropicalis*, Suzuki *et al.* (1983) a value of 1.23 mg O_2/mg phenol for a mixed culture, and Tang *et al.* (1987a,b) a value of 1.4 mg O_2/mg phenol also for a mixed culture. Theoretically, complete oxidation of phenol requires 2.38 mg O_2/mg phenol. However, not all the phenol is oxidized, mainly due to biofilm growth. Thus, the theoretic value of complete oxidation is not expected to be reached (Tang and Fan, 1987a).

6.4 Conclusion

In all three experiments conducted (at 30°C, at 25°C and without temperature control, i.e. at 17.2°C average temperature), the fluidized bed stratified into two or three layers. In the layers closer to the bottom, the biofilm was thinner and appeared denser, whereas no significant differences were observed in the size of the particle cores between the different layers. It was assumed that the differences in the biofilm were mainly due to different microbial compositions, caused by differences in the many factors influencing biofilm development.

In the top layer of the stratified bed, the biofilm developed differently at the different temperatures tested with regard to rate, thickness and structure. Again, the predominance of different species was regarded as the main reason for the differences. At 17.2°C average temperature and at 30°C, a loose, fluffy, unevenly shaped, thick biofilm developed after different operating times, resulting in sloughing of the biofilm in the former experiment. Conversely, the

biofilm grown at 25°C was firm and relatively even in shape and structure. Here, the initial growth rate appeared much faster than in the other two cases. However, the final thickness remained far below the thicknesses reached by the fluffy biomass. Image analysis techniques proved to be a very useful tool to determine the mean biofilm thickness on bioparticles.

Apart from the very start of the experiments where adsorption of phenol to the activated carbon caused the phenol uptake to be large, the reduction in phenol concentration was small due to a very short hydraulic retention time. However, the volumetric phenol uptake rates reached were comparable with results obtained by other researchers. In accordance with expectation, the peak uptake rates increased with increasing temperature. Yet, sloughing and development of extremely fluffy biofilm were followed by decrease in phenol uptake in the experiments conducted at ~17.2°C and at 30°C, respectively. Thus, the phenol uptake at the end of the experiments was the highest at 25°C.

The inlet dissolved oxygen concentration decreased slightly as the temperature rose in agreement with theory. The outlet concentration was low in all three experiments (though considerably higher at 17.2°C average temperature). As, at the same time, the phenol concentration in the outlet was high, the system was regarded as oxygen-limited. A better aeration device would have to be used to increase the inlet dissolved oxygen concentration and thus supply more oxygen to the microorganisms.

Since the biofilm that developed at 25°C showed the most favourable characteristics, this temperature was employed in the subsequent study of the effect of different inlet phenol concentrations on the performance of the fluidized bed system.

CHAPTER 7

FLUIDIZED BED STUDIES USING DIFFERENT INLET PHENOL CONCENTRATIONS

7.1 Introduction

After investigation of the influence of different reactor temperatures, it was of interest to examine the effect of different inlet phenol concentrations on the biofilm development, and on the performance of the fluidized bed system during start-up in general. It is commonly recognized that the substrate loading rate influences not only the growth rate but also the structure of the developing biofilm. Trulear and Characklis (1982), for example, observed in a system without inhibition that the biofilm density increased with substrate loading rate. However, literature reporting on the direct examination of the relationship between substrate loading and biofilm properties appears to be extremely scarce.

The growth characteristics at different phenol concentrations of the culture grown freely suspended in batch fermentation have been investigated previously (Chapter 4). The results of that study were used as a rudimentary guideline for the concentrations to be used and for the behaviour to expect. However, it is known that the relationship between substrate concentration and growth in biofilm systems differs from that in suspended growth systems. This difference is mainly caused by the buffering qualities of biofilm systems, which in turn are predominantly due to adsorption of substrate to the carrier material and to diffusional limitations.

Thus, the present study was conducted not only to investigate the influence of the inlet phenol concentration on the performance of the fluidized bed system during start-up, but also to gain an impression of the difference between the response of the previously tested suspended growth system and the employed attached growth system to varying phenol concentrations.

7.2 Results

Inlet phenol concentrations of about 35 mg/l, 100 mg/l, 330 mg/l and 520 mg/l were used in four separate experiments. As a result of the preceding investigations of the effect of different reactor temperatures on the performance of the fluidized bed system (Chapter 6), a reactor temperature of 25°C was employed. Thus, the data presented for an inlet phenol concentration of 100 mg/l are the same as those presented in Chapter 6 for a reactor temperature of 25°C. The experimental conditions are described in Section 3.3.

7.2.1 Biofilm Development

As in the experiments investigating the effect of different reactor temperatures, the biofilm did not develop evenly throughout the fluidized bed. Again, in all the experiments, two or three layers (always a bottom and a top layer, and in some cases a middle layer) containing particles of different biofilm thickness formed within the fluidized bed. In the experiment using 330 mg/l inlet phenol concentration, the height of the fluidized bed decreased suddenly after eight days (c. 190 h). This was accompanied by the development of additional layers. However, the differences between these layers were not as clear as in all other cases. At this stage of the experiment, bioparticles with loose biofilm moved

upwards through the unoccupied upper area of the fluidized bed zone and the solid-liquid disengagement zone, and were washed out. This wash out of particles continued for two days.

As described in Section 6.2.1, due to a small number of particles circulating to the top of the fluidized bed zone shortly after the start of the experiment (the number increasing with time), no gradual increase of bed height with growth of biofilm took place. The only exception was the experiment conducted at 520 mg/l inlet phenol concentration. Here, the height of the fluidized bed increased gradually after it had initially remained unchanged for eight days (c. 190 h). The time course of the heights of the different layers within the fluidized bed for all four experiments is given in Figure 7.1.

In the experiment with an initial phenol concentration of 520 mg/l, during the first six days (c. 140 h) very few of the activated carbon particles were washed out due to tiny air bubbles being attached to their surface. For the first ten days (c. 230 h) large air bubbles formed continuously under the mesh at the bottom of the fluidized bed, causing the bed to be relatively turbulent. When growth commenced after about six days (c. 140 h), particles with well grown biofilm accumulated at the top of the activated carbon bed. Free biomass flakes circulated between the top of the expanding bed and the top of the fluidized bed zone. Until day 13 (c. 300 h) the transition between the bottom and the top layer was fluent. The top layer contained bioparticles of a wide range of biofilm thicknesses throughout the experiment, although becoming more uniform with time. A photographic illustration of the development of the fluidized bed in this experiment can be seen in Figure 7.2.

Bioparticles from the top layer were sampled daily in all experiments. However, in the experiment using 520 mg/l inlet phenol concentration, sampling was

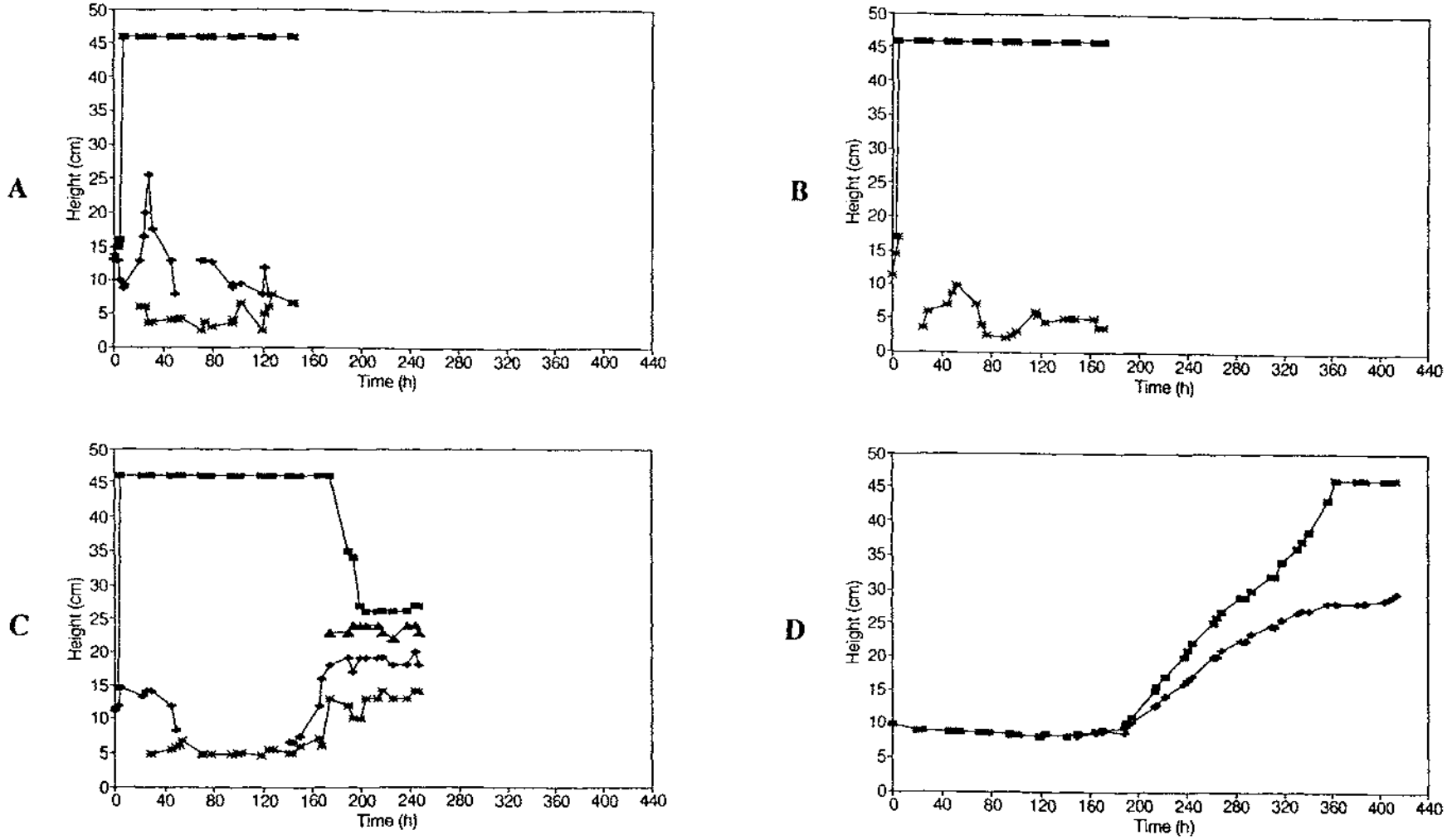

Figure 7.1 Time course of the heights of the different layers of the fluidized bed at different inlet phenol concentrations (**A**: 35 mg/l, **B**: 100 mg/l, **C**: 330 mg/l, **D**: 520 mg/l)

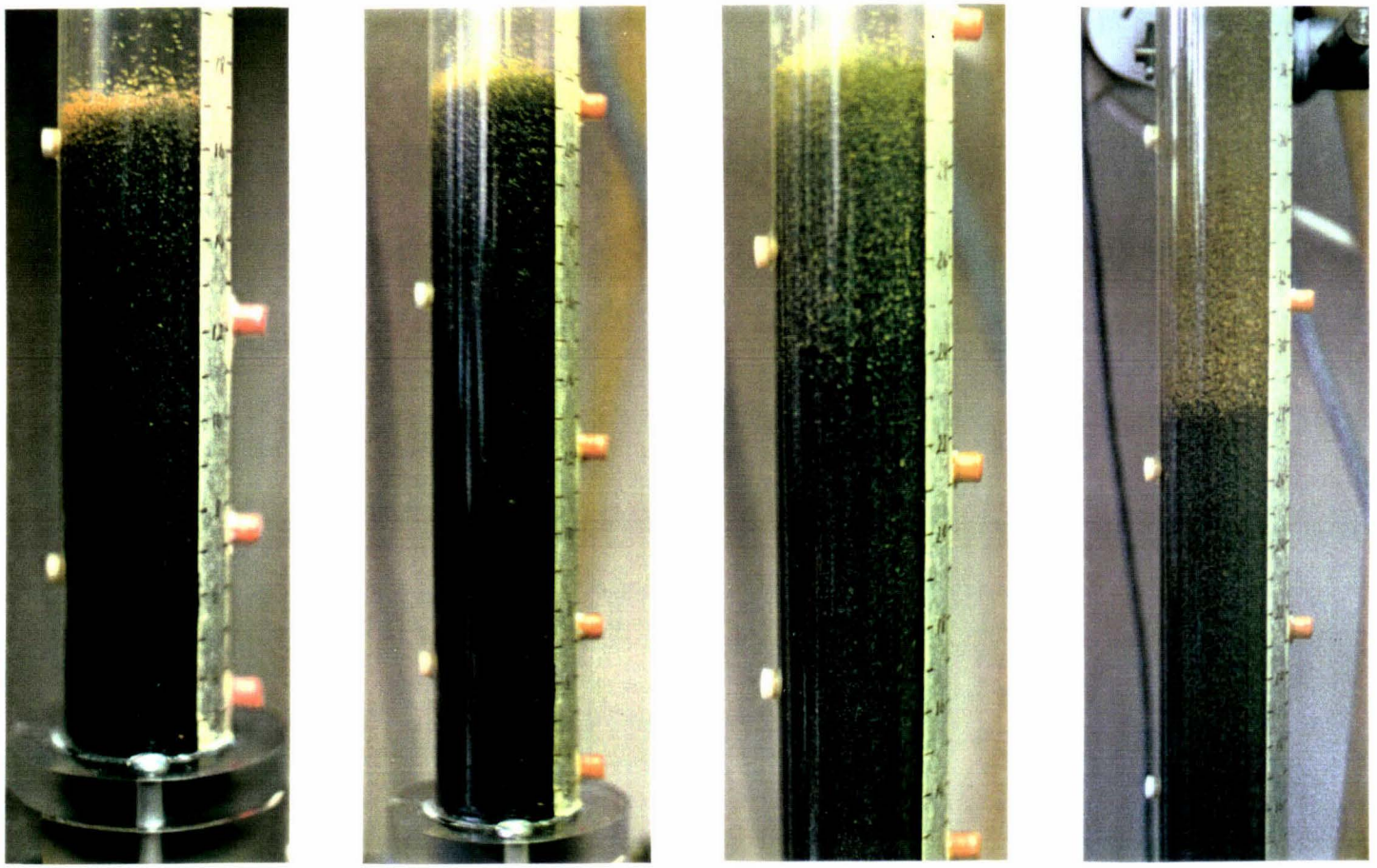

c. 220 h c. 240 h c. 290 h c. 380 h

Figure 7.2 Photographic illustration of the development of the fluidized bed in the experiment using 520 mg/l inlet phenol concentration

started only on day ten (c. 220 h) due to a lack of obvious growth prior to this time. The measured mean biofilm thicknesses over time for all four experiments are shown in Figure 7.3. It can be seen that the biofilm thickness increased the fastest at 100 mg/l inlet phenol concentration, followed by 35 mg/l, then 330 mg/l, and finally 520 mg/l. However, the thickness reached was the least at 100 mg/l inlet phenol concentration. At 35 mg/l the biofilm thickness was slightly greater, followed by 520 mg/l and then 330 mg/l. The colour of the biofilm darkened with time in all experiments. The differences between the structure of the biofilm grown at different phenol concentrations were not as strong as the differences observed in the experiments described in Chapter 6. However, obvious differences were apparent.

The loosest, least dark and most fragile biofilm was observed in the experiment with an inlet phenol concentration of 330 mg/l. However, contrary to the loose biofilm which developed in the experiments using different reactor temperatures (Chapter 6), the outline of the biofilm was smooth and the biofilm developed relatively evenly around the activated carbon particles. From day four (c. 80 h) bioparticles with broken biofilm were noticed under the microscope. Figure 7.4 shows bioparticles from this experiment; apart from undamaged ones, one with biofilm in the process of breaking and one which has lost part of its biofilm are shown. Some particles carried biofilm of even looser looking structure as can be seen in Figure 7.5. From day eight (c. 170 h) the contour of the biofilm was rough. From day nine (c. 190 h) the biofilm was bulky and of uneven thickness, but started to appear more dense (Figure 7.6). However, avoiding damage of the biofilm when sampling continued to be difficult.

The biofilm that developed at an inlet phenol concentration of 35 mg/l (Figure 7.7) was less dense than that at 100 mg/l (Figure 6.6). On the last day of the former experiment the biofilm density seemed to be considerably less than on

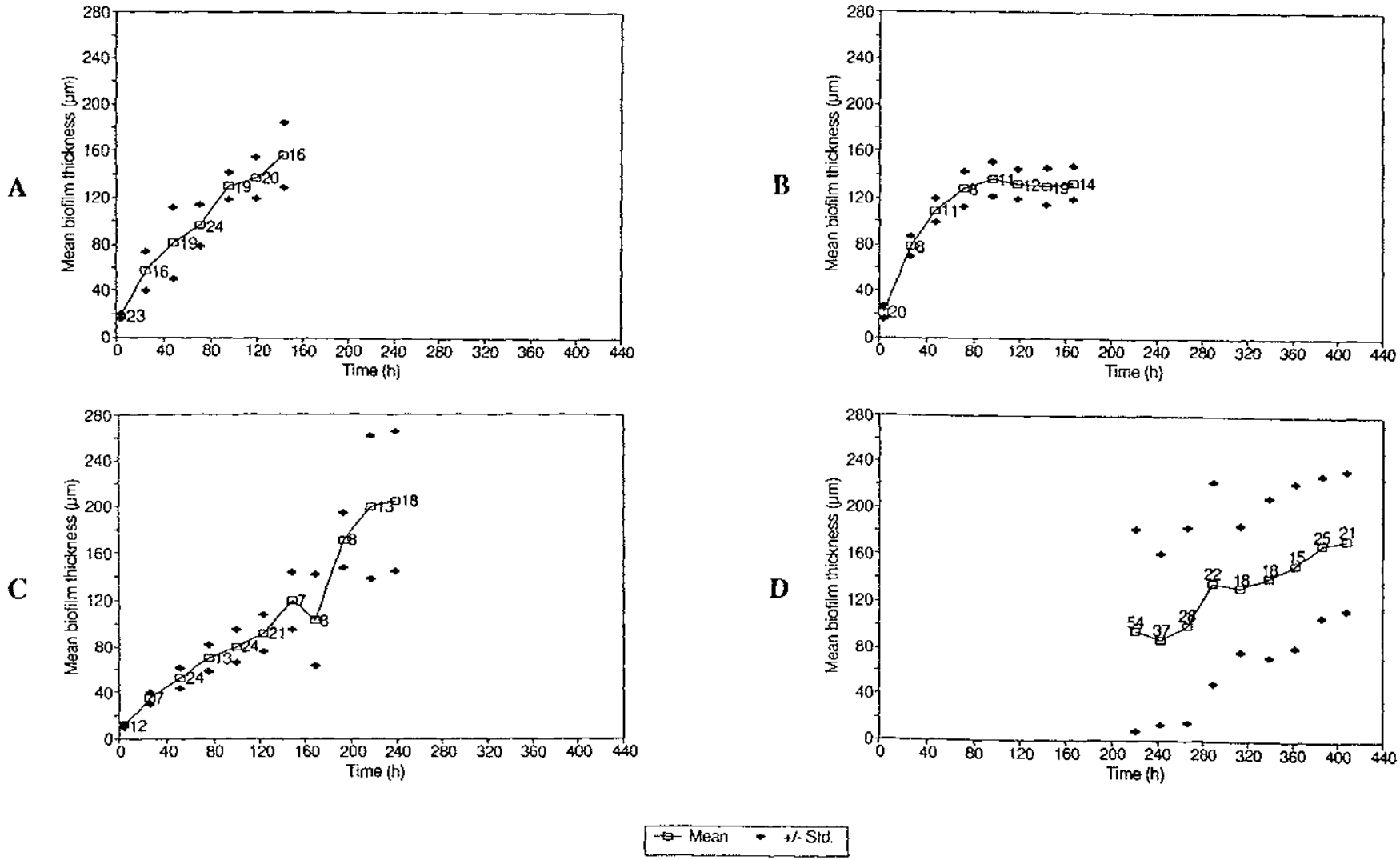

Figure 7.3 Time course of the mean biofilm thickness in the top layer at different inlet phenol concentrations, Interior labels: sample size (**A**: 35 mg/l, **B**: 100 mg/l, **C**: 330 mg/l, **D**: 520 mg/l)

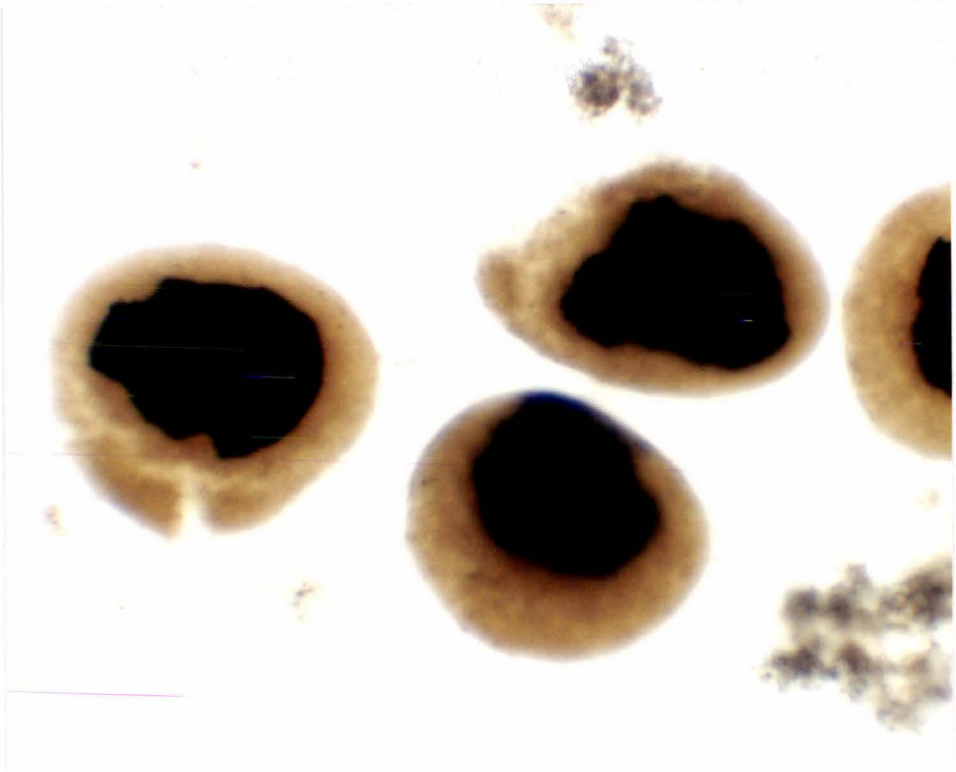

Figure 7.4 Photograph of biofilm grown in the top layer at 330 mg/l inlet phenol concentration, time: c. 120 h (70.5x)

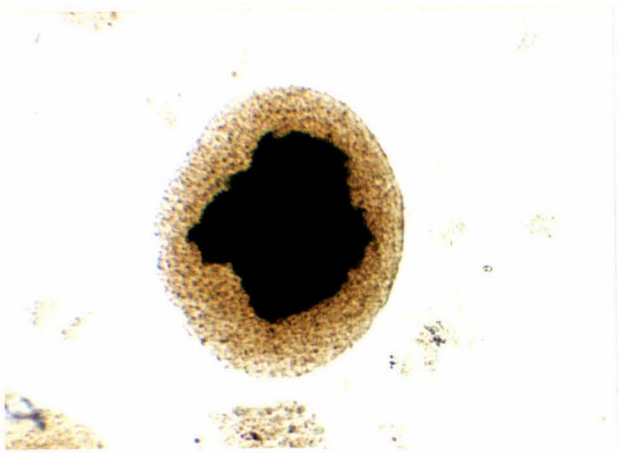

Figure 7.5 Photograph of very loose looking biofilm grown in the top layer at 330 mg/l inlet phenol concentration, time: c. 100 h (70.5x)

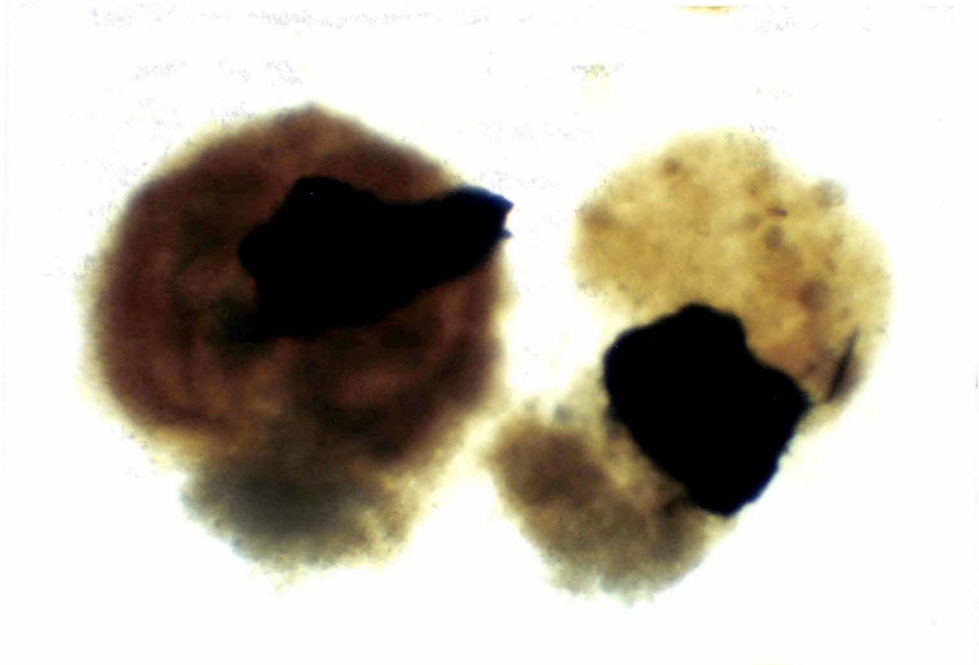

Figure 7.6 Photograph of bulky biofilm grown in the top layer at 330 mg/l inlet phenol concentration, time: c. 190 h (70.5x)

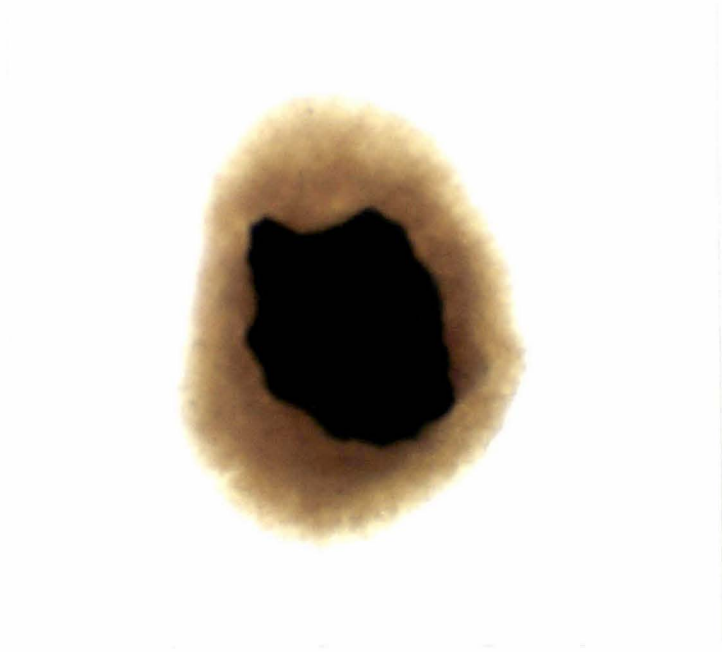

Figure 7.7 Photograph of biofilm grown in the top layer at 35 mg/l inlet phenol concentration, time: c. 120 h (70.5x)

the preceding days. In both cases the biofilm was of relatively uniform thickness and its contour was smooth. However, in the experiment conducted at 100 mg/l inlet phenol concentration the outline of the bioparticles was slightly more irregular than in the experiment conducted at 35 mg/l. No breakage of the biofilm was observed in either of the two experiments.

The densest looking biofilm occurred at 520 mg/l inlet phenol concentration. The outline of the bioparticles was initially crenate, becoming smoother with time. Due to the very dark shade of the biofilm the interface between the activated carbon core and the biofilm could only be guessed at or, in most cases, was not visible at all. Where judgement was possible, the thickness of the biofilm seemed to be relatively uniform per particle. Breakage of the biofilm did not occur. An example of a bioparticle from this experiment can be seen in Figure 7.8.

From the bottom layer, bioparticles were sampled daily in the experiment conducted with an inlet phenol concentration of 520 mg/l, commencing after eleven days (c. 260 h). The biofilm in this layer was smoother and of slightly different colour than in the top layer, as can be seen in Figure 7.9. The mean biofilm thickness at the end of the experiment was about half of that in the top layer. The time course of the mean biofilm thickness in the bottom layer is given in Figure 7.10.

In the other experiments, in the case of a middle layer being present, a few samples were taken from this layer. In all these cases, the biofilm was thinner, darker and smoother than in the top layer. The only exception occurred in the experiment conducted at 330 mg/l inlet phenol concentration. When the second layer from the bottom reappeared in the latter experiment after about six days (c. 140 h), it consisted of particles covered by a thicker biofilm than the

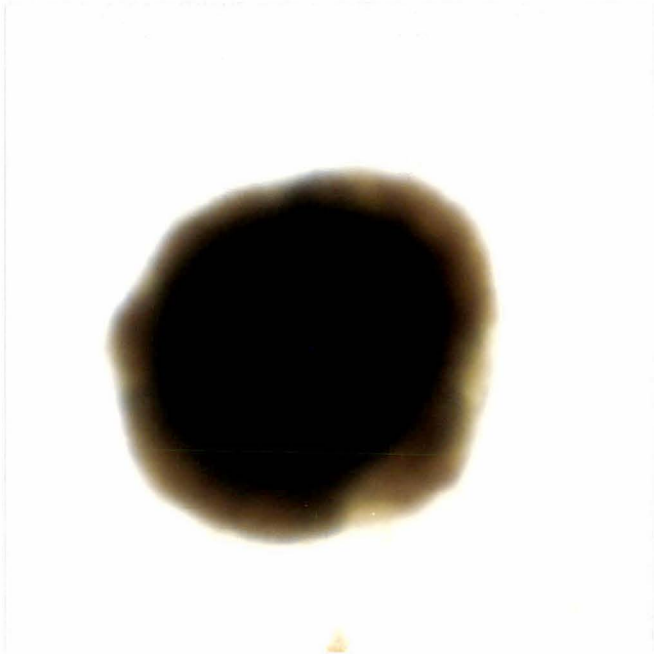

Figure 7.8 Photograph of biofilm grown in the top layer at 520 mg/l inlet phenol concentration, time: c. 360 h (70.5x)

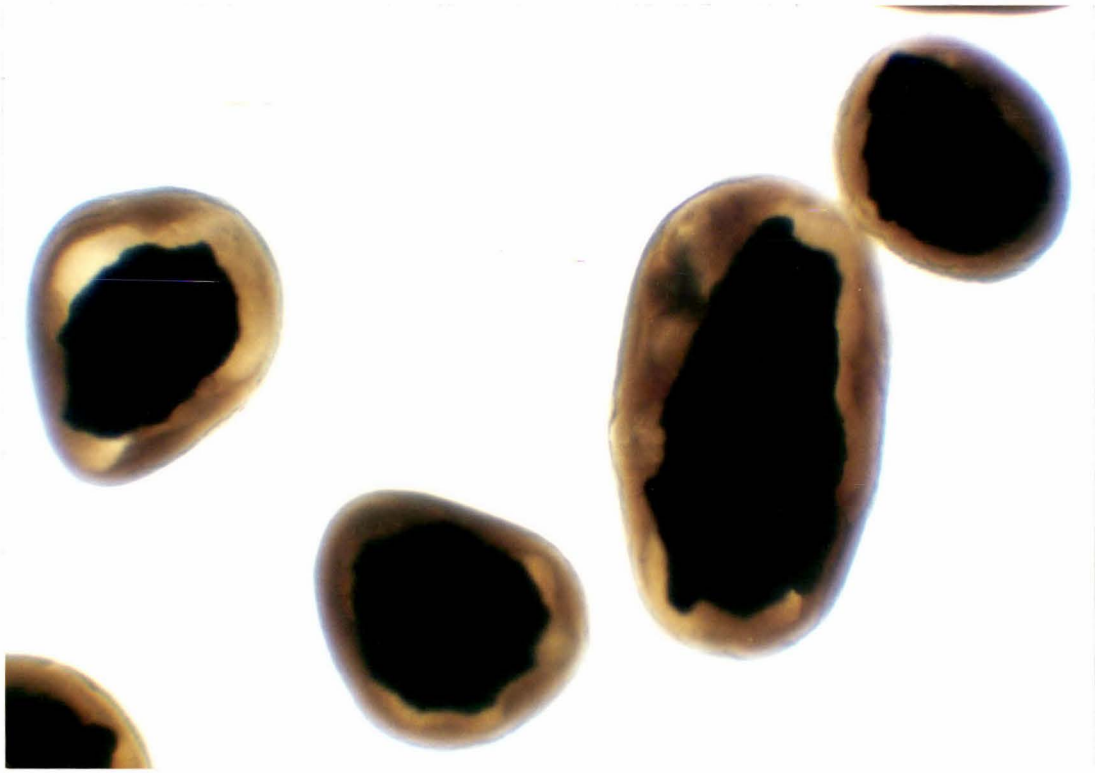

Figure 7.9 Photograph of biofilm grown in the bottom layer at 520 mg/l inlet phenol concentration, time: c. 410 h (70.5x)

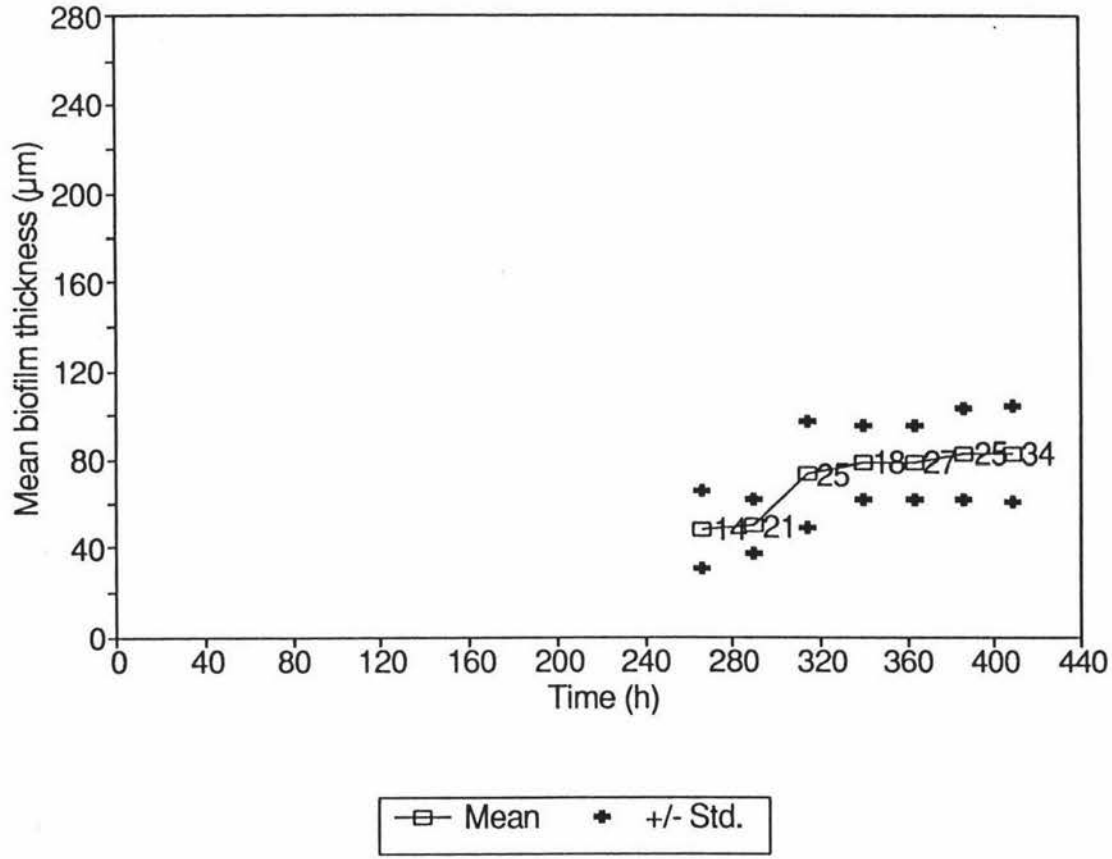

Figure 7.10 Time course of the biofilm thickness in the bottom layer at 520 mg/l inlet phenol concentration

particles in the rest of the fluidized bed. In the subsequent course of the experiment this layer contained some particles with extremely thick biofilm. An example can be seen in Figure 7.11. The lines and different shades in the picture are the result of a number of photographs being combined.

Without needing magnification, it was clearly visible that the particles in the very bottom layer of the experiments using an inlet phenol concentration of 35 mg/l, 100 mg/l and 330 mg/l had hardly any biomass on their surfaces.

7.2.2 Substrate Consumption

The phenol concentration in the medium below and above the fluidized bed during the course of all four experiments is given in Figure 7.12. It can be seen that in all cases the reduction in phenol concentration was large immediately after starting the experiments, but small during the course of the experiments. In the experiment conducted at an inlet phenol concentration of 35 mg/l, the volumetric phenol uptake rate reached about 230 mg/(l·h), but decreased to about 170 mg/(l·h) at the end of the experiment. With inlet phenol concentrations of 100 mg/l, 330 mg/l and 520 mg/l, volumetric uptake rates of about 220 mg/(l·h), 160 mg/(l·h) and 210 mg/(l·h) were achieved, respectively. The peak volumetric uptake rate was reached the fastest in the experiment conducted at 100 mg/l inlet phenol concentration, followed by the one at 35 mg/l, then 330 mg/l and finally 520 mg/l. For all four experiments, the course of the volumetric uptake rates is given in Figure 7.13. The volumetric uptake rates relate to the volume of the fluidized bed zone of the reactor, i.e. the area between the mesh and the bottom of the solid-liquid disengagement zone (Figure 3.3).

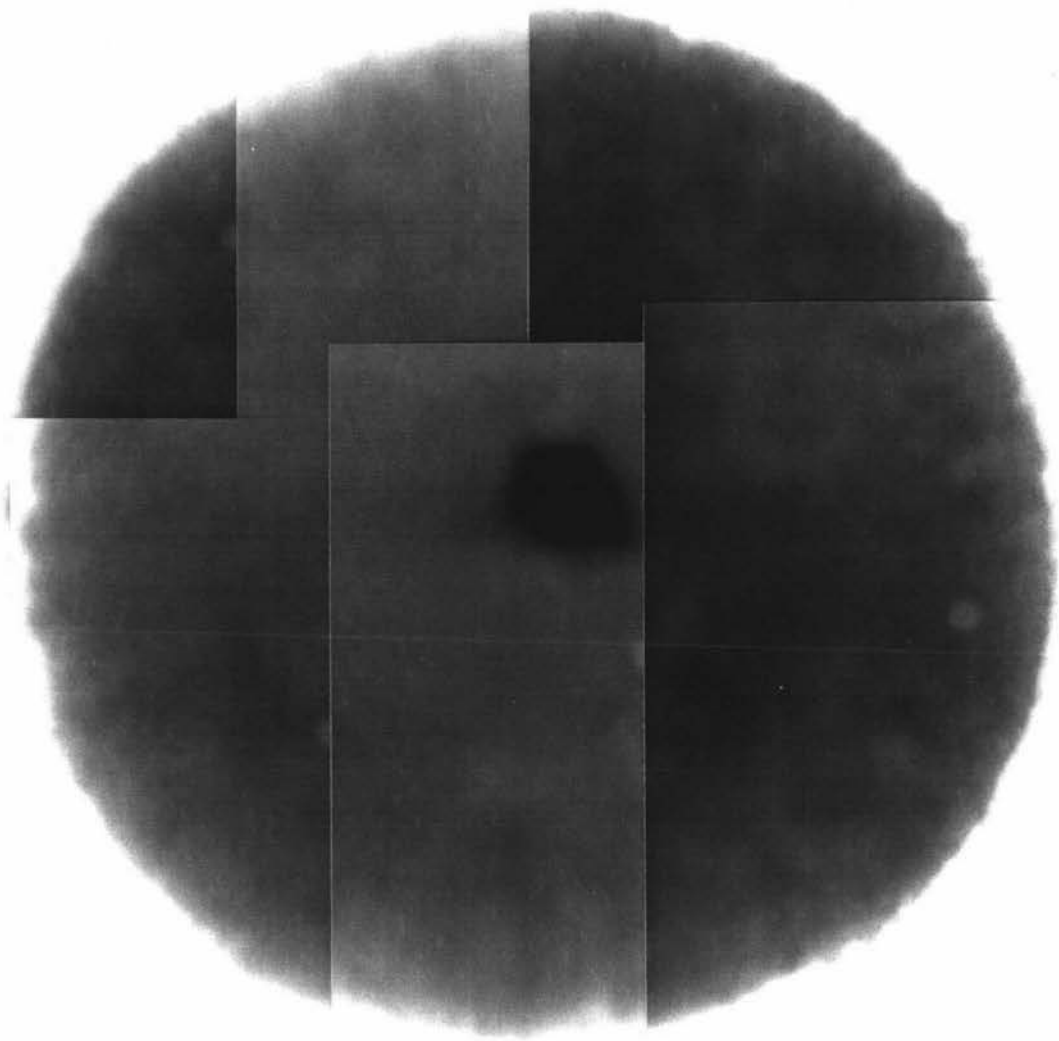

Figure 7.11 Photograph of bioparticle with extremely thick biofilm found in the second layer from the bottom at 330 mg/l inlet phenol concentration, time: c. 240 h (49x)

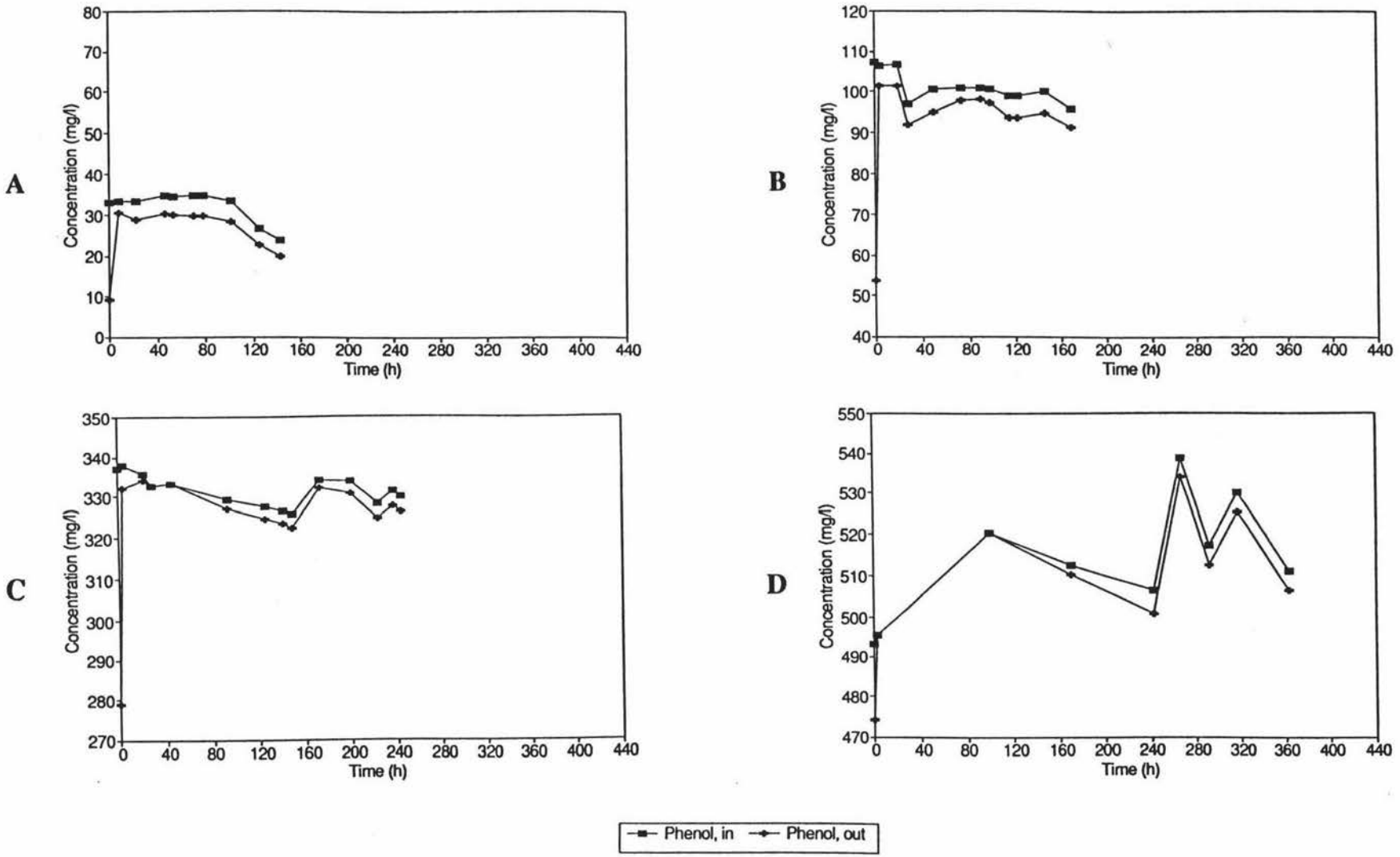

Figure 7.12 Time course of the phenol concentration at different inlet phenol concentrations (**A**: 35 mg/l, **B**: 100 mg/l, **C**: 330 mg/l, **D**: 520 mg/l)

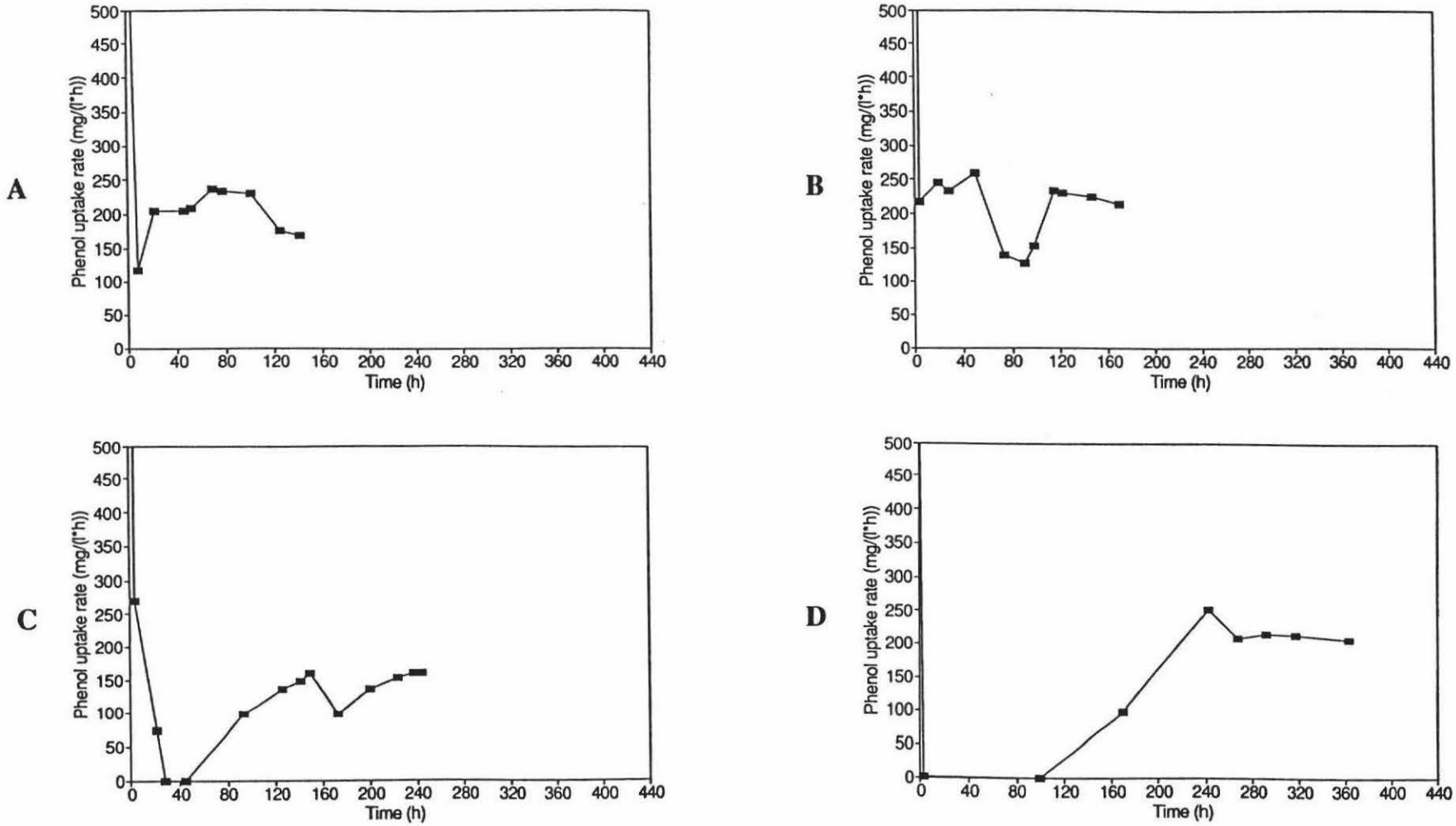

Figure 7.13 Time course of the volumetric phenol uptake rate at different inlet phenol concentrations (A: 35 mg/l, B: 100 mg/l, C: 330 mg/l, D: 520 mg/l)

The inlet and outlet dissolved oxygen concentrations can be seen in Figure 7.14. The inlet concentration decreased drastically in the course of the experiment conducted at an inlet phenol concentration of 35 mg/l, and to a small extent in the experiment conducted at 100 mg/l. The oxygen uptake reached values of over 90% in all experiments excluding the one conducted at an inlet phenol concentration of 330 mg/l. This almost complete oxygen uptake was reached after the shortest amount of time in the experiment using an inlet phenol concentration of 100 mg/l, followed by the one using 35 mg/l and then the one using 520 mg/l. Using an inlet phenol concentration of 330 mg/l, the oxygen uptake reached only about 70%.

The amount of dissolved oxygen required for the degradation of phenol was about 1.3 mg O_2/mg phenol at 35 mg/l inlet phenol concentration, about 1.5 mg O_2/mg phenol at 100 mg/l, and about 1.6 mg O_2/mg phenol at inlet phenol concentrations of 330 mg/l and 520 mg/l.

7.3 Discussion

The possible reasons for the fluidized bed to stratify into layers of particles of different biofilm thickness and different biofilm structure have been discussed in Section 6.3, as have the observed differences in darkness of the biofilm. Contrary to the rule, in the second half of the experiment using an inlet phenol concentration of 330 mg/l, the second layer from the bottom contained the particles with the thickest biofilm. This must mean that the density of this biofilm was much higher than the density of the biofilm in the top layer(s). An explanation for the formation of some giant bioparticles cannot be given.

The sudden decrease in bed height in the same experiment was caused by the

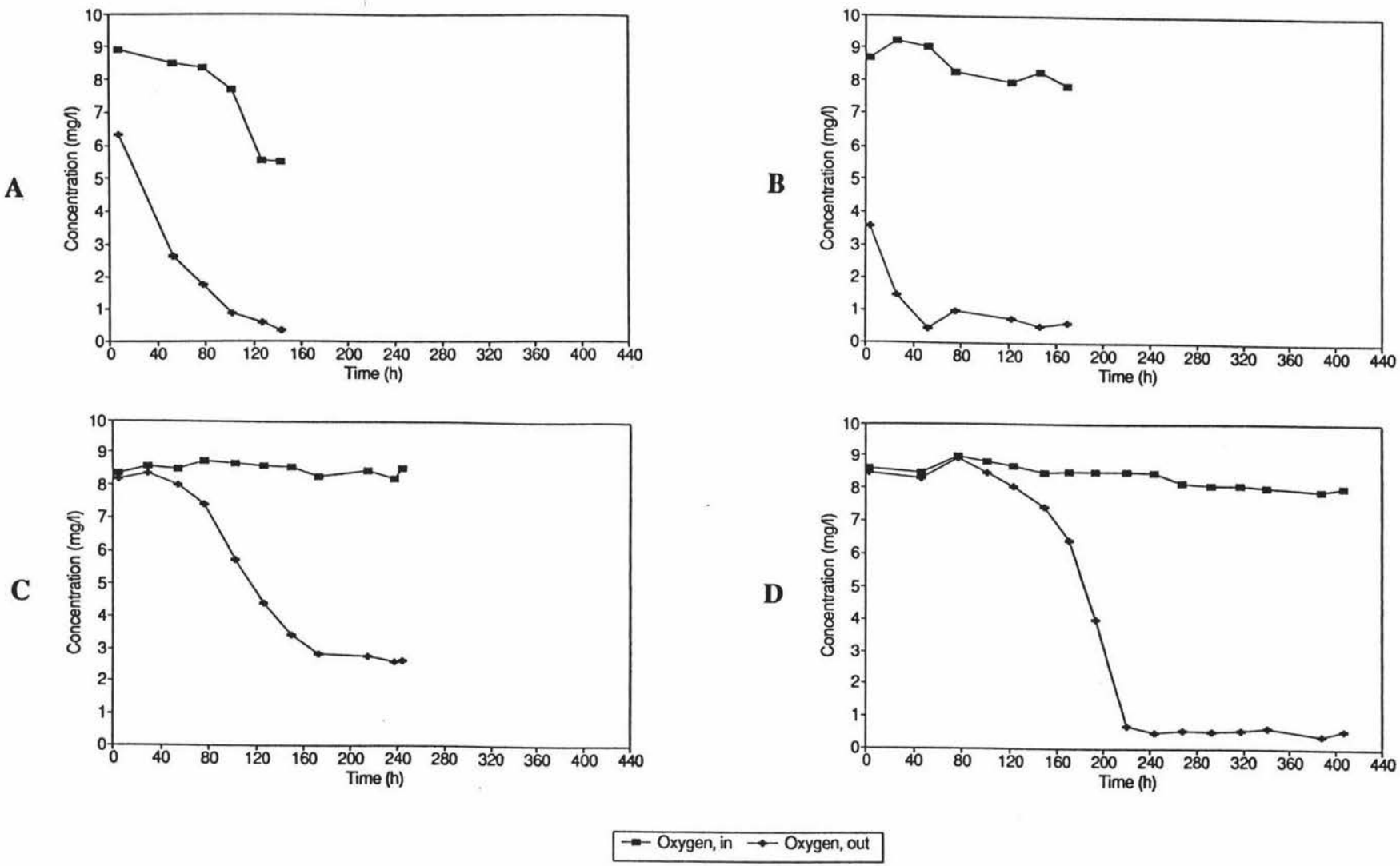

Figure 7.14 Time course of the oxygen concentration at different inlet phenol concentrations (**A**: 35 mg/l, **B**: 100 mg/l, **C**: 330 mg/l, **D**: 520 mg/l)

wash out of bioparticles with very loose biofilm. At the same time as the bed height decreased, an additional layer formed within the fluidized bed and the height of the two layers closest to the bottom suddenly increased. From this the conclusion can be drawn that detachment and subsequent wash out of parts of the looser biofilm also contributed to the decrease in bed height. This assumption is supported by the preceding observation; that the biofilm was fragile and tended to break (Figure 7.5). Further, the uneven thickness and rough contours of the biofilm after the bed height had decreased, accompanied by an increase in variation in the biofilm thickness per sample, suggest that parts of the biofilm had detached themselves.

Shortly before the bed height started to decrease, the measured mean biofilm thickness in the top layer also decreased, even though only temporarily. Since the contours of the biofilm in this sample looked rough, not smooth as did the contours of undamaged biofilm in this experiment, and since the biofilm had been very fragile, it was assumed that the biofilm thickness in the top layer itself did not actually decrease but that the lower value was caused by breakage and subsequent detachment of the very loose biofilm during sampling. Further, the shape of the graph of mean biofilm thickness versus time suggests that the discussed value was an aberration.

As wash out of bioparticles with very loose biofilm proceeded for two days, the continued increase in biofilm thickness did not cause the bed to regain height during this period. On the last day of the fluidized bed operation the wash out had stopped. As a consequence, the height of the bed increased slightly. Overall, it has to be assumed that in the second half of the experiment the accuracy of the results for the biofilm thickness decreased somewhat, because with increasing thickness it became more difficult to avoid damage to the biofilm when sampling. Yet, due to the wash out of the very loose biofilm, breakage

when sampling did not become a major problem.

The experiment conducted at an inlet phenol concentration of 520 mg/l was the only experiment in which the height of the fluidized bed increased gradually. In all other experiments, an increasing amount of particles with relatively loose and thick biofilm circulated to the top of the fluidized bed zone within a short period of time. This differing behaviour was mainly due to the relatively high turbulence in the fluidized bed at the beginning of the experiment, caused by the continuous formation of big air bubbles beneath the mesh at the bottom of the fluidized bed zone. The increased shear stress occasioned by the more turbulent behaviour of the bed made it impossible for fast growing, loose biofilm to develop. In addition, the high phenol concentration possibly also prevented the development of this type of biofilm. The formation of big air bubbles beneath the mesh at the bottom of the fluidized bed zone ceased after some growth had developed. The reason for their presence during the initial phase of the experiment is not clear, neither is the reason for the presence of tiny air bubbles attached to some activated carbon particles in the beginning of this experiment.

The variation in biofilm thicknesses in the top layer of the experiment conducted at 520 mg/l inlet phenol concentration was very high, even clearly visible without magnification. The phenomenon of bioparticles with very different biofilm thicknesses accumulating in the same layer is a consequence of the high density of the biofilm in this experiment. The latter causes the gravitational force on bioparticles of different biofilm thicknesses to be relatively similar, whereas differences in the thickness of loose biofilm cause significant differences in the gravitational force on the bioparticles. The fact that the particle cores of the sampled bioparticles in the top layer of this experiment were not visible made it necessary to use an altered procedure for the determination of the biofilm thickness, viz. using an average value for the size

of the cores (see Section 3.4.4). The inaccuracies caused by this approach also added to the variation in the measured mean biofilm thickness per sample. In the graph of mean biofilm thickness versus time (Figure 7.3), the two values that are slightly out of line are believed to be due to the sample having contained by chance more of the bioparticles with thicker film.

Comparing the four different inlet phenol concentrations tested, the rate of increase in biofilm thickness in the top layer was the highest at 100 mg/l, followed by 35 mg/l, then 330 mg/l and finally 520 mg/l. Thus, phenol inhibition was clearly apparent at a concentration of 330 mg/l. In comparison, Wisecarver and Fan (1989) proposed a model for a three-phase fluidized bed bioreactor for phenol degradation using activated carbon as carrier, which predicts phenol inhibition to occur only at a concentration of 800 mg/l. The results of the fluidized bed experiments are in accordance with those of the batch culture kinetic studies (Chapter 4). In the latter, for all three kinetic models fitted, the specific growth rate, μ, was slightly greater at 100 mg/l phenol concentration than at 35 mg/l. At the other two concentrations it was considerably smaller (see Figure 4.4). As mentioned in Chapter 4, several researchers (e.g. Chi and Howell, 1976; Sokol and Howell, 1981; Sokol, 1988) have reported that the inhibition characteristics are influenced by the phenol concentration prevailing in the culture from which the microorganisms were taken. Thus, the fact that in both, the fluidized bed and the batch culture studies, comparatively high growth rates were found at 100 mg/l phenol concentration, is probably related to the fact that the inoculum was grown at a phenol concentration of 100 mg/l.

However, it is known that biofilms are less sensitive to substrate inhibition than free cell systems (Van Ede *et al.*, 1993). Therefore, it is assumed that fastest increase in biofilm thickness would be achieved at a higher phenol concentration

than the concentration at which fastest growth in the batch culture experiments was observed. Additional experiments at phenol concentrations between 50 mg/l and 300 mg/l are necessary to determine the phenol concentration at which inhibition starts to occur in the biofilm system. It has to be noted, though, that the increase in biofilm thickness is not a true measure of growth, but the net result of biomass production and biomass removal by shear, the removal rate increasing with the mass of attached biofilm (Trulear and Characklis, 1982). Further, the biofilm thickness is influenced by extracellular by-products and the density with which the cells are packed in the biofilm.

The observed biofilm density was the highest at 520 mg/l inlet phenol concentration, followed by 100 mg/l, then 35 mg/l and finally 330 mg/l. The differences were the smallest between the experiments using an inlet phenol concentration of 35 mg/l and the one using 100 mg/l. However, the biofilm that developed at an inlet phenol concentration of 100 mg/l looked considerably denser than that at 35 mg/l. On the last day of the latter experiment, the biofilm seemed to be less dense than on the preceding days. This coincided with a decrease in inlet phenol concentration occurring towards the end of this experiment. Thus, for non-inhibitory phenol concentrations, the biofilm density decreased with decreasing phenol concentration. This statement, however, is based on very few observations. Yet, a decrease in biofilm density with decreasing substrate concentration under non-inhibitory conditions has also been observed by Trulear and Characklis (1982).

From the results of the experiment conducted at 330 mg/l, it could be concluded that inhibitory phenol concentrations might also induce the formation of loose biofilm. The observation that at 520 mg/l inlet phenol concentration the biofilm was the densest of all experiments does not necessarily contradict this assumption. Since the flow characteristics in the fluidized bed at the beginning

of the latter experiment were comparatively turbulent, any loose biofilm would have had difficulty remaining attached to the particles. Thus, the formation of dense biofilm was enforced by the hydrodynamic behaviour of the bed. However, it is also possible that the high phenol concentration employed in this experiment, favoured microorganisms which form denser biofilm. In any event, more phenol concentrations have to be tested to verify assumptions made on the basis of the present study.

The biofilm thickness reached was the smallest at 100 mg/l inlet phenol concentration, followed by 35 mg/l, then 520 mg/l and finally 330 mg/l. However, as the densities of the biofilms at the different concentrations varied, the thicknesses cannot be directly compared. In addition, it has to be noted that a high support particle concentration causes high particle to particle attrition, and this in turn causes the biofilm to be thin and dense (Chang *et al.*, 1991; Trinet *et al.*, 1991). Thus, since from the very start of the experiment using 100 mg/l inlet phenol concentration only one small bottom layer developed (i.e. the particle concentration in the top layer was comparatively high), enhanced attrition probably contributed to the biofilm thickness in the top layer reaching its maximum at a relatively low value and an early point in time. Further, it should not be forgotten that the measured biofilm thickness is no indication for the amount of active biomass present, as biomass further away from the bulk liquid tends to become inactive due to a lack in supply of substrate caused by diffusional limitations.

Image analysis in combination with the trapezoid formula used proved to be a very beneficial tool for determining the mean biofilm thickness. However, in the experiment conducted at 520 mg/l inlet phenol concentration, the determined values for the mean biofilm thicknesses in the top layer are all slight overestimates, as an altered method for calculation of the biofilm thickness had

to be employed due to the invisibility of the outlines of the particle cores (see Section 3.4.4). In general, all biofilm thicknesses observed must be regarded as somewhat larger than they were in reality, because the three-dimensional bioparticles became flatter when put on a glass slide for microscopy (see Section 3.4.4).

The achievement of only a small reduction in phenol concentration in the growth medium during its passage through the fluidized bed is discussed in Section 6.3. The high reduction in phenol concentration at the start of the experiments is due to adsorption of phenol to the activated carbon particles. As the quantity of adsorbate that can be taken up by an adsorbent is a function of the concentration of the adsorbate (Tchobanoglous, 1991), more phenol was removed from the medium as the phenol concentration in the growth medium increased. However, in the experiment using an inlet phenol concentration of 520 mg/l, the initial phenol reduction observed was comparatively small. This could be due to the fact that in this experiment adsorption of phenol onto the activated carbon proceeded at a faster rate than in the other experiments. Thus, at the time the measurement was taken (half an hour after start of the experiment), the adsorption equilibrium might have been nearly reached already. Possible reasons for the faster rate of adsorption are firstly the high phenol concentration in the medium, and secondly the small growth on the particles as the colonization of activated carbon particles slows down phenol adsorption (Ehrhardt and Rehm, 1985; Kindzierski *et al.*, 1992). Moreover, it is conceivable that the presence of tiny air bubbles attached to activated carbon particles at the beginning of this experiment blocked adsorption sites and thus reduced the adsorptive capacity of the activated carbon.

As higher inlet phenol concentrations were used, the absolute fluctuations with time in the inlet phenol concentration increased. Yet, relative to the value of the

inlet phenol concentration, the fluctuations were in a similar range in all four experiments. These fluctuations were mainly caused by the hygroscopic nature of phenol, which causes errors when weighing, and by the method employed for measuring the volume when mixing the medium (see Section 3.3.5). However, the variations in inlet phenol concentration did not seem to affect the degradation rate.

In the experiment using an inlet phenol concentration of 35 mg/l, the inlet phenol concentration and the inlet dissolved oxygen concentration decreased considerably after five days operation (c. 120 h). This was due to a large amount of growth occurring in the aeration tank and in the gas-liquid disengagement tank. Thus, the experiment was stopped. In the experiment conducted at 100 mg/l inlet phenol concentration, a much smaller amount of growth in the same tanks caused the inlet dissolved oxygen concentration to decrease slightly with time.

The phenol uptake rate started increasing earliest in the experiment using an inlet phenol concentration of 100 mg/l, followed by the one using 35 mg/l, then 330 mg/l and finally 520 mg/l. The same applied for the dissolved oxygen uptake. This was in accordance with the rate of increase in biofilm thickness in the top layer.

In the experiments conducted at inlet phenol concentrations of 35 mg/l and 100 mg/l, the initial rates of phenol degradation were masked by physical phenol adsorption to the carrier particles. Conversely, in the experiments conducted at inlet phenol concentrations of 330 mg/l and 520 mg/l, the phenol reduction decreased to zero after the adsorptive capacity of the activated carbon had been reached. In the case of the latter experiment, this was in agreement with the observation that hardly any growth occurred at the time. Yet, in the experiment

conducted at 330 mg/l phenol concentration, though growth was comparatively slow, marked biofilm was present when the zero phenol reduction was observed. It is assumed that the substrate needed for growth was obtained from the activated carbon particles to which it had adsorbed previously, and that at the same time the adsorption equilibrium changed because the increasing growth on the carbon particles hindered the phenol adsorption (Ehrhardt and Rehm, 1989; Kindzierski *et al.*, 1992).

The volumetric uptake rates reached were not significantly different in all of the experiments conducted except for the one using 330 mg/l inlet phenol concentration. In general, similar final phenol uptake rates were anticipated, because oxygen was the limiting factor in the system, as discussed in Section 6.3. Therefore, it is assumed that the decrease in phenol uptake rate towards the end of the experiment using 35 mg/l inlet phenol concentration, was caused by the decrease in oxygen concentration at the time, rather than by the simultaneous decrease in phenol concentration. The fact that in the experiment conducted at 330 mg/l inlet phenol concentration the phenol uptake rate reached was smaller than in all other experiments can be attributed to the wash out of carrier particles and biomass which occurred in this experiment. Further, it is possible that the comparatively loose biofilm contributed to the reduced phenol uptake rate since it has been reported that loose, thick biofilm coincides with low phenol uptake rates (Fan *et al.*, 1987).

As wash out of bioparticles with loose biofilm and wash out of detached biofilm occurred in the experiment conducted at an inlet phenol concentration of 330 mg/l, the phenol uptake rate decreased temporarily. The reason for the phenol uptake rate passing through a trough in the experiment using 100 mg/l inlet phenol concentration is unknown. Overall, not too much significance should be placed on the results of the volumetric phenol uptake rate since the differences

between inlet and outlet phenol concentration were only small.

Comparing volumetric phenol uptake rate and biofilm thickness, it can be observed that in all the experiments at a certain point the volumetric phenol uptake rate stopped increasing in spite of further increase in biofilm thickness. This is the point at which diffusional limitations in the biofilm become critical and the biofilm closest to the carrier becomes inactive (Shieh and Keenan, 1986).

In all of the experiments except the one conducted at 330 mg/l inlet phenol concentration, the dissolved oxygen uptake reached over 90%, i.e. the dissolved oxygen in the medium was virtually consumed. Thus, as discussed in Section 6.3, oxygen was regarded the limiting factor in the system. In the latter experiment, the reason for the increase in oxygen uptake coming to a halt at a level of about 70% was again the wash out of particles with very loose biofilm and the wash out of detached biofilm.

The amount of oxygen required for the degradation of phenol found in this study (1.3-1.6 mg O_2/mg phenol) was in agreement with the values found by other workers (see Section 6.3).

7.4 Conclusion

At all four inlet phenol concentrations tested (35 mg/l, 100 mg/l, 330 mg/l and 520 mg/l), the fluidized bed stratified into layers of bioparticles with different biofilm thickness and different biofilm structure. Differences in the microbial composition of the biofilm caused by the multitude of factors influencing biofilm development were probably the main reason for this phenomenon.

Apart from the very start of the experiments where adsorption of phenol to the activated carbon governed the phenol uptake, the reduction in phenol concentration was small due to a very short hydraulic retention time. However, the volumetric phenol uptake rates reached were comparable with results obtained by other researchers. The concentration of dissolved oxygen in the outlet reached very low values. Thus, the system was oxygen-limited.

Distinct differences between the behaviour of the fluidized bed system at the different inlet phenol concentrations were found. The biofilm thickness in the top layer increased the fastest at an inlet phenol concentration of 100 mg/l, followed by 35 mg/l, then 330 mg/l and finally 520 mg/l. The increases in phenol and dissolved oxygen uptakes behaved accordingly. These results were in agreement with the results gained in the batch culture kinetic studies (Chapter 4), where the same order applied for the specific growth rates at phenol concentrations of the above values. However, since it is known that biofilms are less sensitive to substrate inhibition than free cells, it is assumed that phenol inhibition would start to occur at a higher phenol concentration in the fluidized bed system than it did in the batch culture kinetic studies. Additional experiments between 50 mg/l and 300 mg/l inlet phenol concentration are necessary to determine the substrate concentration at which the biofilm thickness increases fastest.

The few observations obtained could indicate that for non-inhibitory phenol concentrations the biofilm density increases with increasing phenol concentration. For inhibitory phenol concentrations, it was not possible to determine a relationship between biofilm density and phenol concentration on the basis of the present observations, as the loosest biofilm was observed at 330 mg/l inlet phenol concentration and the densest at 520 mg/l. However, in the latter experiment, the formation of dense biofilm was induced by turbulent flow

patterns at the start of the experiment, caused by big air bubbles forming under the mesh at the bottom of the fluidized bed zone.

The biofilm thickness that was reached in the top layer was the smallest at 100 mg/l inlet phenol concentration, followed by 35 mg/l, then 520 mg/l and finally 330 mg/l. However, since the densities of the biofilm and the particle concentration, and thus in turn the shear stress, in the top layer varied between the different experiments, the biofilm thicknesses cannot be directly compared.

Image analysis techniques in combination with the trapezoid formula employed proved to be a very useful and convenient tool to determine the mean biofilm thickness, giving representative values for all shapes of bioparticles.

The volumetric phenol uptake rates reached were about the same in all experiments except the one conducted at 330 mg/l. A similar uptake was expected, as the culture system was oxygen-limited. The main reason for the lower uptake in the latter experiment was wash out of bioparticles with loose biofilm and wash out of detached biofilm. For the same reasons, the dissolved oxygen uptake in this experiment was slightly lower.

Since in this study only four different inlet phenol concentrations were tested and no replicates were conducted, the results gave only an insight into the effect of different inlet phenol concentrations, and into the complex interactions occurring in fluidized bed bioreactors. Further experiments are necessary to determine more closely the relationship between phenol concentration and biofilm development during start-up.

CHAPTER 8

FINAL DISCUSSION AND CONCLUSIONS

Batch culture studies to determine the kinetic behaviour of the mixed microbial culture employed in this work showed that the culture was well adapted to phenol as inhibitory substrate. The culture was faster growing than other phenol degrading cultures described in the literature. The highest specific growth rates were obtained for initial phenol concentrations of between 30 and 130 mg/l, the results giving a scatter cloud of data points in this area. Three substrate inhibition models were fitted to the experimental data; the Teissier-Edwards model, the Haldane model and the Aiba-Edwards model. All three fitted the data well, without showing a statistically significant difference in the goodness of fit. However, the lowest variance was obtained for the Teissier-Edwards model. The phenol concentrations at which the fitted functions go through their maximum value were between 57 and 88 mg/l, corresponding to specific growth rates of between 0.64 and 0.65 h^{-1}.

In order to investigate the biofilm development of the mixed culture on fluidized activated carbon particles, an experimental apparatus was established. Test runs showed that the most critical part of the apparatus was the liquid distributor at the bottom of the liquid-solid fluidized bed bioreactor. An effective liquid distribution device is necessary to prevent turbulent flow patterns at the bottom of the fluidized bed. An important requirement is to ensure that blockage of the liquid distributor by biomass or coalescing air bubbles cannot occur. Other critical factors that were decided on during preliminary test runs were initial bed expansion, flow rate, support particle size, and amount of support particles used,

these parameters all being interdependent.

The fluidized bed studies which were conducted confirmed that the use of image analysis techniques is a very effective means of measuring the biofilm thickness on fluidized support particles. A trapezoid formula, which has also been used by Senthilnathan *et al.* (1990b, 1991), was employed to calculate the mean biofilm thickness from the projected areas and the perimeters of the bioparticle and the particle core. This formula provides a reliable estimate of the mean biofilm thickness for all shapes of particle cores and for nonuniform biofilms. Whereas Senthilnathan *et al.* (1990b) used a light pen to trace the circumference of the particle core and the bioparticle, in the present study the computer program identified these boundaries by segmentation. This clearly improves the accuracy of the measurement, as operator errors are eliminated and the objectivity of the procedure is increased. The placement of the bioparticles on a glass slide for microscopy proved to introduce slight errors as the biofilm flattened to some degree when placed on the glass slide. In order to obtain comparable results, this method was, however, retained throughout the study. For future studies, the more work intensive sample preparation employed by some researchers (Dudley *et al.*, 1993; Senthilnathan *et al.*, 1990b), viz. embedment of the bioparticles in agar in a petri dish, would be preferable.

In all fluidized bed experiments, the bed stratified into layers (in most cases two or three) containing bioparticles with different biofilm thickness and different biofilm structure, the biofilm densities having been only visually observed, not measured. The disparate biofilm development was attributed, above all, to differences in the microbial composition of the biofilm caused by the multitude of factors influencing biofilm development. Since sampling was easiest from the upper part of the fluidized bed, the main focus was on the development of the biofilm in the top layer. Another common feature of all experiments was that,

apart from the very start of the experiments where adsorption of phenol to the activated carbon governed the phenol uptake, the reduction in phenol concentration was small due to a very short hydraulic retention time. However, the volumetric phenol uptake rates reached were comparable with results obtained by other researchers. The dissolved oxygen concentration in the outlet reached very low values. Thus, the system was oxygen-limited.

Different reactor temperatures led to distinct differences in the morphology of the biofilm in the top layer. Without temperature control, i.e. at 17.2°C average temperature, and at 30°C, a loose, fluffy, unevenly shaped, thick biofilm developed after different operating times. Conversely, at 25°C the biofilm was firm and relatively even in shape. Here, the final thickness remained far below the thicknesses reached by the fluffy biofilm. Since the biofilm that developed at 25°C showed the most favourable characteristics, this temperature was used for the experiments investigating the effect of different inlet phenol concentrations.

The biofilm thickness in the top layer increased the fastest at an inlet phenol concentration of 100 mg/l, followed by 35 mg/l, then 330 mg/l and finally 520 mg/l. The increase in phenol and dissolved oxygen uptakes behaved accordingly. These results were in agreement with the results obtained in the batch culture kinetic studies, where the same order applied for the specific growth rates at phenol concentrations of the above values. However, since it is known that immobilized microorganisms are less sensitive to inhibition than free cells, it is assumed that phenol inhibition would start to occur at a higher phenol concentration in the fluidized bed system than it did in batch culture. Additional experiments between 50 mg/l and 300 mg/l inlet phenol concentration are necessary to determine the substrate concentration at which the biofilm thickness increases fastest. The biofilm thicknesses reached cannot be directly compared

since they depend on factors which varied between the different experiments, such as biofilm density and shear stress.

In the case of the few observations obtained at non-inhibitory phenol concentrations, the biofilm density increased with increasing phenol concentration. This is in agreement with the results of Trulear and Characklis (1982). For inhibitory phenol concentrations, a relationship between phenol concentration and biofilm density could not be determined as in these experiments the flow patterns were very different. Thus, they were the dominating factor influencing the biofilm density. However, out of the four phenol concentrations tested, the loosest biofilm formed in the experiment using 330 mg/l inlet phenol concentration. This biofilm, though, was far less loose than the biofilm that developed at 17.2°C average temperature and at 30°C.

In conclusion, this study has shown that image analysis is a very useful tool to determine the mean biofilm thickness on fluidized support particles. Within the scope of this work, only an insight into the effect of different reactor temperatures and different inlet phenol concentrations on the biofilm development during start-up could be obtained. Additional experiments are necessary to determine more closely these relationships. In future investigations special attention should be paid to obtaining accurate values for the biofilm volume, employing the image processing method proved effective in this study, thus allowing reliable determination of biofilm densities.

REFERENCES

Adams, H.L., Thomas, C.R. (1988),
The Use of Image Analysis for Morphological Measurements on Filamentous Microorganisms,
Biotechnol. Bioeng., **32**, 707-712.

Allsop, P.J., Chisti, Y., Moo-Young, M., Sullivan, G.R. (1993),
Dynamics of Phenol Degradation by *Pseudomonas putida*,
Biotechnol. Bioeng., **41**, 572-580.

Annachhatre, A.P., Khanna, P. (1987),
Unsteady-State Biofilm Kinetics,
J. Environ. Eng., **113**, 429-333.

Anselmo, A.M., Mateus, M., Cabral, J.M.S., Novais, J.M. (1985),
Degradation of Phenol by Immobilized Cells of *Fusarium flocciferum*,
Biotechnol. Lett., **7**, 889-894.

Anselmo, A.M., Cabral, J.M.S., Novais, J.M. (1989),
The Adsorption of *Fusarium flocciferum* Spores on Celite Particles and their Use in the Degradation of Phenol,
Appl. Microbiol. Biotechnol., **31**, 200-203.

Anselmo, A.M., Novais, J.M. (1992),
Degradation of Phenol by Immobilized Mycelium of *Fusarium flocciferum* in Continuous Culture,
Wat. Sci. Tech., **25**, 161-168.

Antai, S.P., Crawford, D.L. (1983),
Degradation of Phenol by *Strepyomyces setonii*,
Can. J. Microbiol., **29**, 142-143.

Applegate and Bryers (1991),
Effects of Carbon and Oxygen Limitations and Calcium Concentration on Biofilm Removal Processes,
Biotechnol. Bioeng., **37**, 17-25.

Atkinson, B., Mavituna, F. (1991a),
Continuous Reactor Systems - Fluidized Bed,
In: Biochemical Engineering and Biotechnology Handbook, 2nd ed.,
Stockton Press, New York, pp. 652-664.

Atkinson, B., Mavituna, F. (1991b),
Immobilized Cell Systems,
In: Biochemical Engineering and Biotechnology Handbook, 2nd ed.,
Stockton Press, New York, pp. 768-784.

Bayly, R.C., Dagley, S. (1969),
Oxoenic Acids as Metabolites in the Bacterial Degradation of Catechols,
Biochem. J., **111**, 303-307.

Beltrame, P., Beltrame, P.L., Carniti, P., Pitea, D. (1980),
Kinetics of Phenol Degradation by Activated Sludge in a Continuous-Stirred Reactor,
J. Wat. Pollut. Control Fed., **52**, 126-133.

Beltrame, P., Beltrame, P.L., Carniti, P. (1984),
Influence of Feed Concentration on the Kinetics of Biodegradation of Phenol in a Continuous Stirred Reactor,
Water Res., **18**, 403-407.

Bettmann, H., Rehm, H.J. (1984),
Degradation of Phenol by Polymer Entrapped Microorganisms,
Appl. Microbiol. Biotechnol., **20**, 285-290.

Bhamidimarri, S.M.R. (1985),
Biofilm Characteristics and their Role in a Fluidized-Bed Bioreactor,
Ph.D. Thesis, University of Queensland, St. Lucia, Australia.

Bhamidimarri, S.M.R., Greenfield, P.F., Bell, P.R.F. (1987),
Biofilm Characteristics in a Fluidized-Bed Bioreactor,
Proc. 42nd Ind. Waste Conf., Purdue Univ., 103-111.

Bhamidimarri, S.M.R. (1990),
Adsorption and Attachment of Microorganisms to Solid Supports,
In: Wastewater Treatment by Immobilized Cells, Tyagi, R.D., Vembu, K. (eds.),
CRC Press, Boca Raton, Ann Arbor, Boston, pp. 29-43.

Bhamidimarri, S.M.R., Greenfield, P.F. (1990),
Unified Models for Phenol Degradation in a Fluidized Bed Biofilm Reactor,
Chemeca, **18**, 493-507.

Bhamidimarri, S.M.R., See, T.T. (1992),
Shear Loss Characteristics of an Aerobic Biofilm,
Wat. Sci. Tech., **26**, 595-600.

Bignami, L., Eramo, B., Gavasci, R., Ramadori, R., Rolle, E. (1991),
Modelling and Experiments on Fluidized-Bed Biofilm Reactors,
Wat. Sci. Tech., **24**, 47-58.

Bucke, C. (1986),
Methods of Immobilising Cells,
In: Process Engineering Aspects of Immobilised Cell Systems,
Webb, C., Black, G.M., Atkinson, B. (eds.),
Institution of Chemical Engineers, Rugby, pp. 20-34.

Buswell, J.A. (1975),
Metabolism of Phenol and Cresols by *Bacillus stearothermophilus*,
J. Bacteriol., **124**, 1077-1083.

Chang, H.T., Rittmann, B.E. (1987),
Mathematical Modeling of Biofilm on Activated Carbon,
Environ. Sci. Technol., **21**, 273-280.

Chang, H.T., Rittmann, B.E., Amar, D., Heim, R., Ehlinger, O., Lesty, Y. (1991),
Biofilm Detachment Mechanisms in a Liquid-Fluidized Bed,
Biotechnol. Bioeng., **38**, 499-506.

Characklis, W.G., Bakke, R., Trulear, M.G. (1985),
Fundamental Considerations of Fixed Film Systems,
In: Comprehensive Biotechnology, Moo-Young, M. (ed.), Vol.4,
Pergamon Press, Oxford, pp. 945-961.

Chi, C.T., Howell, J.A. (1976),
Transient Behaviour of a Continuous Stirred Tank Biological Reactor Utilizing Phenol as an Inhibitory Substrate,
Biotechnol. Bioeng., **18**, 63-80.

Colvin, R.J., Rozich, A.R. (1986),
Phenol Growth Kinetics of Heterogeneous Populations in a Two-Stage Continuous Culture System,
J. Wat. Pollut. Control Fed., **58**, 326-332.

Cooper, P.F., Atkinson, B. eds. (1981),
Biological Fluidized Bed Treatment of Water and Wastewater,
John Wiley & Sons, London, New York.

Cooper, P.F. (1985),
Biological Fluidized Bed Reactors for Treatment of Sewage and Industrial Effluents,
In: Comprehensive Biotechnology, Moo-Young, M. (ed.), Vol.4,
Pergamon Press, Oxford, pp. 993-1006.

Cooper, P.F. (1986),
The Two Fluidised Bed Reactor for Wastewater Treatment,
In: Process Engineering Aspects of Immobilised Cell Systems,
Webb, C., Black, G.M., Atkinson, B. (eds.),
Institution of Chemical Engineers, Rugby, pp. 179-204.

D'Adamo, P.D., Rozich, A.F., Gaudy, A.F., Jr. (1984),
Analysis of Growth Data with Inhibitory Carbon Sources,
Biotechnol. Bioeng., **26**, 397-402.

Davidson, P.M., Branen, A.L. (1981),
Antimicrobial Activity of Non-halogenated Phenolic Compounds,
J. Food. Prot., **44**, 623-632.

Diamadopoulos, E., Samaras, P., Sakellaropoulos, G.P. (1992),
The Effect of Activated Carbon Properties on the Adsorption of Toxic Substances,
Wat. Sci. Tech., **25**, 153-160.

Dudley, B.T., Howgrave-Graham, A.R., Bruton, A.G., Wallis, F.M. (1993),
Image Analysis to Quantify and Measure UASB Digester Granules,
Biotechnol. Bioeng., **42**, 279-283.

Edwards, V.H. (1970),
The Influence of High Substrate Concentrations on Microbial Kinetics,
Biotechnol. Bioeng., **12**, 679-712.

Ehrhardt, H.M., Rehm, H.J. (1985),
Phenol Degradation by Microorganisms Adsorbed on Activated Carbon,
Appl. Microbiol. Biotechnol., **21**, 32-36.

Ehrhardt, H.M., Rehm, H.J. (1989),
Semicontinuous and Continuous Degradation of Phenol by *Pseudomonas putida* P8 Adsorbed on Activated Carbon,
Appl. Microbiol. Biotechnol., **30**, 312-317.

Ellis, B.E. (1977),
Degradation of Phenolic Compounds by Fresh-Water Algae,
Plant. Sci. Lett., **8**, 213-216.

Fan, L.-S., Fujie, K., Long, T.-R., Tang, W.-T. (1987),
Characteristics of Draft Tube Gas-Liquid-Solid Fluidized-Bed Bioreactor with Immobilized Living Cells for Phenol Degradation,
Biotechnol. Bioeng., **30**, 498-504.

Fan, L.-S., Leyva-Ramos, R., Wisecarver, K.D., Zehner, B.J. (1990),
Diffusion of Phenol through a Biofilm Grown on Activated Carbon Particles in a Draft-Tube Three-Phase Fluidized-Bed Bioreactor,
Biotechnol. Bioeng., **35**, 279-286.

Feist, C.F., Hegemann, G.D. (1969),
Phenol and Benzoate Metabolism by *Pseudomonas putida*: Regulation of Tangential Pathways,
J. Bacteriol., **100**, 869-877.

Gantzer, C.J. (1989),
Inhibitory Substrate Utilization by Steady-State Biofilms,
J. Environ. Eng., **115**, 302-319.

Gorris, L.G.M., van Deursen, J.M.A., van der Drift, C., Vogels, G.D. (1988),
Influence of Waste Water Composition on Biofilm Development in Laboratory Methanogenic Fluidized Bed Reactors,
Appl. Microbiol. Biotechnol., **29**, 95-102.

Gorris, L.G.M., van Deursen, J.M.A., van der Drift, C., Vogels, G.D. (1989),
Biofilm Development in Laboratory Methanogenic Fluidized Bed Reactors,
Biotechnol. Bioeng., **33**, 687-693.

Gurujeyalakshmi, G., Oriel, P. (1989),
Isolation of Phenol-Degrading *Bacillus stearothermophilus* and Partial Characterization of the Phenol Hydroxylase,
Appl. Environ. Microbiol., **55**, 500-502.

Hackel, U., Klein, J., Megnet, R., Wagner, F. (1975),
Immobilisation of Microbial Cells in Polymeric Matrices,
Europ. J. Appl. Microbiol., **1**, 291-293.

Han, K., Levenspiel, O. (1988),
Extended Monod Kinetics for Substrate, Product, and Cell Inhibition,
Biotechnol. Bioeng., **32**, 430-437.

Heipieper, H.J., Keweloh, H., Rehm, H.J. (1991),
Influence of Phenols on Growth and Membrane Permeability of Free and Immobilized *Escherichia coli*,
Appl. Environ. Microbiol., **57**, 1213-1217.

Hill, G.A., Robinson, C.W. (1975),
Substrate Inhibition Kinetics: Phenol Degradation by *Pseudomonas putida*,
Biotechnol. Bioeng., **17**, 1599-1615.

Holladay, D.W., Hancher, C.W., Scott, C.D. (1978),
Biodegradation of Phenolic Waste Liquors in Stirred-Tank, Packed-Bed, and Fluidized-Bed Bioreactors,
J. Wat. Pollut. Control Fed., **50**, 2573-2589.

Jähne, B. (1991),
Digital Image Processing, Concepts, Algorithms and Scientific Applications,
Springer-Verlag, Berlin, Heidelberg, New York.

Jones, G.L., Jansen, F., McKay, A.J. (1973),
Substrate Inhibition of the Growth of Bacterium NCIB 8250 by Phenol,
J. Gen. Microb., **74**, 139-148.

Karel, S.F., Libicki, S.B., Robertson, C.R. (1985),
The Immobilization of Whole Cells: Engineering Principles,
Chem. Eng. Sci., **40**, 1321-1354.

Keweloh, H., Heipieper, H.J., Rehm, H.J. (1989),
Protection of Bacteria against Toxicity of Phenol by Immobilization in Calcium Alginate,
Appl. Microbiol. Biotechnol., **31**, 383-389.

Keweloh, H., Weyrauch, G., Rehm, H.J. (1990),
Phenol-Induced Membrane Changes in Free and Immobilized *Escherichia coli*,
Appl. Microbiol. Biotechnol., **33**, 66-71.

Kim, B.R., Suidan, M.T. (1989),
Approximate Algebraic Solution for a Biofilm Model with the Monod Kinetic Expression,
Wat. Res., **23**, 1491-1498.

Kim, J.W., Humenick, M.J., Armstrong, N.E. (1981),
A Comprehensive Study on the Biological Treatabilities of Phenol and Methanol, I. Analysis of Bacterial Growth and Substrate Removal Kinetics by a Statistical Method,
Water Res., **15**, 1221-1231.

Kindzierski, W.B., Gray, M.R., Fedorak, P.M., Hrudey, S.E. (1992),
Activated Carbon and Synthetic Resins as Support Material for Methanogenic Phenol-Degrading Consortia - Comparison of Surface Characteristics and Initial Colonization,
Water Environ. Res., **64**, 766-775.

Klein, J., Hackel, U., Wagner, F. (1979),
Phenol Degradation by *Candida tropicalis* Whole Cells Entrapped in Polymeric Ionic Networks,
Immobilized Microbial Cells, ACS Symp. Ser. No. 106, Am. Chem. Soc., Washington, DC.

Klein, J., Vorlop, K.-D. (1985),
Immobilization Techniques - Cells,
In: Comprehensive Biotechnology, Vol.2, Moo-Young, M. (ed.),
Pergamon Press, Oxford, pp. 203-224.

Klein, J. (1988),
Matrix Design for Microbial Cell Immobilization,
In: Bioreactor Immobilized Enzymes and Cells: Fundamentals and Applications,
Moo-Young, M. (ed.), Elsevier Applied Science, London, New York, pp. 1-8.

Klekner, V., Kosaric, N. (1992),
Degradation of Phenols by Algae,
Environ. Tech., **13**, 493-501.

Koch, B., Ostermann, M., Höke, H., Hempel, D.-C. (1991),
Sand and Activated Carbon as Biofilm Carriers for Microbial Degradation of Phenols and Nitrogen-Containing Aromatic Compounds,
Water Res., **25**, 1-8.

Kunii, D., Levenspiel, O. (1991),
Fluidization Engineering, 2nd ed.,
Butterworth-Heinemann, Boston, London.

Lee, D.D., Scott, C.D., Hancher, C.W. (1979),
Fluidized Bed Bioreactor for Coal-Conversion Effluents,
J. Wat. Pollut. Control Fed., **51**, 974-984.

Li, J., Humphrey, A.E. (1989),
Kinetic and Fluorometric Behavior of a Phenol Fermentation,
Biotechnol. Lett., **11**, 177-182.

Lin, S.H. (1991),
A Mathematical Model for a Biological Fluidized Bed Reactor,
J. Chem. Tech. Biotechnol., **51**, 473-482.

Livingston, A.G., Chase, H.A. (1989),
Modeling Phenol Degradation in a Fluidized-Bed Bioreactor,
AIChE J., **35**, 1980-1992.

Lu, Y., Ganczarczyk, J.J. (1983),
Application of Carrier/Activated Sludge Process for Treatment of Phenolic Wastewater,
Proc. 38th Ind. Waste Conf., Purdue Univ., 643-657.

Luong, J.H.T. (1987),
Generalization of Monod Kinetics for Analysis of Growth Data with Substrate Inhibition,
Biotechnol. Bioeng., **29**, 242-248.

McFeters, G.A. (1984),
Biofilm Development and Its Consequences - Group Report,
In: Microbial Adhesion and Aggregation, Marshall, K.C. (ed.),
Springer-Verlag, Berlin Heidelberg, New York, pp. 109-124.

Mizobuchi, T., Morita, S., Yano, T. (1980),
Stability and Phase-Plane Analyses of Continuous Phenol Biodegradation: A Simple Case,
J. Ferment. Technol., **58**, 33-38.

Mol, N., Kut, O.M., Dunn, I.J. (1992),
Adsorption toxischer Schocks auf verschiedenartigen Trägermaterialien in anaeroben Biofilm-Fließbettreaktoren,
Chem.-Ing.-Tech., **64**, 878.

Molin, G., Nilsson, I. (1985),
Degradation of Phenol by *Pseudomonas putida* ATCC 11172 in Continuous Culture at Different Ratios of Biofilm Surface to Culture Volume,
Appl. Environ. Microbiol., **50**, 946-950.

Mörsen, A., Rehm, H.J. (1987),
Degradation of Phenol by a Mixed Culture of *Pseudomonas putida* and *Cryptococcus elinovii* Adsorbed on Activated Carbon,
Appl. Microbiol. Biotechnol., **26**, 283-288.

Mörsen, A., Rehm, H.J. (1990),
Degradation of Phenol by a Defined Mixed Culture Immobilized by Adsorption on Activated Carbon and Sintered Glass,
Appl. Microbiol. Biotechnol., **33**, 206-212.

Mulcahy, L.T., Shieh, W.K., LaMotta, E.J. (1981),
Simplified Mathematical Models for a Fluidized Bed Biofilm Reactor,
AIChE Symp. Series, **77**, 273-285.

Muslu, Y. (1992),
Developments in Modelling Biofilm Reactors,
J. Biotechnol., **23**, 183-191.

Neujahr, H.J., Varga, J.M. (1970),
Degradation of Phenols by Intact Cells and Cell-free Preparations of *Trichosporon cutaneum*,
Europ. J. Biochem., **13**, 37-44.

Nishijima, W., Tojo, M., Okada, M., Murakami, A. (1992),
Biodegradation of Organic Substances by Biological Activated Carbon - Simulation of Bacterial Activity on Granular Activated Carbon,
Wat. Sci. Tech., **26**, 2031-2034.

Ong, S.K., Bowers, A.R. (1990),
Steady-State Analysis for Biological Treatment of Inhibitory Substrates,
J. Environ. Eng., **116**, 1013-1028.

Pawlowsky, U., Howell, J.A. (1973),
Mixed Culture Biooxidation of Phenol. I. Determination of Kinetic Parameters,
Biotechnol. Bioeng., **15**, 889-896.

Phillips, C.R., Poon, Y.C. (1988),
Immobilization of Cells,
Springer-Verlag, Berlin, Heidelberg, New York.

Quail, B.E., Hill, G.A. (1991),
A Packed-column Bioreactor for Phenol Degradation: Model and Experimental Verification,
J. Chem. Tech. Biotechnol., **52**, 545-557.

Reichl, U., Buschulte, T.K., Gilles, E.D. (1990),
Study of the Early Growth and Branching of *Streptomyces tendae* by Means of an Image Processing System,
J. Microsc., **158**, 55-62.

Rittmann, B.E., Manem, J.A. (1992),
Development and Experimental Evaluation of a Steady-State, Multispecies Biofilm Model,
Biotechnol. Bioeng., **39**, 914-922.

Ro, K.S., Neethling, J.B. (1990),
Terminal Settling Characteristics of Bioparticles,
Res. J. Water Pollut. Control Fed., **62**, 901-906.

Ro, K.S., Neethling, J.B. (1991),
Biofilm Density for Biological Fluidized Beds,
Res. J. Water Pollut. Control Fed., **63**, 815-818.

Rouxhet, P.G., Mozes, N. (1990),
Physical Chemistry of the Interface between Attached Micro-organisms and their Support,
Wat. Sci. Tech., **22**, 1-16.

Rozich, A.F., Gaudy, A.F., Jr. (1983a),
Response of Phenol-Acclimated Activated Sludge Process to Quantitative Shock Loading,
Proc. 38th Ind. Waste Conf., Purdue Univ., 725-736.

Rozich, A.F., Gaudy, A.F., Jr., D'Adamo, P.D. (1983b),
Predictive Model for Treatment of Phenolic Wastes by Activated Sludge,
Water. Res., **17**, 1453-1466.

Rozich, A.F., Gaudy, A.F., Jr., D'Adamo, P.D. (1985),
Selection of Growth Rate Model for Activated Sludges Treating Phenol,
Water. Res., **19**, 481-490.

Sáez, P.B., Rittmann, B.E. (1988),
Improved Pseudoanalytical Solution for Steady-State Biofilm Kinetics,
Biotechnol. Bioeng., **32**, 379-385.

Scott, C.D. (1987)
Immobilized Cells: A Review of Recent Literature,
Enzyme Microb. Technol., **9**, 66-73.

Senthilnathan, PR., Ganczarczyk, J.J. (1990a),
Application of Biomass Carriers in Activated Sludge Process,
In: Wastewater Treatment by Immobilized Cells, Tyagi, R.D., Vembu, K. (eds.),
CRC Press, Boca Raton, Ann Arbor, Boston, pp. 103-141.

Senthilnathan, PR., Li, D.-H., Ganczarczyk, J.J. (1990b),
Image Analysis of Biomass Immobilized on Micro-Carriers,
Proc. 44th Ind. Waste Conf., Purdue Univ., 175-181.

Senthilnathan, PR., Ganczarczyk, J.J. (1991),
Discussion of: Terminal Settling Characteristics of Bioparticles (By: Ro, K.S., Neethling, J.B., 1990),
Res. J. Water Pollut. Control Fed., **63**, 819.

Shieh, W.K. (1980),
Suggested Kinetic Model for the Fluidized-Bed Biofilm Reactor,
Biotechnol. Bioeng., **22**, 667-676.

Shieh, W.K., Sutton, P.M., Kos, P. (1981),
Predicting Reactor Biomass Concentration in a Fluidized-Bed System,
J. Wat. Pollut. Control Fed., **53**, 1574-1584.

Shieh, W.K., Mulcahy, L.T., LaMotta, E.J. (1982),
Mathematical Model for the Fluidized Bed Biofilm Reactor,
Enzyme Microb. Technol., **4**, 269-275.

Shieh, W.K., Keenan, J.D. (1986),
Fluidized Bed Biofilm Reactors for Wastewater Treatment,
In: Advances in Biochemical Engineering/Biotechnology, Vol.33, Fiechter, A. (ed.), Springer-Verlag, Berlin, Heidelberg, 131-169.

Shimizu, T., Uno, T., Dan, Y., Nei, N., Ichikawa, K. (1973),
Continuous Treatment of Waste Water Containing Phenol by *Candida tropicalis*,
J. Ferment. Technol., **51**, 809-812.

Skowlund, C.T. (1990),
Effect of Biofilm Growth on Steady-State Biofilm Models,
Biotechnol. Bioeng., **35**, 502-510.

Sokol, W., Howell, J.A. (1981),
Kinetics of Phenol Oxidation by Washed Cells,
Biotechnol. Bioeng., **23**, 2039-2049.

Sokol, W. (1987),
Oxidation of Inhibitory Substrate by Washed Cells (Oxidation of Phenol by *Pseudomonas putida*),
Biotechnol. Bioeng., **30**, 921-927.

Sokol, W. (1988),
Uptake Rate of Phenol by *Pseudomonas putida* Grown in Unsteady State,
Biotechnol. Bioeng., **32**, 1097-1103.

Stanier, R.Y., Ornston, L.N. (1973),
The β-ketoadipate Pathway,
Adv. Microbiol. Physiol., **9**, 89-152.

Suzuki, M., Momonoi, S., Harada, H. (1983),
Phenolic Wastewater Treatment in a Loop-Type Bioreactor,
Proc. Symp. Biol. Wastewater Treatments, Sandi, Japan, 34.

Szetela, R.W., Winnicki, T.Z. (1981),
A Novel Method for Determining the Parameters of Microbial Kinetics,
Biotechnol. Bioeng., **23**, 1485-1490.

Takahashi, S., Itoh, M., Kaneko, Y. (1981),
Treatment of Phenolic Wastes by *Aureobasidium pullulans* Adhered to the Fibrous Supports,
Europ. J. Appl. Microbiol. Biotechnol., **13**, 175-178.

Tanaka, A., Tosa, T., Kobayashi, T. eds. (1993),
Industrial Application of Immobilized Biocatalysts,
Marcel Dekker, New York, Basel, Hong Kong.

Tang, W.-T., Fan, L.-S. (1987a),
Steady State Phenol Degradation in a Draft-Tube, Gas-Liquid-Solid Fluidized-Bed Bioreactor,
AIChE J., **33**, 239-249.

Tang, W.-T., Wisecarver, K., Fan, L.-S. (1987b),
Dynamics of a Draft Tube Gas-Liquid-Solid Fluidized Bed Bioreactor for Phenol Degradation,
Chem. Eng. Sci., **42**, 2123-2134.

Tchobanoglous, G. (1991),
Wastewater Engineering: Treatment, Disposal, Reuse / Metcalf & Eddy, Inc.,
3rd ed., revised by Tchobanoglous, G., Burton, F.L.,
McGraw-Hill, New York, London, Singapore, p. 318.

Trambouze, P., Van Landeghem, H., Wauquier, J.P. (1988),
Chemical Reactors, Design/Engineering/Operation,
Gulf Publishing Company, Houston, Texas, pp. 416-438, 463-470.

Trinet, F., Heim, R., Amar, D., Chang, H.T., Rittmann, B.E. (1991),
Study of Biofilm and Fluidization of Bioparticles in a Three-Phase Liquid-Fluidized-Bed Reactor,
Wat. Sci. Tech., **23**, 1347-1354.

Trulear, M.G., Characklis, W.G. (1982),
Dynamics of Biofilm Processes,
J. Wat. Pollut. Control Fed., **54**, 1288-1301.

Van Ede, C.J., Bollen, A.M., Beenackers, A.A.C.M. (1993),
Analytical Effectiveness Calculations Concerning the Degradation of an Inhibitive Substrate by a Steady-State Biofilm,
Biotechnol. Bioeng., **42**, 267-278.

Vembu, K., Tyagi, R.D. (1990),
Fluidized Bed Reactors in Wastewater Treatment,
In: Wastewater Treatment by Immobilized Cells, Tyagi, R.D., Vembu, K. (eds.),
CRC Press, Boca Raton, Ann Arbor, Boston, pp. 253-265.

Wanner, O., Gujer, W. (1986),
A Multispecies Biofilm Model,
Biotechnol. Bioeng., **28**, 314-328.

Wayman, M., Tseng, M.C. (1976),
Inhibition-Threshold Substrate Concentrations,
Biotechnol. Bioeng., **18**, 383-387.

Wisecarver, K.D., Fan, L.-S. (1989),
Biological Phenol Degradation in a Gas-Liquid-Solid Fluidized Bed Reactor,
Biotechnol. Bioeng., **33**, 1029-1038.

Worden, R.M., Donaldson, T.L. (1987),
Dynamics of a Biological Fixed Film for Phenol Degradation in a Fluidized-Bed Bioreactor,
Biotechnol. Bioeng., **30**, 398-412.

Yanase, H., Zuzan, K., Kita, K., Sogabe, S., Kato, N. (1992),
Degradation of Phenols by Thermophilic and Halophilic Bacteria Isolated from a Marine Brine Sample,
J. Ferment. Bioeng., **74**, 297-300.

Yang, R.D., Humphrey, A.E. (1975),
Dynamics and Steady State Studies of Phenol Biodegradation in Pure and Mixed Culture,
Biotechnol. Bioeng., **27**, 1211-1235.

Zilli, M., Converti, A., Lodi, A., Del Borghi, M., Ferraiolo, G. (1993), Phenol Removal from Waste Gases with a Biological Filter by *Pseudomonas putida*,
Biotechnol. Bioeng., **41**, 693-699.